BROOKHAVEN NATIONAL LABORATORY

BNL-107612-2015-IR

Depth-dependent Vertical-to-Horizontal (V/H) Ratios of Free-Field Ground Motion Response Spectra for Deeply Embedded nuclear Structures

X. Wei, M. Miranda, M.E. Rosario,
C.J. Costantino, J. Braverman

February 2015

Nuclear Science & Technology Department

Brookhaven National Laboratory

U.S. Nuclear Regulatory Commission
Office of New Reactors

DISCLAIMER

BNL-107612-2015-IR

Depth-dependent Vertical-to-Horizontal (V/H) Ratios of Free-Field Ground Motion Response Spectra for Deeply Embedded Nuclear Structures

X. Wei[1], M. Miranda[2], M. E. Rosario[3], C. J. Costantino[4], and J. Braverman[5]

[1]Currently at WSP Group, [2]Currently Assistant Professor at Hofstra University,
[3]Visiting Research Associate at BNL from University of Puerto Rico at Mayaguez,
[4]C.J. Costantino and Associates, [5]Brookhaven National Laboratory

February 25, 2015

Nuclear Science and Technology Department
Brookhaven National Laboratory

Prepared for
Office of New Reactors
U.S. Nuclear Regulatory Commission

Abstract

This report documents the results of a study to determine the depth-dependent V/H ratios of ground motion response spectra in the free field. The V/H ratios reported herein were developed from a worldwide database of surface and downhole acceleration recordings obtained from 45 vertical array stations. This database was specifically compiled for this project, and includes information from a diversity of active tectonic regions (California, Alaska, Taiwan, Japan), site conditions (rock to soft soil), ground motion intensity levels (PGAs between 0.01 g and 0.50 g), magnitudes (between ML 2.78 and JMA 8.1), epicentral distances (between 3.2 km and 812 km), and source depths (between 1.2 km and 112 km), as well as sensors at surface and at a wide range of depths relevant to the project.

To study the significance of the depth effect, V/H ratios from all the records were sorted into a number of depth bins relevant to the project, and statistics (average, standard deviation, coefficient of variation, 16th, 50th, and 84th percentiles) of the V/H ratios within each bin were computed. Similar analyses were repeated, controlling for different site conditions, ground motion intensity levels, array locations, and source depths, to study their relative effect on the V/H ratios.

Our findings confirm the importance of the depth effect on the V/H ratios. The research findings in this report can be used to provide guidance on the significance of the depth effect, and the extent to which this effect should be considered in the seismic design of deeply embedded SMR structures and NPP structures in general.

Table of Contents

List of Tables

List of Figures

1. Introduction

1.1 Background

In the seismic design of nuclear power plant (NPP) structures, the vertical ground motion response spectra (RS) are typically developed by multiplying the horizontal ground motion RS with empirically-based, frequency-dependent, vertical-to-horizontal (V/H) spectral ratios. Since conventional NPP structures normally have shallow foundations (embedment less than 40 ft), the U.S. Nuclear Regulatory Commission (NRC) accepts the use of surface V/H ratios for such structures. Any uncertainties in the design ground motions, including uncertainties associated with the depth-dependence of the V/H ratios, are judged to be compensated by the conservatism of the Soil Structure Interaction (SSI) analysis methodology typically followed in the site-specific seismic design of NPP structures.

In recent years, several Small Modular Reactor (SMR) designs have been submitted to the NRC for review and licensing approval. Currently proposed SMR structures are deeply embedded as much as 140 ft from the ground surface, which is substantially deeper than the aforementioned shallow foundations of conventional NPP structures.

A review of the literature could only find a small number of studies performed to investigate the depth-dependence of the V/H ratios [1, 2]. It should also be noted that these studies were based on a relatively limited number of acceleration recordings from vertical (downhole) seismic arrays. Nevertheless, these studies indicate that the extrapolation of surface V/H ratios to significantly greater depths may not be conservative in the frequency range of interest to the seismic design of SMR structures.

1.2 Objective

The objective of this project is to develop depth-dependent V/H ratios of ground motion RS in the free field, based on available downhole acceleration recordings from a number of vertical arrays that have been instrumented to date. These depth-dependent V/H ratios may then be used to characterize vertical motions in the seismic design of deeply embedded SMR structures.

The research results can also be used to provide guidance on the significance of the depth effect, and the extent to which this effect should be considered in the seismic design of NPP structures.

It should be emphasized that all recorded downhole acceleration records correspond to in-column motions in the free field. It follows that any depth-dependent V/H ratios derived from such records must also correspond to in-column motions, as opposed to outcrop motions. This important distinction should be taken into consideration in any application of empirically-based, depth-dependent V/H ratios used for seismic design purposes.

1.3 Approach

The V/H ratios reported herein were developed from a worldwide database of surface and downhole acceleration recordings obtained from a number of vertical array stations. This database was specifically compiled for this project, and includes information from a diversity of

active tectonic regions, site conditions, ground motion intensity levels, earthquake magnitudes, epicentral distances, and sensors located at the ground surface and at a wide range of depths of interest to the project.

Each acceleration record at the surface and at depth includes three components: two horizontal and one vertical. For each acceleration record component, the corresponding 5% damped response spectrum (RS) was calculated; the average horizontal RS was then computed as the geometric mean of the RS of the two horizontal components. Finally, the frequency-dependent V/H ratios at the surface or at depth were calculated by dividing the vertical RS by the average horizontal RS.

Distinct V/H ratios were calculated for each acceleration record set at the surface and at depth, for each seismic event recorded at a given array.

To study the significance of the depth effect, V/H ratios from all the records were sorted into several depth bins, and statistics (average, standard deviation, coefficient of variation, 16^{th}, 50^{th}, and 84^{th} percentiles) of the V/H ratios within each bin were estimated. Similar analyses were repeated, controlling for different site conditions, ground motion intensity levels, array locations, and source depths, to study their relative effects on the V/H ratios.

It should be noted that the same seismic event may be recorded at several array stations. Since accelerations recorded at different arrays, but corresponding to the same event, tend to have noticeable differences in amplitude and frequency content (due to differences in source-to-site paths, local site conditions, etc.) they are considered to originate form separate “events” for the purposes of the database. Statistical bias may be introduced by this approach if the same event is recorded by two arrays that have similar site conditions and are located relatively close to each other. Only 6 (out of 267) database events are judged to fall in this category, however, so that any such bias is likely to be very small.

2. Collection of Vertical Seismic Array Data

2.1 Data Sources

The study is based on downhole recordings in the free field with maximum surface peak ground accelerations (PGA) of at least 0.01 g, and sensor depths ranging from near the surface to more than 300 ft below grade.

To collect as many downhole recordings as possible, the authors performed an exhaustive search of electronic databases accessible through the internet, and contacted well-known researchers and private consultants. Major databases and institutions inquired include the following: Center for Engineering Strong Motion Data (CESMD) of the California Geological Survey (CGS), California Strong Motion Instrumentation Program (CSMIP); National Strong-Motion Project (NSMP), U.S. Geological Survey (USGS); COSMOS Virtual Data Center; Pacific Earthquake Engineering Research (PEER) Center at the University of California, Berkeley; Pacific Engineering and Analysis, Inc.; Network for Earthquake Engineering Simulation at the University of California, Santa Barbara (NEES at UCSB); Southern California Earthquake

Center (SCEC) at the University of Southern California; Northeastern University; KiK-net, Japan; Building Research Institute (BRI), Japan; Institute of Engineering Seismology and Earthquake Engineering, Institute of Earth Sciences (IES) at the Academia Sinica, Taiwan; and National Central University (NCU) of Taiwan.

Recordings meeting the project requirements (e.g., minimum PGA of 0.01 g, recordings away from the influence of adjacent large/heavy structures, available site shear wave velocity, and available soil information) were obtained from the online data repositories of CGS-CESMD [3], USGS-NSMP [4], and NEES at UCSB [5]. In addition, researchers at BRI and NCU provided data from vertical arrays in Japan [6] and Taiwan [7], respectively, as well as corresponding site information.

2.2 Data Summary

2.2.1 Array Stations

The data used in this study were recorded at 45 different array stations located in California; Anchorage, Alaska; the Sendai District in Japan; and the Taipei Basin in Taiwan. Figure 1 shows a map of the different array stations considered. A summary of available information for each array station is provided in Table 1, which includes array station code, name, sensor depths, free field information, and local site information and site classification.

Sensor depths range from near the surface down to 1644 ft, although the study focuses primarily on depths representative of deeply embedded SMR designs; i.e. 0 to 200 ft. Records for depths greater than 200 ft were included to illustrate trends in depth variation.

As indicated by the free field information in Table 1, all records were obtained from array stations that were judged to be representative of the free field; i.e., located sufficiently far away from adjacent heavy structures (e.g., dams).

Local site information, including a majority of shear wave velocity profiles, was obtained from the referenced data repositories, for the arrays located in California and Alaska, and from research reports for the arrays located in Japan and Taiwan.

Shear wave velocity profiles of 6 (out of 45) arrays could not be obtained. These arrays are: Alameda-Posey & Webster, Crockett-Carquinez Bridge #2, Vallejo-Highway 37/Napa River East, Seven Oaks Dam Downstream Array, and Superstition Mountain Peak in California; and Water Conservancy Bureau in Panchiao, Taiwan.

The Vs30 parameter shown in Table 1 for each array station corresponds to the average shear wave velocity of the rock or soil layers in the top 30 m at the site (equivalent-travel time). This parameter was obtained directly from the data repositories or was computed from the available shear wave velocity profiles. In only two cases, Vs30 was extrapolated from shear wave velocity profiles available for the vicinity of the site (Vs30 for Crockett-Carquinez Bridge #2 was assumed to be similar to Crockett-Carquinez Bridge #1 since the two stations are located 500 ft apart in relatively flat terrain; Vs30 for Water Conservancy Bureau, Panchiao, Taiwan, was estimated from geotechnical studies of the Taipei basin [8,9]).

In Table 1, local site conditions at each array station are categorized as rock (class B), soft rock or very dense soil (class C), stiff soil (class D), or soft soil (class E), according to the site classification defined in the well-known NEHRP provisions [10], which depends on the parameter Vs30. The full NEHRP site classification as a function of Vs30 is reproduced in Table 3. The number of arrays located in class B, C, D, and E sites are 2, 11, 28, and 4, respectively.

Since soft soil (class E) sites are unlikely to be considered for NPP construction, the V/H ratios obtained from arrays in class E sites are provided only for the purpose of illustrating the trends in variation with respect to site conditions.

In some cases, even stiff soil (class D) sites may not be considered suitable for NPPs since the definition of competent foundation material for such structures is associated with a shear wave velocity of 1000 ft/s (305 m/s), which is in the middle of the Vs30 range for class D. Furthermore, a site classification more appropriate to deeply embedded SMRs would need to consider the average shear wave velocity of the layers in the top 60 m, rather than 30 m, at the site.

Therefore, for class D sites only, an additional sub-classification was implemented in this study in the following manner. First, a parameter Vs60 was defined as the average shear wave velocity of the rock or soil layers in the top 60 m at the site. If Vs60 is greater than approximately 350 m/s, the site was classified as D1. If Vs60 is less than approximately 250 m/s, the site was classified as D3. All remaining sites that are not D1 or D3 were classified as D2. The number of arrays in class D1, D2, and D3 sites are 13, 5, and 10, respectively, and are designated in Table 1 in parenthesis after the main site classification.

In light of the above discussions, the study focuses on V/H ratios obtained from arrays in class B, C, and D1 sites.

2.2.2 Acceleration Records

Over 300 sets of downhole acceleration records from different seismic events recorded at the 45 vertical array stations were collected and processed as part of this study. V/H ratios were calculated and plotted for all these records. An initial review of the V/H ratio plots resulted in the elimination of several sets of records because of obvious data errors. In addition, as discussed in the BRI report [6], several Japanese records are not reliable at frequencies below approximately 0.3 Hz because of the small amplitudes of components in the low frequency range. Based on the reliable frequency range recommended in the BRI report, as well as to avoid any numerical artifacts from the data processing or filtering, the RS used in the calculation of all the V/H ratios were all truncated below 0.5 Hz.

A total of 267 sets of downhole records were utilized in the final calculations reported herein. Since each set has records at two or more depths, the 267 sets result in 965 individual records at surface or at depth.

Table 2 provides detailed information of the 267 sets of records, including: data source; name and code of the array station; and seismic event information, including event name or ID, recording date and time, maximum surface PGA, magnitude, epicentral distance, and source

depth. It is noted that the maximum surface PGA is the maximum peak ground acceleration of the three components recorded at the surface.

The number of records obtained from arrays in class B, C, D1, D2, D3, and E sites are 37, 187, 297, 110, 269, and 65, respectively (a total of 965).

The data used in this study was recorded between 1987 and 2012. The 125 sets of records from the U.S. are fairly new, with 90% recorded within the last 10 years, 50% recorded within the last 5 years, and the latest one recorded near the end of 2012. The 20 sets of records from Taiwan were recorded between 1994 and 1999, and the 122 sets of records from Japan were recorded between 1987 and 1998.

The magnitudes of the earthquakes shown in Table 2 are given in different scales; i.e., ML, Mw and JMA. Unit conversion was not performed because these scales are relatively similar in the range of magnitudes being considered in this study. Additional accuracy was not warranted because dependence on magnitude was not directly investigated. Magnitudes range between ML 2.78 and JMA 8.1.

Earthquake source depths range between 1.2 km and 112 km. About 50% of the records correspond to earthquakes with source depths less than or equal to 14 km, and about 80% of the records correspond to earthquakes with source depths less than 70 km, which means that the majority of the records correspond to “shallow-focus” earthquakes. Epicentral distances range between 3.2 km and 812 km; the percentages of records that correspond to epicentral distances less than 15 km, 50 km, and 150 km are about 27%, 49%, and 80%, respectively.

The largest PGA shown in Table 2 is 0.49 g, recorded at the Los Angeles-La Cienega array during the 2001 West Hollywood earthquake. Of the 267 sets of records, about 50% have PGAs less than 0.032 g, and about 87% have PGAs less than 0.10 g.

In summary, as shown in Table 1 and Table 2, the records utilized in this study cover a diversity of active tectonic regions, site conditions, ground motion intensity levels, magnitudes, epicentral distances, and sensors at the surface and at a wide range of depths relevant to the project.

3. Analysis of Vertical Seismic Array Data

3.1 Data Analysis

As outlined in Section 1.3, each seismic event recorded at a given array generates acceleration records at or close to the surface, as well as at the various depths where the seismometers (sensors) of the array are embedded. Each acceleration record at the surface or at depth includes three components: two horizontal and one vertical. For each acceleration record component, the RS at 5% damping was calculated; then, the average horizontal RS was computed as the geometric mean of the RS of the two horizontal components, using the equation given below.

$$RS_{hor.ave.} = \sqrt{a_{hor.1} \cdot a_{hor.2}}$$

Finally, the frequency-dependent V/H ratios at the surface or at depth were calculated by dividing the vertical RS by the average horizontal RS.

As mentioned in the prior section, a total of 267 sets of downhole records were utilized in the final calculations reported herein. Since each set has records at two or more depths, the 267 sets result in 965 individual records at surface or at depth. Distinct V/H ratios were computed for each of these 965 individual records.

To study the significance of the depth effect, V/H ratios from the records were sorted into several depth bins, and statistics (average, standard deviation, coefficient of variation, 16^{th}, 50^{th}, and 84^{th} percentiles) of the ratios within each bin were estimated. Similar analyses were repeated, controlling for different site conditions, ground motion intensity levels, array locations, and source depths, to study their relative effects on the V/H ratios.

3.2 Analysis Results and Findings

3.2.1 Depth Effect

The following bins were defined to study the depth effect: (1) depth 0-7 ft below grade (this bin is treated as representative of the surface); (2) depth 7-50 ft below grade; (3) depth 50-100 ft below grade; (4) depth 100-150 ft below grade; (5) depth 150-200 ft below grade; (6) depth 200-300 ft below grade; and (7) depths greater than 300 ft below grade.

Only V/H ratios obtained from arrays in class B, C, and D1 sites were considered in the study of the depth effect. This reduced the total number of ratios from 965 to 521, which were distributed in the seven depth bins as follows: 154, 71, 81, 65, 62, 57, and 31, from the shallowest to the deepest. Table 4 provides more detailed on how the data is distributed in terms of depth bins and site classes.

Statistics (average, standard deviation, coefficient of variation, 16^{th}, 50^{th}, and 84^{th} percentiles) of the V/H ratios within each depth bin were estimated using standard techniques. In addition, normalized average V/H ratios for the six deeper bins were calculated by dividing their average V/H ratios by the average V/H ratios of the 0-7 ft bin. This information is presented in Figures 2 through 5.

As shown in Figure 2 (top), all average V/H ratios for the various depth bins are less than 1.0, with the exception of ratios for the depth bin >300 ft, which has a peak of approximately 1.17 at 1.2 Hz. This peak is mainly due to data from Japan. Depths greater than 300 ft, however, are beyond the range of interest for this study.

Figure 2 (bottom) shows the normalized average V/H ratios corresponding to the six deeper bins. This plot is used to illustrate how the frequency-dependent variation of the average V/H ratios at depth differs from that at the surface. The plot shows that, for most frequencies below approximately 10 Hz, the average V/H ratios at depth are greater than the average V/H ratios at the surface. In the frequency range of 1 to 6 Hz, the average V/H ratios at depth may be up to two times the average V/H ratios at the surface. With the increase of depth, the peak of the

normalized average V/H ratios increase in magnitude and shift to the lower frequencies. For the depth bin 150-200 ft, which is of most interest for the seismic design of deeply embedded SMR structures, the average V/H ratios are between 1.2 and 1.9 times the average V/H ratios at the surface in the frequency range of 1 to 6 Hz, and about the same at frequencies above 10 Hz.

The depth effect illustrated in Figure 2 is generally consistent with previous findings by Darragh et al. [1], which were based on only 59 sets of records from 10 vertical arrays. The present findings also provide further validation to the explanation by Beresnev et al. [2], who indicate that the vertical component of ground motion increases with depth at low frequencies (below about 10 Hz) where SV waves dominate, but not at high frequencies (above about 10 Hz) where P waves dominate.

3.2.2 Site Condition Effect

To study the effect of site conditions on the average V/H ratios at depth, the analysis discussed in the preceding Section 3.2.1 was repeated, independently, for the V/H ratios obtained from arrays in class B and C (combined), D1, D2, D3, D (D1, D2, and D3 combined), and E sites. The total number of ratios obtained from arrays in class B and C, D1, D2, D3, D, and E sites is 224, 297, 110, 269, 676, and 65, respectively. Table 4 provides more detailed information on how the data is distributed in terms of depth bins and site classes.

Figures 6 through 17 show average V/H ratios and normalized average V/H ratios computed for the various site conditions indicated above. Coefficients of variation and percentiles are not provided because, in several instances, the number of data in the depth bins is insufficient to yield meaningful statistics. In this regard, we note the following: in Figures 10 and 11 (class D2 sites), depth bin 7-50 ft has only 3 ratios and depth bin 150-200 ft has only 6 ratios; in Figures 12 and 13 (class D3 sites), depth bin 100-150 ft has only 6 ratios; and in Figures 16 and 17 (class E sites), depth bin 7-50 ft has only 5 ratios, depth bin 100-150 ft has only 6 ratios, depth bin 150-200 ft has only 2 ratios, and depth bin >300 ft has only 6 ratios. The reader is cautioned that the average V/H ratios computed for such small sample sizes are probably lacking in statistical power; nevertheless, they are shown in the figures to illustrate trends and for completeness.

Comparisons of the normalized average V/H ratios for the different site classes indicate that, with the decrease in site stiffness, from rock to soft soil, the ratio of the average V/H ratios at depth relative to the ratios at the surface tends to increase, for most frequencies below approximately 10 Hz. In the frequency range of 1 to 6 Hz, the average V/H ratios at depth may be up to 2.0, 2.5, and 3.9 times the average V/H ratios at the surface for site classes B and C, D, and E, respectively.

3.2.3 Ground Motion Intensity Effect

To study the effect of ground motion intensity on the average V/H ratios at depth, the analysis discussed in the preceding sections was repeated, independently, for the V/H ratios obtained from events with PGAs in the ranges 0.01-0.10 g, 0.10-0.20 g, 0.20-0.50 g, and 0.10-0.50 g (0.10-0.20g and 0.20-0.50 g combined), from arrays in class B, C, and D1 sites only. The total

number of ratios obtained from events with PGA ranges 0.01-0.10 g, 0.10-0.20 g, 0.20-0.50 g, and 0.10-0.50 g is 466, 30, 25, and 55, respectively. Table 5 provides more detailed information on how the data is distributed in terms of depth bins and PGA ranges.

Figures 18 through 25 show average V/H ratios and normalized average V/H ratios computed for the various PGA ranges indicated above. Coefficients of variation and percentiles are not provided because, for PGAs above 0.10 g, the number of data in the depth bins is insufficient to yield meaningful statistics. In this regard, we note the following: in Figures 20 and 21 (PGA range 0.10-0.20 g), 6 out of 7 depth bins have 6 or fewer ratios, and 2 bins have only 2 ratios; in Figures 22 and 23 (PGA range 0.20-0.50 g), 6 out of 7 depth bins have 6 or fewer ratios, and 2 bins have only 1 ratio; and in Figures 24 and 25 (PGA range 0.10-0.50 g), 4 out of 7 depth bins have 7 or fewer ratios. As indicated for previous cases, the reader is cautioned that the average V/H ratios computed for such small sample sizes are probably lacking in statistical power; they are shown in the figures to illustrate trends and for completeness.

Direct comparisons of average V/H ratios and normalized average V/H ratios, for PGAs below 0.10 g (Figure 18) and above 0.10 g (Figure 24), are difficult because of the small sample sizes used to compute the latter. Comparisons between the data for depth bins 0-7 ft, 7-50 ft, 50-100 ft, and 200-300 ft, all of which have at least 7 ratios, indicate a moderate increase of between 10% and 20% in the normalized average V/H ratios for PGAs above 0.10 g relative to those below 0.10 g, in the frequency range of 1 to 6 Hz.

The differences identified above may suggest a possible trend but are not conclusive. To obtain more definitive results, it is necessary to obtain a substantial amount of additional records from events with PGAs greater than 0.10 g from arrays in class B, C, and D1 sites. It is noted again that 87% of the 267 sets of records compiled for this study have PGAs less than 0.10 g.

3.2.4 Array Location Effect

To study the effect of array location on the average V/H ratios at depth, the data from arrays in class B, C, and D sites was separated into five array location groups: CGS-CESMD and USGS-NSMP sites in California; NEES at UCSB sites in California; NEES at UCSB site in Anchorage, Alaska; sites in the Sendai District, Japan; and sites in the Taipei Basin, Taiwan. Table 6 provides detailed information on how the data is distributed in terms of depth bins and array locations.

Figures 26 through 35 show average V/H ratios and normalized average V/H ratios computed for the various array locations indicated above. A review of these figures indicates that the normalized average V/H ratios generally follow the same depth-dependent trends identified in Section 3.2.1 for the overall results (illustrated in Figure 2, bottom). In other words, there does not appear to be any location-specific characteristic that leads to significant deviations from the overall results for normalized average V/H ratios, as discussed in Section 3.2.1.

However, Figures 28 and 29 (NEES at UCSB sites in California) show average V/H ratios significantly greater than 1.0 for the depth bin 0-7 ft, in frequency range of 20 to 30 Hz. This does deviate from the overall results shown in Figure 2 (top), where average V/H ratios are less

than 1.0 for all depth bins except for a small peak of 1.17 at a frequency of approximately 1.2 Hz, for the depth bin >300 ft. Similarly, Figures 30 and 31 (NEES at UCSB site in Anchorage, Alaska) show average V/H ratios significantly greater than 1.0 for depth bins 0-7 ft, 7-50 ft, and 200-300 ft, in the frequency range of 8 to 30 Hz. It should be noted that these large averages appear to be caused by a relatively small number of V/H ratios and do not have an impact on normalized average V/H ratios.

The deviations described above may be due to events with relatively small epicentral distances. As indicated in NUREG 6728 [11], ground motions from events with near-source distances (less than 15 km) tend to have vertical components that exceed the horizontal components at high frequencies. The average epicentral distance of events used in the study is: 60 km for CGS-CESMD and USGS-NSMP sites in California; 26 km for NEES at UCSB sites in California; 34 km for NEES at UCSB site in Anchorage, Alaska; 163 km for sites in the Sendai District, Japan; and 77 km for sites in the Taipei Basin, Taiwan. This suggests that the impact of small epicentral distances is probably significant only for the average results from NEES at UCSB sites in California (average epicentral distance 26 km) and Anchorage, Alaska (average epicentral distance 34 km), which is in agreement with the data shown in Figures 26 through 35.

Additional research is necessary to investigate the relative impact of small epicentral distances on the overall trends discussed in Section 3.2.1. The epicentral distances of all events used in the study are listed in Table 2. Approximately 27% of all events correspond to epicentral distances of 15 km or less.

3.2.5 Source Depth Effect

To study the effect of earthquake source depth on the V/H ratios, the data from the NEES at UCSB site in Anchorage, Alaska, was separated into two source depth ranges: 0-40 km and 40-70 km. Figures 36 and 37 show average V/H ratios and normalized average V/H ratios computed for the two depth ranges. A comparison of the two figures indicates that source depth has a moderate effect on average V/H ratios and a relatively minor effect on normalized average V/H ratios, for all depth bins considered.

The comparison also indicates that the large average V/H ratios at high frequencies noted in Section 3.2.4 tend to be more pronounced for the 0-40 km depth range. The reason for this trend may really be due to the effect of small epicentral distances since, for this particular array, events with source depths in the 0-40 km range also have an average epicentral distance of 18 km, which is close to the near-source distance of 15 km. In contrast, events with source depths in the 40-70 km range have an average epicentral distance of 44 km.

The source depths of all events used in the study are listed in Table 2. As discussed in previous sections, the source depths of all events used in the study range between 1.2 km and 112 km. About 50% of events correspond to source depths of 14 km or less, and about 80% of events correspond to source depths of 70 km or less, which means that the majority of the events correspond to “shallow-focus” earthquakes.

3.2.6 Comparison to V/H ratios defined in NUREG 6728 and RG 1.60

The 16th, 50th, and 84th percentiles of the V/H ratios obtained from all arrays in class B, C, and D1 sites, as discussed in Section 3.2.1, were compared to V/H ratios recommended by (a) NUREG 6728 for Western US soft rock (WUS-R) sites and PGAs less than 0.20 g; (b) NUREG 6728 for Central and Eastern US rock (CEUS-R) sites and PGAs less than 0.20 g; and (c) RG 1.60 [12]. These comparisons are illustrated in Figures 38 and 39 for each of the seven depth bins considered in the study. Recommendations for PGAs less than 0.20 g were used in light of the fact that 87% of the 267 sets of records compiled for this study have PGAs less than 0.10 g.

For the depth bin 0-7ft (i.e., at or close to the surface), it is observed that the frequency-dependent V/H ratios recommended by NUREG 6728 for WUS-R sites follow the shape of the 50th percentile curve reasonably closely, but are somewhat larger, for most frequencies between 0.5 and 50 Hz. The V/H ratios recommended by NUREG 6728 for CEUS-R sites and by RG 1.60 are substantially different, in terms of the shape of the curve, from the 50th percentile curve. This is to be expected since the data used to generate the 50th percentile curve corresponds to the same depth and similar site conditions, PGA, and tectonic settings as the data used as basis for the NUREG 6728 recommendations for WUS-R sites.

In contrast, for all of the depth bins below the surface, it is observed that the frequency-dependent V/H ratios recommended by NUREG 6728 or RG 1.60 do not resemble the shape of the 50th percentile curve. The discrepancies become more pronounced with increasing depth. For the depth bin 150-200 ft, which is of most interest for the seismic design of deeply embedded SMR structures, the 50th percentile curve exceeds the V/H ratios recommended by NUREG 6728 for WUS-R sites by a significant margin for frequencies below 7 Hz (by a factor of more than 2.0 at about 3 Hz). On the other hand, the V/H ratios recommended from RG 1.60 envelope the 50th percentile curve for all frequencies between 0.5 and 50 Hz; however, even this conservative recommendation is exceeded by the 84th percentile curve for frequencies below 6 Hz.

4. Conclusions

This study focused on the development of depth-dependent V/H ratios of ground motion response spectra in the free field. The V/H ratios reported herein were developed from a worldwide database of surface and downhole acceleration recordings obtained from 45 vertical array stations. This database was specifically compiled for this project, and includes information from a diversity of active tectonic regions (California, Alaska, Taiwan, Japan), site conditions (rock to soft soil), ground motion intensity levels (PGAs between 0.01 g and 0.50 g), magnitudes (between ML 2.78 and JMA 8.1), epicentral distances (between 3.2 km and 812 km), and source depths (between 1.2 km and 112 km), as well as sensors at surface and at a wide range of depths relevant to the project.

A total of 267 sets of downhole records were utilized in the final calculations. Since each set has records at two or more depths, the 267 sets result in 965 individual records at surface or at depth.

To study the significance of the depth effect, V/H ratios from all the records were sorted into seven depth bins relevant to the project, and statistics (average, standard deviation, coefficient of variation, 16th, 50th, and 84th percentiles) of the V/H ratios within each bin were computed. Similar analyses were repeated, controlling for different site conditions, ground motion intensity levels, array locations, and source depths, to study their relative effect on the V/H ratios. Only V/H ratios obtained from arrays in NEHRP class B, C, and a subset of D (designated as D1) sites were considered in the study of the depth effect and the ground motion intensity effect.

Our findings confirm the importance of the depth effect on the average V/H ratios. For most frequencies below approximately 10 Hz, the average V/H ratios at depth are significantly greater than the average V/H ratios at the surface. In the frequency range of 1 to 6 Hz, the average V/H ratios at depth may be up to two times the average V/H ratios at the surface. With the increase of depth, the peak of the normalized average V/H ratios seems to increase in magnitude and shift to the lower frequencies. For the depth bin 150-200 ft, which is of most interest for the seismic design of deeply embedded SMR structures, the average V/H ratios are between 1.2 and 1.9 times the average V/H ratios at the surface in the frequency range of 1 to 6 Hz, and about the same at frequencies above 10 Hz.

Comparisons of average V/H ratios for different site conditions indicate that, with the decrease in site stiffness from rock to soft soil, the normalized average V/H ratios tends to increase for most frequencies below approximately 10 Hz. In the frequency range of 1 to 6 Hz, the average V/H ratios at depth may be up to 2.0, 2.5, and 3.9 times the average V/H ratios at the surface for NEHRP class B and C, D, and E sites, respectively.

Direct comparisons of average V/H ratios for PGAs below 0.10 g and above 0.10 g are difficult because of the relative scarcity of records for the latter case. Limited comparisons indicate a moderate increase of between 10% and 20% in the normalized average V/H ratios in the frequency range of 1 to 6 Hz, for PGAs above 0.10 g relative to those below 0.10 g. These differences suggest a possible trend but are not conclusive. To obtain more definitive results, it is necessary to obtain a substantial amount of additional records from events with PGA greater than 0.10 g. It is noted that 87% of the records compiled for this study have PGA less than 0.10 g.

Comparisons of average V/H ratios for different array locations and source depths reveal a small to moderate effect on the average V/H ratios in the frequency range of 8 to 30 Hz, which appears to be linked to a number of events with small epicentral distances recorded at NEES at UCSB sites in California and Alaska. It has been previously observed (see, e.g., NUREG 6728) that ground motions from events with near-source distances (less than 15 km) tend to have vertical components that exceed the horizontal components at high frequencies. Additional research is needed to investigate the relative impact of small epicentral distances on the overall trends identified in this study. It is noted that 27% of the records compiled for this study correspond to epicentral distances of 15 km or less.

The 16th, 50th, and 84th percentiles of the V/H ratios used to study the depth effect were compared to V/H ratios recommended by (a) NUREG 6728 for WUS-R sites (PGA less than 0.20 g); (b) NUREG 6728 for CEUS-R sites (PGA less than 0.20 g); and (c) RG 1.60.

For the depth bin closest to the surface, the V/H ratios recommended by NUREG 6728 for WUS-R sites were found to be somewhat larger but generally following the shape of the 50th percentile curve, for most frequencies between 0.5 and 50 Hz. In contrast, the V/H ratios recommended by NUREG 6728 for CEUS-R sites and by RG 1.60, in terms of the shape of the curves, were found to differ significantly from the 50th percentile curve. This is to be expected since the data used to generate the 50th percentile curve is similar to the data used as basis for the NUREG 6728 recommendations for WUS-R sites.

For the depth bins below the surface, the V/H ratios recommended by NUREG 6728 and RG 1.60 were all found to differ significantly from the shape of the 50th percentile curve. This difference becomes more pronounced with increasing depth. For the depth bin 150-200 ft, which is of most interest for the seismic design of deeply embedded SMR structures, the 50th percentile curve exceeds the V/H ratios recommended by NUREG 6728 for WUS-R sites by a large margin for frequencies below 7 Hz (by a factor of more than 2.0 at about 3 Hz).

It is important to mention that the V/H ratios recommended from RG 1.60 do provide a conservative envelope of the 50th percentile curve for all depth bins from the surface down to the 150 - 200 ft bin, which is the region of interest for the deeply embedded SMR structures. However, the V/H ratios recommended from RG 1.60 are exceeded by the 84th percentile curve at some frequency range for all depth bins.

The research findings summarized above can be used to provide guidance on the significance of the depth effect, and the extent to which this effect should be considered in the seismic design of deeply embedded SMR structures and NPP structures in general.

Finally, the authors emphasize that all downhole acceleration records used in this study correspond to in-column motions in the free field. It follows that any depth-dependent V/H ratios derived from such records must also correspond to in-column motions, as opposed to outcrop motions. This important distinction should be taken into consideration in any application of empirically-based, depth-dependent V/H ratios used for seismic design purposes.

Acknowledgement

This study was supported by the U.S. Nuclear Regulatory Commission, Office of New Reactors.

We gratefully acknowledge the following researchers for their generous support with the data collection: Dr. J. H. Steidl of the University of California, Santa Barbara; Prof. K-L. Wen and Mr. J-Y. Huang of the National Central University of Taiwan; and Mr. Toshihide Kashima of the International Institute of Seismology and Earthquake Engineering, Japan.

References

[1] Darragh, R., W. Silva, and N. Gregor, “Bay Bridge Downhole Array Analyses.” Final Report submitted to Earth Mechanics, Inc., Pacific Engineering and Analysis, 1999.

[2] Beresnev, I.A., A. M. Nightengale, and W. J. Silva, “Properties of Vertical Ground Motions.” Bulletin of the Seismological Society of America, Vol. 92, No.8, pp. 3152-3164, 2002.

[3] California Strong Motion Instrumentation Program, California Geological Survey. Data repository available online at http://www.strongmotioncenter.org/

[4] National Strong Motion Project, U.S. Geological Survey. Data repository available online at http://nsmp.wr.usgs.gov/

[5] Network for Earthquake Engineering Simulation at the University of California, Santa Barbara. Data repository available online at http://www.nees.ucsb.edu/

[6] Sendai Dense Array Earthquake Observation, General Report, Building Research Institute and Japan Association for Building Research Promotion, December, 1999. Partial data repository (digital data for surface accelerations only) available online at http://smo.kenken.go.jp/smdb

[7] Taipei Basin Downhole Seismic Network, Institute of Earth Sciences, Academia Sinica, Taiwan. Descriptive information (no digital data) available online at http://www.earth.sinica.edu.tw/~smdmc

[8] Wang, C-Y., Y-H. Lee, M-L. Ger, and Y-L. Chen, “Investigating Subsurface Structures and P and S wave Velocities in the Taipei Basin.” Terrestrial, Atmospheric and Oceanic Sciences, Vol. 15, No. 4, pp. 609-627, 2004.

[9] Huang, W-G., B-S. Huang, J-H. Wang, K-C. Chen, K-L. Wen, S-J. Tsao, Y-C. Hsieh, and C-H. Chen, “Seismic observations in the Taipei metropolitan area using the downhole network.” Terrestrial, Atmospheric and Oceanic Sciences, Vol. 21, No. 3, pp. 615-625, 2010.

[10] BSSC, “NEHRP Recommended Provisions for Seismic Regulations for New Buildings and Other Structures (FEMA 450).” Building Seismic Safety Council, National Institute of Building Sciences, 2004.

[11] McGuire, R.K., W.J. Silva, and C. J. Costantino, “NUREG/CR-6728 Technical Basis for Revision of Regulatory Guidance on Design Ground Motions: Hazard and Risk Consistent Ground Motion Spectra Guidelines.” Report to the U.S. Nuclear Regulatory Commission, 2001.

[12] U.S. NRC, “Regulatory Guide 1.60: Design Response Spectra of Nuclear Power Plants.” U.S. Nuclear Regulatory Commission, 1973.

Table 1 List of Vertical Array Stations

CGS-CSMIP (California Strong Motion Instrumentation Program)

Station Code	Station	Sensor Depths	Free Field Information	Site Geology	V_s Profile	V_{s30} (m/s, appr.)	Site Class
1794	El Centro - Meloland	0, 30, 100, 185 m (0, 99, 330, 640 ft)	140 ft from a bridge abutment, 62 ft from a highway	Deep alluvium	Yes	186	D (D3)
3192	San Diego - Coronado East	0, 13, 30, 91 m (0, 42, 97, 300 ft)	close to a bridge pier and two story building	Shallow alluvium over soft rock (sandstone)	Yes	280	D (D1)
3193	San Diego - Coronado West	0, 11.6, 22.9, 40.1, 103 m (0, 38, 75, 138, 358 ft)	100 ft from a bridge pier	Thin fill/alluvium over soft rock (sandstone)	Yes	210	D (D2)
13186	Corona - I15/Hwy 91	0, 7.9, 21.6, 41.8 m (0, 28, 71, 137 ft)	about 100 ft from bridge piers, 20 ft from a highway	Shallow alluvium over rock (granodiorite)	Yes	280	D (D1)
14783	Los Angeles - Vincent Thomas W1	0, 30, 91 m (0, 100, 300 ft)	about 120 ft from a bridge pier	Deep alluvium	Yes	200	D (D3)
14784	Los Angeles - Vincent Thomas W2	0, 15, 30 m (0, 50, 100 ft)	about 120 ft from a bridge pier	Deep alluvium	Yes	179	E
14786	Los Angeles - Vincent Thomas West	0, 30, 91 m (0, 100, 300 ft)	about 120 ft from a bridge pier	Deep alluvium	Yes	200	D (D3)
23792	San Bernardino - I10/215 W	0, 10.7, 35, 92.1 m (0, 35, 115, 302 ft)	100 ft from a bridge pier	Deep alluvium	Yes	271	D (D1)
24400	Los Angeles - Obregon Park	0, 69.5 m (0, 228 ft)	close to one story building	Deep alluvium over rock (sandstone)	Yes	349	D (D1)
24703	Los Angeles - La Cienega	0, 18, 100, 252 m (0, 60, 330, 827 ft)	next to highways	Deep alluvium	Yes	260	D (D2)
24764	Tarzana - Cedar Hill B	0, 60 m, (0, 197 ft)	close to single family houses	Thin alluvium over shale	Yes	411	C
36520	Parkfield - Turkey Flat #2	0, 11, 23 m (0, 35, 77 ft)	free field	Shallow alluvium over rock (sandstone)	Yes	492	C
36529	Parkfield - Turkey Flat #1	0, 24 m (0, 79 ft)	free field	Rock (sandstone)	Yes	907	B
58137	Alameda - Posey & Webster	0, 5.2, 12.2, 36.6 m (0, 17, 40, 120 ft)	free field	Deep alluvium	No	208	D (D3)
58204	Oakland - Bay Bridge	0, 17, 46, 91, 162 m (0, 56, 150, 299, 530 ft)	50 ft from a bridge pier	Alluvium (fill)	Yes	150	E
58642	Treasure Island	0, 7, 16, 31, 44, 104, 122 m (0, 24, 51, 102, 145, 340, 400 ft)	close to a two story building	Shallow fill over deep alluvium (Bay mud)	Yes	150	E
58961	San Francisco - Bay Bridge	0, 14, 40 m (0, 46, 131 ft)	about 100 ft from bridge a bridge pier	Fill over shallow alluvium over soft rock	Yes	400	C
58964	Half Moon Bay - Tunitas	0, 5, 12, 45 m (0, 17 , 39, 147 ft)	next to a highway	Alluvium over soft rock (siltstone)	Yes	353	D (D1)
58968	Foster City - San Mateo Bridge	0, 17.7, 24, 38.3 m (0, 53, 72, 115 ft)	90 ft from a highway, 10 ft from a local road	Shallow alluvium over rock (chert/greenstone)	Yes	215	D (D1)
68206	Crockett - Carquinez Bridge #1	0, 45.7 m, (0, 150 ft)	about 50 ft from a bridge pier, 20 ft from a two story house	Shallow clay over rock (sed.)	Yes	340	D (D1)
68259	Crockett - Carquinez Bridge #2	0, 61, 125 m (0, 201, 410 ft)	20 ft from a bridge pier	Shallow clay over soft rock	No	340	D (D1)
68310	Vallejo - Hwy 37/Napa River East	0, 17.9, 44.5 m (0, 59, 146 ft)	50 ft from a bridge abutment	Bay mud	No	552	C
68323	Benicia - Martinez Bridge South	0, 11, 35 m (0, 36, 114 ft)	50 ft from a bridge pier	Thin alluvium over soft rock	Yes	500	C
89734	Eureka	0, 19, 33, 56, 136 m (0, 62, 109, 185, 446 ft)	10 ft from a highway	Deep alluvium	Yes	220	D (D2)

USGS-NSMP (National Strong-Motion Project)

Station Code	Station	Sensor Depths	Free Field Information	Site Geology	V_s Profile	V_{s30} (m/s, appr.)	Site Class
5300	Seven Oaks Dam Downstream Array, Redlands, CA	0, 16.2 m (0, 53 ft)	about 1500 ft from Seven Oaks Dam	Rock	No	685	C
286	Superstition Mtn. Pk., Imperial Valley, CA	0, 35.7 m (0, 117 ft)	free field		No	362	C

NEES at UCSB

Station Code	Station	Sensor Depths	Free Field Information	Site Geology	V_s Profile	V_{s30} (m/s, appr.)	Site Class
GVDA	Garner Valley Downhole Array, CA	0, 6, 15, 22, 50, 150, 501 m (0, 20, 49, 72, 164, 492, 1644 ft)	200 ft from highway and one story building	Alluvium (0-18 to 25 m) over rock (granite)	Yes	260	D (D1)
HEO	Hollister Earthquake Observatory, CA	0, 53 m (0, 174 ft)	free field at remote rock site (not the main site)	Rock (granite)	Yes	600	C
WLA	Wildlife Liquefaction Array, CA	0, 2.5, 5.5, 7.7, 30, 100 m (0, 8, 18, 25, 98, 328 ft)	free field	Silty clay (0-3 m), silty sand (3-7 m), clay (7-12 m)	Yes	200	D (D3)
8040	Delaney Park Downhole Array, Anchorage, AK	0, 4.6, 10.7, 18.3, 30.5, 45.4, 61 m (0, 15, 35, 60, 100, 150, 200 ft)	200 ft from two story building, 600 ft from high rise building	Soft clay (outwash [0-40 ft], transition [40-60 ft], bootlegger cove formation [60-160 ft]) over till	Yes	300	D (D1)

Taipei Basin Downhole Seismic Network, Institute of Earth Sciences, Academia Sinica, Taiwan (data from Prof. Wen Kuo-Liang)

Station Code	Station	Sensor Depths	Free Field Information	Site Geology	V_s Profile	V_{s30} (m/s, appr.)	Site Class
BS	Water Conservancy Bureau, Panchiao	0, 25, 59 m		Deep alluvium	No	200	D (D3)
SS	Songshan Tobacco Plant	0, 30, 49 m	away from large buildings	Deep alluvium, tertiary rock at 150 m depth	Yes	200	D (D3)
TF	Vocational Advisory Committee for Retired Servicemen, Panchiao	0, 60 m	in the backyard of a two story building	Deep alluvium, tertiary rock at 300 m depth	Yes	215	D (D3)
WK	Sewage Disposal Plant, Wuku	0, 30, 60 m	away from large buildings	Deep alluvium	Yes	200	D (D3)

Sendai Dense Array Earthquake Observation Project, Building Research Institute, Japan (data from Mr. Toshihide Kashima)

Station Code	Station	Sensor Depths	Free Field Information	Site Geology	V_s Profile	V_{s30} (m/s, appr.)	Site Class
MIYA	Miyagino	1, 22, 54 m	in elementary school, away from building	Alluvium (0-26 m) over sedimentary rock	Yes	443	C
NAGA	Nagamachi	1, 29, 81 m	in elementary school, away from building	Alluvium (0-57 m) over sedimentary rock	Yes	192	D (D2)
NAKA	Nakano	1, 30, 61 m	in elementary school, away from building	Alluvium (0-58 m) over sedimentary rock	Yes	183	D (D3)
OKIN	Okino	1, 17, 62 m	in elementary school, away from building	Alluvium (0-50 m) over sedimentary rock	Yes	267	D (D1)
ORID	Oridate	1, 57, 76 m	in elementary school, away from building	Soft sedimentary rock over andesite	Yes	460	C
SHIR	Shiromaru	1, 20, 76 m	in elementary school, away from building	Alluvium (0-50 m) over sedimentary rock	Yes	271	D (D1)
TAMA	Tamagawa	2, 11, 33 m	in junior high school, away from building	Sedimentary rock	Yes	739	C
TRGA	Tsurugaya	2, 37, 62 m	in elementary school, away from building	Sedimentary rock	Yes	816	B
TRMA	Tsurumaki	1, 25, 79 m	in elementary school, away from building	Alluvium (0-80 m) over sedimentary rock	Yes	177	E
TSUT	Tsutsujigaoka	1, 36, 59 m	in elementary school, away from building	Alluvium (0-5 m) over sedimentary rock	Yes	323	D (D1)
ARAH	Arahama	1, 31, 76 m	in elementary school, away from building	Alluvium (0-35 m) over sedimentary rock	Yes	189	D (D2)

Table 2 List of Acceleration Records

CGS-CSMIP (California Strong Motion Instrumentation Program)

Station Code	Station	Earthquake	Year	Month	Day	HRMN	Max. PGA (g)	Magnitude	Epicentral Dist. (km)	Source Depth (km)
1794	El Centro - Meloland	Calexico	2010	Apr	4		0.230	Mw 7.2	59.1	32.3
	"	Calexico	2010	May	22		0.032	Mw 4.9	35.1	5.4
	"	Ocotillo	2010	Apr	10		0.018	Mw 4.5	32.4	6.8
	"	Ocotillo	2010	Jun	14		0.033	ML 5.7	45.3	6.9
	"	Borrego Springs	2010	Jul	7		0.011	ML 5.4	120.7	14.0
3192	San Diego - Coronado East	San Clemente Island	2004	Jun	15		0.027	ML 5.2	75.1	7.0
3193	San Diego - Coronado West	San Clemente Island	2004	Jun	15		0.058	ML 5.2	73	7.0
	"	San Ysidro	2003	Oct	7		0.016	ML 3.6	15.8	16.4
	"	Chino Hills	2008	Jul	29		0.016	Mw 5.4	151.2	13.6
13186	Corona - I15/Hwy 91	Anza	2005	Jun	12		0.035	ML 5.2	98.8	13.5
	"	Chino Hills	2008	Jul	29		0.157	Mw 5.4	21.6	13.6
14783	Los Angeles - Vincent Thomas W1	Inglewood	2009	May	17		0.051	Mw 4.7	21.7	15
	"	Calexico	2010	Apr	04		0.014	Mw 7.2	324.5	32.3
14784	Los Angeles - Vincent Thomas W2	Inglewood	2009	May	17		0.060	Mw 4.7	21.6	15
	"	Calexico	2010	Apr	4		0.017	Mw 7.2	324.8	32.3
14786	Los Angeles - Vincent Thomas West	Hector Mine	1999	Oct	16		0.030	ML 7.1	207.9	6.0
23792	San Bernardino - I10/215 W	Chino Hills	2008	Jul	29		0.049	Mw 5.4	44.8	13.6
	"	Inglewood	2009	May	17		0.010	Mw 4.7	97.7	15
	"	Redlands	2010	Feb	13		0.018	ML 4.1	12.8	8.9
	"	Calexico	2010	Apr	4		0.022	Mw 7.2	274.3	32.3
	"	Beaumont	2011	Sep	14		0.024	ML 4.1	23.9	16.9
24400	Los Angeles - Obregon Park	Chino Hills	2008	Jul	29		0.185	Mw 5.4	39.2	13.6
	"	Whittier Narrows	2010	Mar	16		0.113	ML 4.4	10.7	18
	"	Calexico	2010	Apr	4		0.013	Mw 7.2	334	32.3
24703	Los Angeles - La Cienega	Hector Mine	1999	Oct	16		0.035	ML 7.1	203.9	6.0
	"	West Hollywood	2001	Sep	9		0.490	ML 4.2	4.3	7.9
	"	Chino Hills	2008	Jul	29		0.030	Mw 5.4	57.3	13.6
	"	Marina Del Rey	2009	Jan	23		0.012	ML 3.4	10.3	7
	"	Inglewood	2009	May	17		0.111	Mw 4.7	11.4	15
	"	Whittier Narrows	2010	Mar	16		0.016	ML 4.4	28.6	18
	"	Calexico	2010	Apr	4		0.010	Mw 7.2	349.3	32.3
24764	Tarzana - Cedar Hill B	West Hollywood	2001	Sep	9		0.028	ML 4.2	17.2	7.9
36520	Parkfield - Turkey Flat #2	Parkfield	2004	Sep	28		0.294	ML 6.0	7.7	7.9
36529	Parkfield - Turkey Flat #1	Parkfield	2007	May	22		0.035	Mw 4.0	5.4	9.2
	"	Parkfield	2004	Sep	28		0.244	ML 6.0	7.1	7.9
58137	Alameda - Posey & Webster	Piedmont	2007	Jul	20		0.053	Mw 4.2	8.1	5.8
	"	Alamo	2008	Sep	5		0.018	Mw 4.0	26.1	16.2
	"	Alum Rock	2007	Oct	30		0.011	Mw 5.4	59.4	9.2
	"	Lafayette	2007	Mar	1		0.021	Ml 4.2	20	16.6
	"	Berkeley	2011	Oct	20		0.055	Mw 4.0	8.6	9.8
	"	El Cerrito	2012	Mar	5		0.012	Ml 4.0	15.6	9.2
58204	Oakland - Bay Bridge	Berkeley	2011	Oct	20		0.029	Mw 4.0	8.3	9.8
	"	El Cerrito	2012	Mar	5		0.017	Ml 4.0	12.1	9.2
58642	Treasure Island	Piedmont Area	2006	Dec	20		0.020	ML 3.7	12.7	9
	"	Alum Rock	2007	Oct	30		0.012	Mw 5.4	68.5	9.2
	"	Gilroy	1993	Jan	15		0.014	ML 5.3	120.3	5.0
58961	San Francisco - Bay Bridge	Berkeley	2011	Oct	20		0.023	Mw 4.0	14.9	9.8
58964	Half Moon Bay - Tunitas	Gilroy	2002	May	13		0.027	ML 4.9	83.1	7.6
58968	Foster City - San Mateo Bridge	Alum Rock	2007	Oct	30		0.010	Mw 5.4	45.9	9.2
68206	Crockett - Carquinez Bridge #1	El Cerrito	2012	Mar	5		0.043	Ml 4.0	15.5	9.2
68259	Crockett - Carquinez Bridge #2	El Cerrito	2012	Mar	5		0.018	Ml 4.0	15.6	9.2
68310	Vallejo - Hwy 37/Napa River East	Crockett	2012	Feb	15		0.020	ML 3.6	6.4	9.3
	"	Crockett	2012	Feb	16		0.020	ML 3.5	6	8.3
	"	El Cerrito	2012	Mar	5		0.012	Ml 4.0	21.5	9.2
68323	Benicia - Martinez Bridge South	El Cerrito	2012	Mar	5		0.009	Ml 4.0	20.1	9.2
89734	Eureka	Ferndale	2007	Feb	26		0.010	ML 5.4	62.6	-
	"	Ferndale	2010	Jan	9		0.197	Mw 6.5	54	21.7
	"	Ferndale	2010	Feb	4		0.025	Mw 5.9	77.6	11.2
	"	Eureka Offshore	2000	Sep	22		0.011	ML 4.4	24.4	13.9
	"	Weitchpec	2012	Feb	13		0.038	Mw 5.6	47.9	28.2
	"	Blue Lake	2012	Oct	21		0.017	ML 3.5	22.2	21.7

USGS-NSMP (National Strong-Motion Project)

Station Code	Station	Earthquake	Year	Month	Day	HRMN	Max. PGA (g)	Magnitude	Epicentral Dist. (km)	Source Depth (km)
5300	Seven Oaks Dam Downstream Array, Redlands, CA	Big Bear City	2000	12	2	0828 UTC	0.018	ML 4.1	34	2.7
	"	Big Bear Lake	2001	2	10	21:05 UTC	0.06	ML 5.1	24.8	5.9
	"	Anza	2001	10	31	07:56 UTC	0.01	ML 5.1	86.1	15.2
	"	Big Bear City	2003	2	22	12:19 UTC	0.04	ML 5.4	32	1.2
	"	Big Bear City	2004	11	13	17:39 UTC	0.01	Mw 3.9	35.6	9.6
	"	Anza	2005	6	12	15:41 UTC	0.02	Mw 5.2	80.2	14.1
	"	Yucaipa	2005	6	16	20:53 UTC	0.295	Mw 4.9	10	11.8
	"	Mt. San Gorgonio	2005	10	18	07:31 UTC	0.01	Mw 4.2	32	17
	"	Big Bear City	2005	12	3	07:49 UTC	0.014	Mw 3.9	34.4	5.1
	"	Big Bear Lake	2007	12	19	12:14 UTC	0.04	Ml 4.0	12	10.2
	"	Yucaipa	2008	10	2	09:41 UTC	0.10	Mw 3.8	12.4	12.5
	"	San Bernardino	2009	1	9	03:49 UTC	0.07	Mw 4.5	19	14.1
286	Superstition Mtn. Pk., Imperial Valley, CA	Obsidian Butte	2005	9	2	01:27 UTC	0.02	Mw 5.1	28.7	9.7

Table 2 List of Acceleration Records (continued)

NEES at UCSB

Station Code	Station	Earthquake ID	Year	Month	Day	HRMN	Max. PGA (g)	Magnitude (ML)	Epicentral Dist. (km)	Source Depth (km)
GVDA	Garner Valley Downhole Array, CA	14151440	2005	6	12	15:41 UTC	0.172	5.6	19.97	14
	"	14155260	2005	6	16	20:53 UTC	0.041	4.88	53.42	11.6
	"	14197132	2005	11	8	22:03 UTC	0.036	3.36	15.72	12.9
	"	14243724	2006	7	30	13:32 UTC	0.410	3.16	11.55	15.3
	"	10225585	2007	1	8	03:05 UTC	0.018	2.78	9.33	19.2
	"	14372916	2008	6	3	23:06 UTC	0.028	3.04	5.48	16.2
	"	10353485	2008	10	11	19:33 UTC	0.015	3	3.82	16.5
	"	14403792	2008	11	17	17:41 UTC	0.011	3.79	26.16	11.5
	"	14403732	2008	11	17	12:35 UTC	0.025	4.11	25.64	12.2
	"	14491232	2009	7	26	04:54 UTC	0.060	3.53	5.84	14
	"	10530013	2010	1	16	12:03 UTC	0.045	4.28	43.67	13.9
	"	10701405	2010	6	13	03:08 UTC	0.018	4.9	39.76	12.5
	"	10736069	2010	7	7	23:53 UTC	0.102	5.43	32.53	14
	"	14995172	2011	6	3	05:45 UTC	0.020	3.11	6.58	12.9
	"	15001500	2011	6	14	08:25 UTC	0.022	3.6	6.65	18.1
HEO	Hollister Earthquake Observatory, CA	21532735	2006	8	17	05:44 UTC	0.040	2.95	10.86	8.15
	"	40219230	2008	6	15	03:00 UTC	0.025	3.12	8.99	13.86
	"	51211143	2008	11	13	18:24 UTC	0.044	3.4	7.69	8.6
	"	71271995	2009	9	6	09:47 UTC	0.031	3.87	9.52	20.73
	"	71413856	2010	6	12	06:05 UTC	0.017	3.57	7.68	11.69
	"	71429025	2010	7	21	06:54 UTC	0.014	3.35	8.31	8.51
	"	71509345	2011	1	13	04:00 UTC	0.045	3.92	7.29	8.06
	"	71509330	2011	1	13	03:54 UTC	0.011	3.68	7.45	8.07
	"	71873180	2012	11	1	14:34 UTC	0.019	3.33	6	8.6
WLA	Wildlife Liquefaction Array, CA	30253759	2010	4	5	11:14 UTC	0.037	5.1	54.94	13.1
	"	10597061	2010	4	10	9:12 UTC	0.025	4.5	52.61	6.8
	"	30261759	2010	4	5	13:33 UTC	0.030	5.1	56.86	0
	"	14348588	2008	2	12	4:32 UTC	0.012	4.97	75.12	6
	"	10657533	2010	5	8	18:33 UTC	0.028	4.8	53.62	6
	"	14682004	2010	4	27	10:55 UTC	0.017	4.83	53.97	3.3
	"	10671989	2010	5	19	0:39 UTC	0.053	4.53	55.6	8.9
	"	12217067	2005	9	2	1:27 UTC	0.128	4.5	12.74	4.9
	"	15204969	2012	8	28	2:01 UTC	0.040	4.22	11.01	4.4
	"	14745580	2010	6	15	4:26 UTC	0.078	5.72	57.36	5.4
	"	15201537	2012	8	26	23:33 UTC	0.333	4.61	7.74	7.4
	"	15199689	2012	8	26	19:33 UTC	0.153	4.89	9.67	4.3
	"	14179736	2005	9	2	1:27 UTC	0.128	5.11	12.12	9.8
	"	24597759	2009	12	30	18:48 UTC	0.083	5.8	77.43	6
	"	14607660	2010	4	4	22:40 UTC	0.131	7.2	99.93	10
	"	14898996	2010	12	15	19:16 UTC	0.051	4.37	7.27	13.2
	"	15199681	2012	8	26	19:31 UTC	0.314	5.32	9.23	8.3
	"	15202921	2012	8	27	4:41 UTC	0.330	4.9	8.58	4.1
	"	37088500	2012	8	26	20:57 UTC	0.206	5.5	8.36	9
8040	Delaney Park Downhole Array, Anchorage, AK	5047474	2005	2	16	18:35 UTC	0.014	4.74	12.69	34.8
	"	6208470	2006	7	27	13:18 UTC	0.036	4.7	13.26	35.99
	"	9097480	2009	4	7	20:12 UTC	0.015	4.8	27.98	33.03
	"	9173540	2009	6	22	19:28 UTC	0.011	5.4	91.49	64.59
	"	9231510	2009	8	19	18:19 UTC	0.010	5.1	51.72	66.44
	"	10263490	2010	9	20	21:24 UTC	0.032	4.9	20.67	45.43
	"	12137460	2012	5	16	15:02 UTC	0.019	4.6	10.83	61.72
	"	12339002	2012	12	4	1:42 UTC	0.026	5.8	44.29	53.2

Taipei Basin Downhole Seismic Network, Institute of Earth Sciences, Academia Sinica, Taiwan (data from Prof. Wen Kuo-Liang)

Station Code	Station	Earthquake ID	Year	Month	Day	HRMN	Max. PGA (g)	Magnitude (ML)	Epicentral Dist. (km)	Source Depth (km)
BS	Water Conservancy Bureau, Panchiao		1995	4	24	10:03 UT	0.027	5.3	42	63
	"		1995	6	25	6:59 UT	0.016	6.1	49	40
	"		1995	12	1	3:17 UT	0.082	5.7	48	45
	"		1996	3	5	14:52 UT	0.022	6.4	151	6
SS	Songshan Tobacco Plant		1997	6	24	16:36 UT	0.022	3.7	9	9
	"		1999	5	7	1:03 UT	0.012	5.1	45	3
TF	Vocational Advisory Committee for Retired Servicemen, Panchiao		1995	2	23	5:19 UT	0.029	5.8	95	22
	"		1995	3	24	4:14 UT	0.019	5.6	60	76
	"		1995	12	1	3:17 UT	0.014	5.7	51	45
	"		1997	5	15	10:43 UT	0.017	4.8	56	93
WK	Sewage Disposal Plant, Wuku		1994	5	24	4:00 UT	0.012	6.6	181	5
	"		1994	6	5	1:09 UT	0.025	6.2	79	5
	"		1995	2	23	5:03 UT	0.046	5.8	99	22
	"		1995	3	24	4:13 UT	0.026	5.6	64	76
	"		1995	6	25	6:59 UT	0.069	6.1	56	40
	"		1996	1	22	19:23 UT	0.011	5.1	32	67
	"		1996	3	5	14:52 UT	0.021	6.4	157	6
	"		1996	11	26	8:22 UT	0.013	5.3	104	26
	"		1997	2	10	16:50 UT	0.021	4.9	109	20
	"		1998	5	9	20: 53 UT	0.068	5.3	54	84

Table 2 List of Acceleration Records (continued)

Sendai Dense Array Earthquake Observation Project, Building Research Institute, Japan (data from Mr. Toshihide Kashima)

Station code	Station	Earthquake ID	Year	Month	Day	HRMN	Max. PGA (g)	Magnitude (JMA)	Epicentral Dist. (km)	Source Depth (km)
ARAH	Arahama	EQ9234	1992	12	28	1:21	0.026	5.9	157	34
	"	EQ9305	1993	1	15	20:07	0.026	7.8	595	101
	"	EQ9327	1993	11	27	15:11	0.094	5.9	51	112
MIYA	Miyagino	EQ8701	1987	1	9	15:15	0.022	6.6	190	72
	"	EQ8704	1987	1	21	8:36	0.028	5.5	113	50
	"	EQ8709	1987	2	6	22:16	0.030	6.4	168	30
	"	EQ8719	1987	4	7	9:41	0.032	6.6	135	44
	"	EQ8724	1987	4	23	5:13	0.030	6.5	144	
	"	EQ8740	1987	10	4	19:27	0.027	5.8	129	42
	"	EQ8915	1989	6	24	4:59	0.038	4.1	9	14
	"	EQ9234	1992	12	28	1:21	0.013	5.9	160	34
	"	EQ9305	1993	1	15	20:07	0.019	7.8	594	101
	"	EQ9602	1996	2	17	0:23	0.041	6.5	179	6
	"	EQ9712	1997	12	7	12:50	0.025	5.3	97	83
	"	EQ9819	1998	9	15	16:18	0.027	3.6	13	13
	"	EQ9820	1998	9	15	16:24	0.145	5.0	13	13
	"	EQ9826	1998	9	15	17:56	0.037	4.0	13	13
	"	EQ9839	1998	11	24	4:48	0.031	5.1	66	82
NAGA	Nagamachi	EQ9234	1992	12	28	1:21	0.023	5.9	164	34
	"	EQ9305	1993	1	15	20:07	0.036	7.8	598	101
	"	EQ9327	1993	11	27	15:11	0.092	5.9	56	112
	"	EQ9602	1996	2	17	0:23	0.108	6.5	179	6
	"	EQ9604	1996	4	23	13:08	0.031	5.2	121	76
	"	EQ9701	1997	2	20	5:22	0.053	5.3	97	88
	"	EQ9712	1997	12	7	12:50	0.052	5.3	97	83
	"	EQ9819	1998	9	15	16:18	0.038	3.6	11	13
	"	EQ9820	1998	9	15	16:24	0.181	5.0	11	13
	"	EQ9826	1998	9	15	17:56	0.042	4.0	10	13
	"	EQ9839	1998	11	24	4:48	0.045	5.1	67	82
NAKA	Nakano	EQ8701	1987	1	9	15:15	0.044	6.6	188	72
	"	EQ8704	1987	1	21	8:36	0.050	5.5	106	50
	"	EQ8709	1987	2	6	22:16	0.096	6.4	164	30
	"	EQ8719	1987	4	7	9:41	0.081	6.6	131	44
	"	EQ8724	1987	4	23	5:13	0.111	6.5	141	
	"	EQ8740	1987	10	4	19:27	0.070	5.8	125	42
	"	EQ8915	1989	6	24	4:59	0.039	4.1	16	14
	"	EQ9234	1992	12	28	1:21	0.036	5.9	154	34
	"	EQ9305	1993	1	15	20:07	0.032	7.8	590	101
	"	EQ9327	1993	11	27	15:11	0.106	5.9	46	112
	"	EQ9413	1994	10	4	22:24	0.054	8.1	801	23
	"	EQ9602	1996	2	17	0:23	0.073	6.5	172	6
	"	EQ9701	1997	2	20	5:22	0.026	5.3	98	88
	"	EQ9712	1997	12	7	12:50	0.041	5.3	91	83
	"	EQ9839	1998	11	24	4:48	0.072	5.1	59	82
OKIN	Okino	EQ8915	1989	6	24	4:59	0.037	4.1	11	14
	"	EQ9234	1992	12	28	1:21	0.028	5.9	162	34
	"	EQ9305	1993	1	15	20:07	0.026	7.8	597	101
	"	EQ9327	1993	11	27	15:11	0.127	5.9	54	112
	"	EQ9602	1996	2	17	0:23	0.257	6.5	177	6
	"	EQ9701	1997	2	20	5:22	0.046	5.3	96	88
	"	EQ9819	1998	9	15	16:18	0.022	3.6	14	13
	"	EQ9820	1998	9	15	16:24	0.157	5.0	14	13
	"	EQ9826	1998	9	15	17:56	0.048	4.0	13	13
	"	EQ9839	1998	11	24	4:48	0.041	5.1	64	82
ORID	Oridate	EQ8719	1987	4	7	9:41	0.058	6.6	142	44
	"	EQ8724	1987	4	23	5:13	0.081	6.5	149	
	"	EQ8740	1987	10	4	19:27	0.038	5.8	135	42
	"	EQ8915	1989	6	24	4:59	0.031	4.1	4	14
	"	EQ9234	1992	12	28	1:21	0.009	5.9	169	34
	"	EQ9305	1993	1	15	20:07	0.022	7.8	598	101
	"	EQ9327	1993	11	27	15:11	0.046	5.9	58	112
	"	EQ9413	1994	10	4	22:24	0.022	8.1	812	23
	"	EQ9712	1997	12	7	12:50	0.030	5.3	104	83
	"	EQ9819	1998	9	15	16:18	0.026	3.6	4	13
	"	EQ9820	1998	9	15	16:24	0.269	5.0	4	13
	"	EQ9826	1998	9	15	17:56	0.028	4.0	3	13
	"	EQ9839	1998	11	24	4:48	0.059	5.1	74	82
SHIR	Shiromaru	EQ8915	1989	6	24	4:59	0.028	4.1	13	14
	"	EQ9234	1992	12	28	1:21	0.018	5.9	164	34
	"	EQ9305	1993	1	15	20:07	0.031	7.8	600	101
	"	EQ9327	1993	11	27	15:11	0.084	5.9	57	112
	"	EQ9602	1996	2	17	0:23	0.086	6.5	175	6
	"	EQ9701	1997	2	20	5:22	0.048	5.3	93	88
	"	EQ9712	1997	12	7	12:50	0.094	5.3	93	83
	"	EQ9805	1998	4	9	17:45	0.043	5.4	140	93
	"	EQ9819	1998	9	15	16:18	0.099	3.6	16	13
	"	EQ9820	1998	9	15	16:24	0.217	5.0	16	13
	"	EQ9826	1998	9	15	17:56	0.084	4.0	15	13

Table 2 List of Acceleration Records (continued)

Sendai Dense Array Earthquake Observation Project, Building Research Institute, Japan (data from Mr. Toshihide Kashima)

Station code	Station	Earthquake ID	Year	Month	Day	HRMN	Max. PGA (g)	Magnitude (JMA)	Epicentral Dist.(km)	Source Depth (km)
TAMA	Tamagawa	EQ8701	1987	1	9	15:15	0.011	6.6	181	72
	"	EQ8704	1987	1	21	8:36	0.017	5.5	103	50
	"	EQ8709	1987	2	6	22:16	0.033	6.4	170	30
	"	EQ8719	1987	4	7	9:41	0.035	6.6	136	44
	"	EQ8724	1987	4	23	5:13	0.033	6.5	147	
	"	EQ9234	1992	12	28	1:21	0.018	5.9	150	34
	"	EQ9305	1993	1	15	20:07	0.014	7.8	584	101
	"	EQ9327	1993	11	27	15:11	0.068	5.9	41	112
	"	EQ9413	1994	10	4	22:24	0.021	8.1	795	23
	"	EQ9602	1996	2	17	0:23	0.042	6.5	176	6
	"	EQ9701	1997	2	20	5:22	0.351	5.3	105	88
	"	EQ9712	1997	12	7	12:50	0.036	5.3	95	83
	"	EQ9820	1998	9	15	16:24	0.038	5.0	21	13
TRGA	Tsurugaya	EQ8915	1989	6	24	4:59	0.021	4.1	7	14
	"	EQ9234	1992	12	28	1:21	0.012	5.9	159	34
	"	EQ9305	1993	1	15	20:07	0.014	7.8	591	101
	"	EQ9327	1993	11	27	15:11	0.041	5.9	49	112
	"	EQ9413	1994	10	4	22:24	0.026	8.1	803	23
	"	EQ9602	1996	2	17	0:23	0.043	6.5	181	6
	"	EQ9701	1997	2	20	5:22	0.025	5.3	103	88
	"	EQ9712	1997	12	7	12:50	0.022	5.3	99	83
	"	EQ9820	1998	9	15	16:24	0.081	5.0	13	13
	"	EQ9826	1998	9	15	17:56	0.015	4.0	12	13
	"	EQ9839	1998	11	24	4:48	0.052	5.1	68	82
TRMA	Tsurumaki	EQ8915	1989	6	24	4:59	0.046	4.1	13	14
	"	EQ9234	1992	12	28	1:21	0.042	5.9	156	34
	"	EQ9305	1993	1	15	20:07	0.037	7.8	591	101
	"	EQ9327	1993	11	27	15:11	0.090	5.9	48	112
	"	EQ9602	1996	2	17	0:23	0.096	6.5	175	6
	"	EQ9701	1997	2	20	5:22	0.029	5.3	99	88
	"	EQ9712	1997	12	7	12:50	0.053	5.3	94	83
	"	EQ9819	1998	9	15	16:18	0.035	3.6	18	13
	"	EQ9820	1998	9	15	16:24	0.101	5.0	18	13
	"	EQ9826	1998	9	15	17:56	0.036	4.0	17	13
TSUT	Tsutsujigaoka	EQ8915	1989	6	24	4:59	0.033	4.1	7	14
	"	EQ9234	1992	12	28	1:21	0.018	5.9	162	34
	"	EQ9305	1993	1	15	20:07	0.025	7.8	595	101
	"	EQ9327	1993	11	27	15:11	0.050	5.9	53	112
	"	EQ9413	1994	10	4	22:24	0.037	8.1	807	23
	"	EQ9602	1996	2	17	0:23	0.075	6.5	181	6
	"	EQ9712	1997	12	7	12:50	0.034	5.3	99	83
	"	EQ9819	1998	9	15	16:18	0.016	3.6	11	13
	"	EQ9820	1998	9	15	16:24	0.115	5.0	11	13
	"	EQ9826	1998	9	15	17:56	0.021	4.0	10	13

Table 3 NEHRP Site Classification

Classification	Description	V_{s30} (m/s)
A	hard rock	> 1500
B	rock	760 - 1500
C	very dense soil/soft rock	360-760
D	stiff soil	180-360
E	soft soil	<180
F	special soils requiring site-specific evaluation	

Table 4 Number of V/H ratios obtained from arrays in class B, C, D1, D2, D3, and E sites

Soil Class	Depth Bin						
	0-7 ft	7-50 ft	50-100 ft	100-150 ft	150-200 ft	200-300 ft	>300 ft
B	13	0	2	11	0	11	0
C	70	16	31	19	38	13	0
D1	71	55	48	35	24	33	31
D2	30	3	27	12	6	14	18
D3	69	69	58	6	19	19	29
E	17	5	17	6	2	12	6

Table 5 Number of V/H ratios obtained from events with PGAs in the ranges 0.01g-0.1g, 0.1g-0.2g, and 0.2-0.5g (from arrays in class B, C, and D1 sites only)

PGA (g)	Depth Bin						
	0-7 ft	7-50 ft	50-100 ft	100-150 ft	150-200 ft	200-300 ft	>300 ft
0.01-0.10	137	63	69	62	57	50	28
0.10-0.20	9	4	6	2	3	4	2
0.20-0.50	8	4	6	1	2	3	1

Table 6 Number of V/H ratios obtained from CGS-CESMD and USGS-NSMP sites in California; NEES at UCSB sites in California; NEES at UCSB site in Anchorage, Alaska; Sendai District, Japan; and Taipei Basin, Taiwan (arrays in class B, C, and D sites only)

Array Location	Depth Bin						
	0-7 ft	7-50 ft	50-100 ft	100-150 ft	150-200 ft	200-300 ft	>300 ft
California CGS-CESMD and USGS-NSMP	68	28	48	31	7	9	34
California NEES at UCSB	43	86	34	0	23	0	44
Anchorage, Alaska	8	16	8	15	0	8	0
Sendai District, Japan	114	13	61	37	38	73	0
Taipei Basin, Taiwan	20	0	15	0	19	0	0

Figure 1 Map of Vertical Array Stations

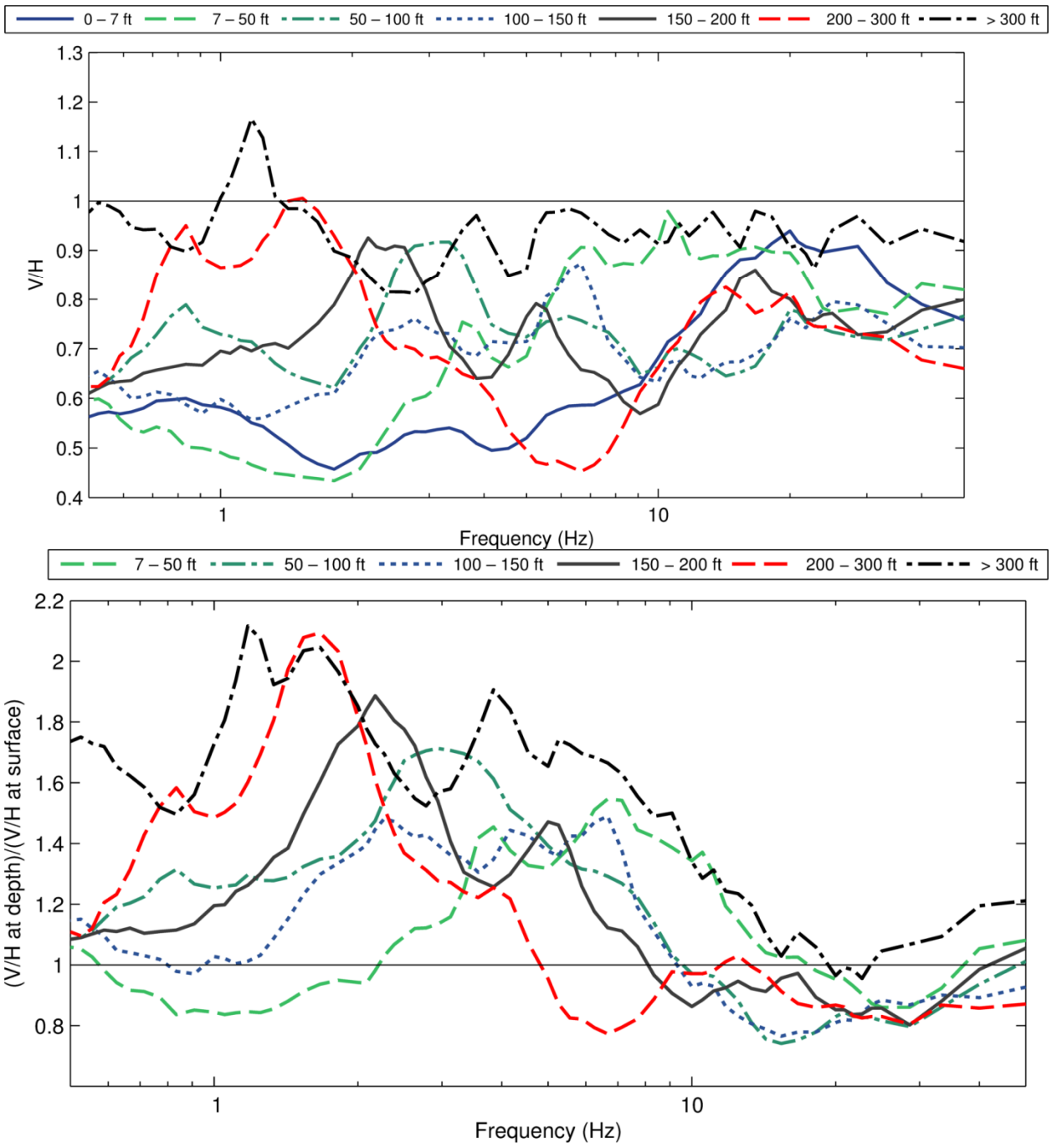

Figure 2 V/H ratios of all records obtained from arrays in class B, C, and D1 site. Average V/H ratios (top) and normalized average V/H ratios (bottom) for each of the seven depth bins:

0-7 ft (154 ratios), 7-50 ft (71 ratios), 50-100 ft (81 ratios), 100-150 ft (65 ratios), 150-200 ft (62 ratios), 200-300 ft (57 ratios), and >300 ft (31 ratios).

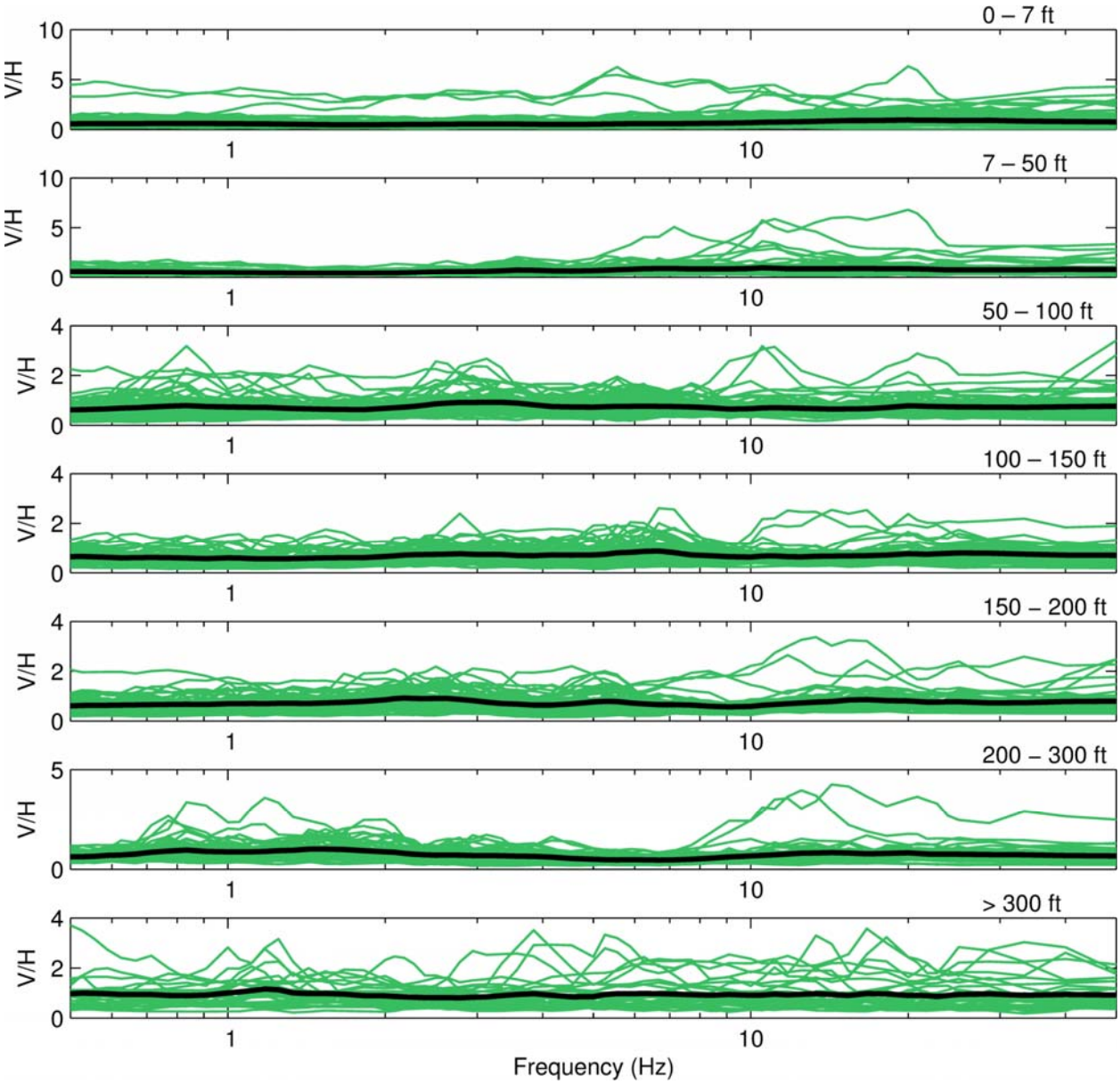

Figure 3 V/H ratios of all records obtained from arrays in class B, C, and D1 sites. Total of 521 V/H ratios plotted in their corresponding depth bins:

0-7 ft (154 ratios), 7-50 ft (71 ratios), 50-100 ft (81 ratios), 100-150 ft (65 ratios), 150-200 ft (62 ratios), 200-300 ft (57 ratios), and >300 ft (31 ratios). The thick black lines correspond to the averages for each bin.

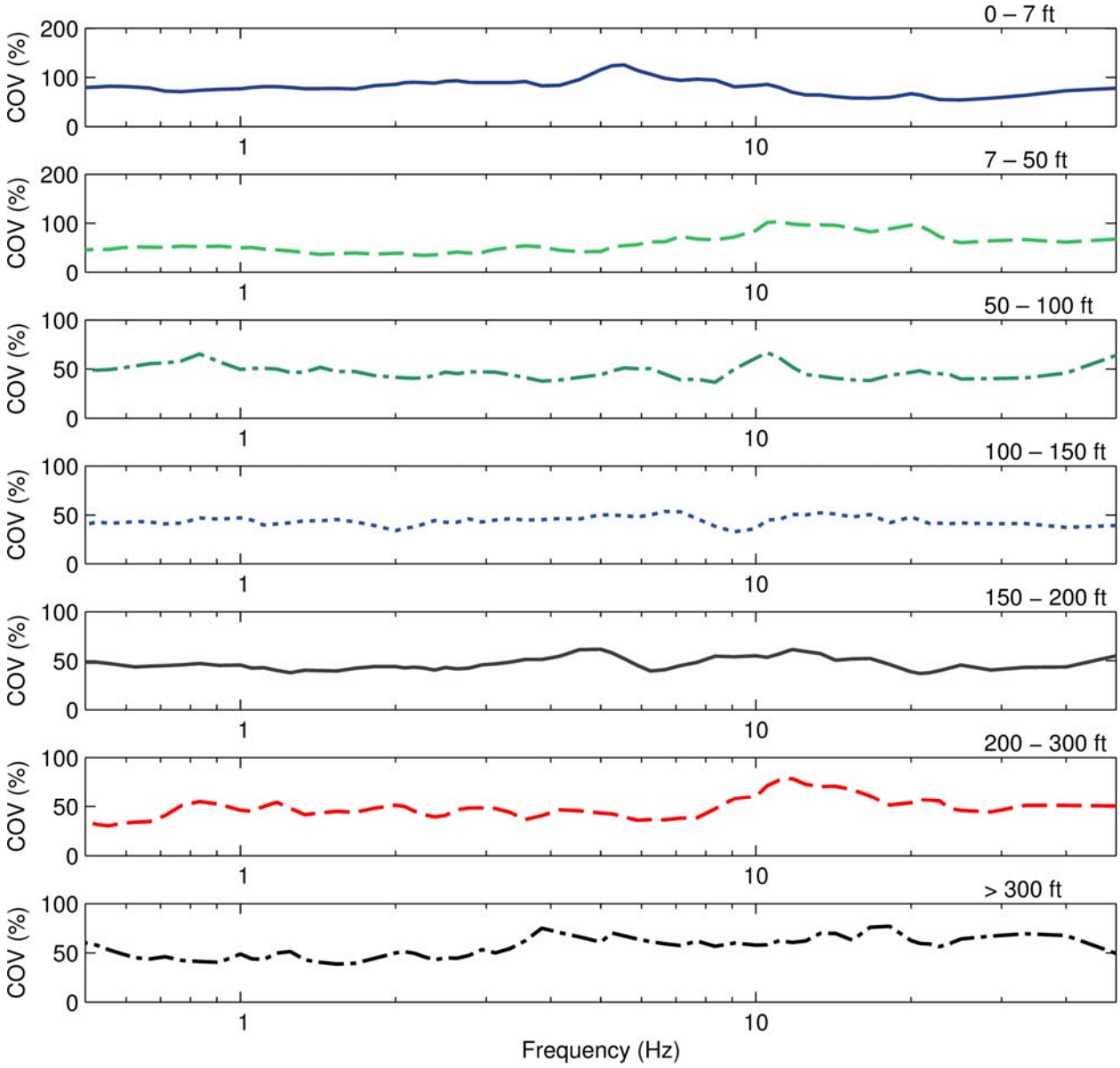

Figure 4 V/H ratios of all records obtained from arrays in class B, C, and D1 sites. Coefficients of variation of the V/H ratios within each of the seven depth bins:

0-7 ft (154 ratios), 7-50 ft (71 ratios), 50-100 ft (81 ratios), 100-150 ft (65 ratios), 150-200 ft (62 ratios), 200-300 ft (57 ratios), and >300 ft (31 ratios).

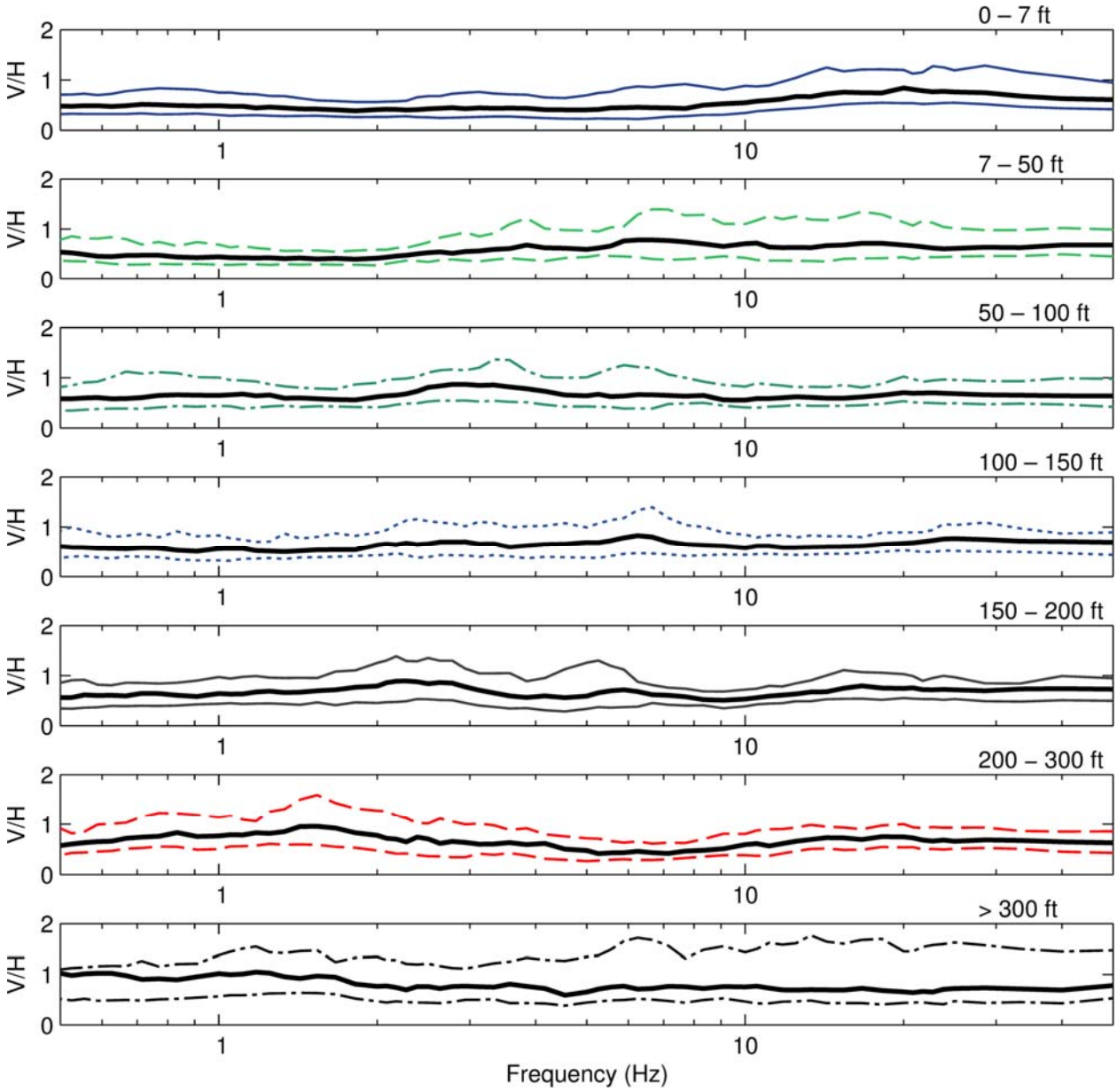

Figure 5 V/H ratios of all records obtained from arrays in class B, C, and D1 sites. Percentiles (16th, 50th, 84th) of the V/H ratios within each of the seven depth bins:

0-7 ft (154 ratios), 7-50 ft (71 ratios), 50-100 ft (81 ratios), 100-150 ft (65 ratios), 150-200 ft (62 ratios), 200-300 ft (57 ratios), and >300 ft (31 ratios). The thick black lines correspond to 50th percentiles for each bin.

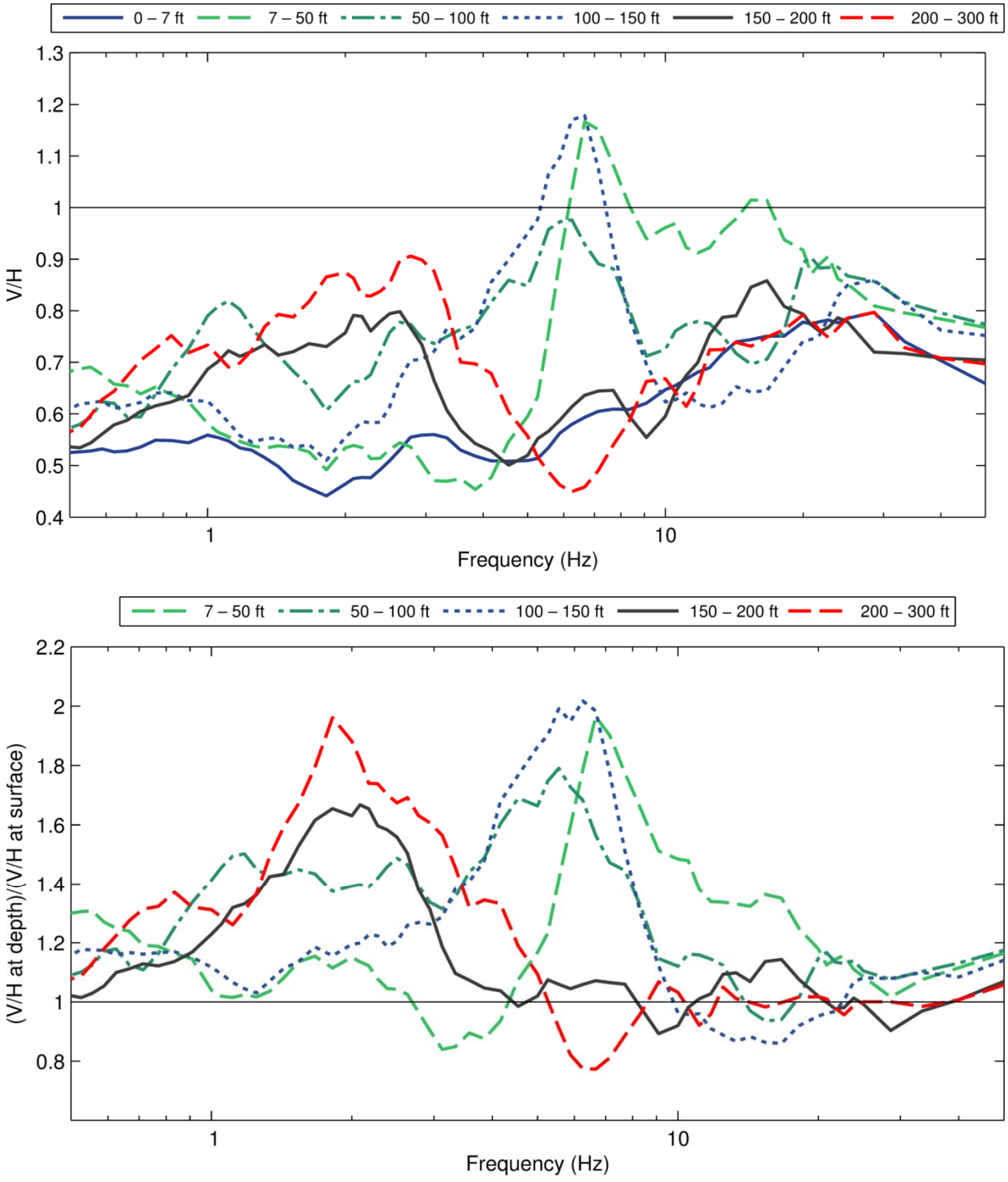

Figure 6 V/H ratios of all records obtained from arrays in class B and C sites. Average V/H ratios (top) and normalized average V/H ratios (bottom) for each of the six depth bins:

0-7 ft (83 ratios), 7-50 ft (16 ratios), 50-100 ft (33 ratios), 100-150 ft (30 ratios), 150-200 ft (38 ratios), and 200-300 ft (24 ratios). There was no data in depth bin >300 ft.

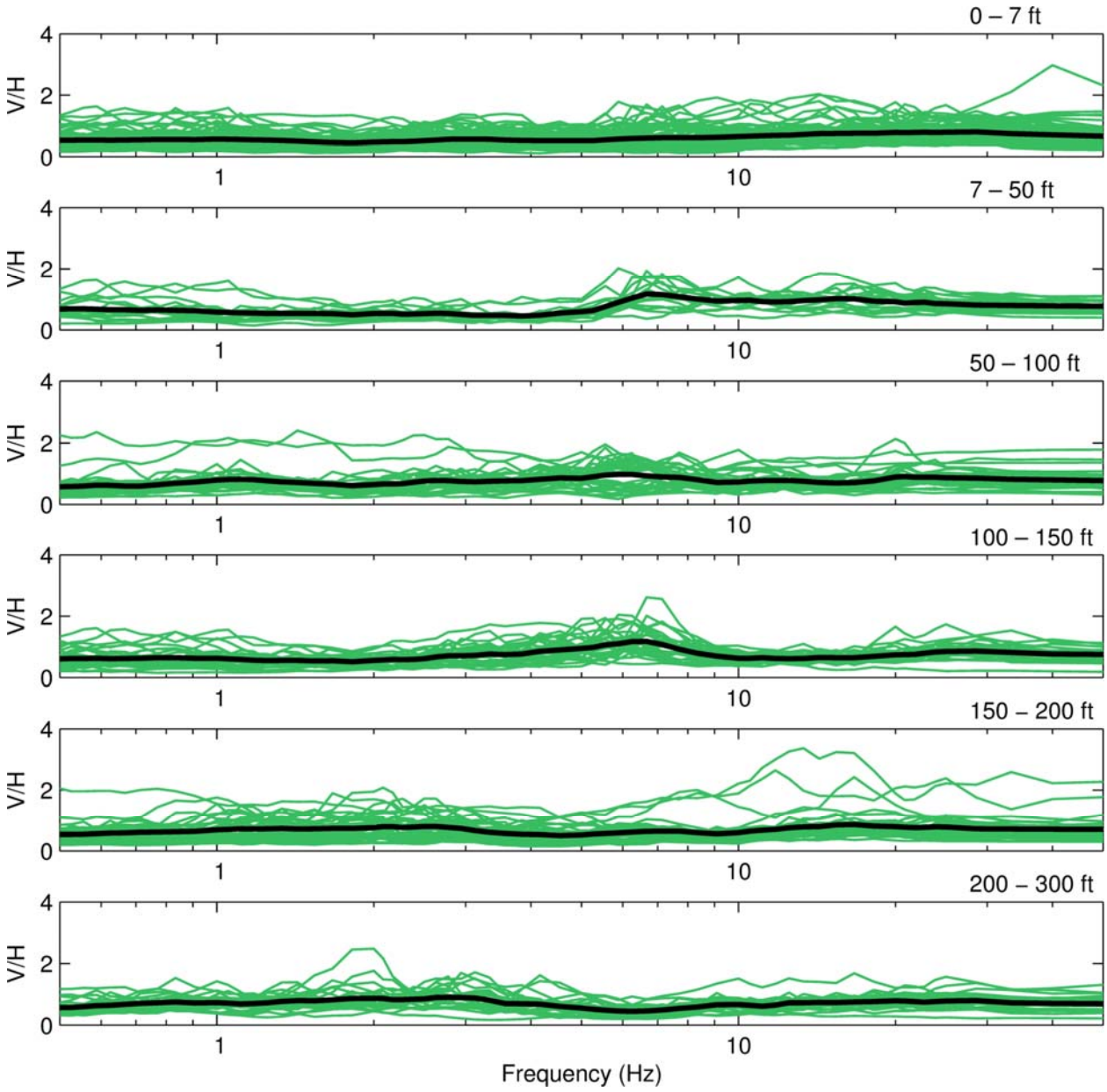

Figure 7 V/H ratios of all records obtained from arrays in class B and C sites

Total of 224 V/H ratios plotted in their corresponding depth bins: 0-7 ft (83 ratios), 7-50 ft (16 ratios), 50-100 ft (33 ratios), 100-150 ft (30 ratios), 150-200 ft (38 ratios), and 200-300 ft (24 ratios). There was no data in depth bin >300 ft. The thick black lines correspond to the averages for each bin.

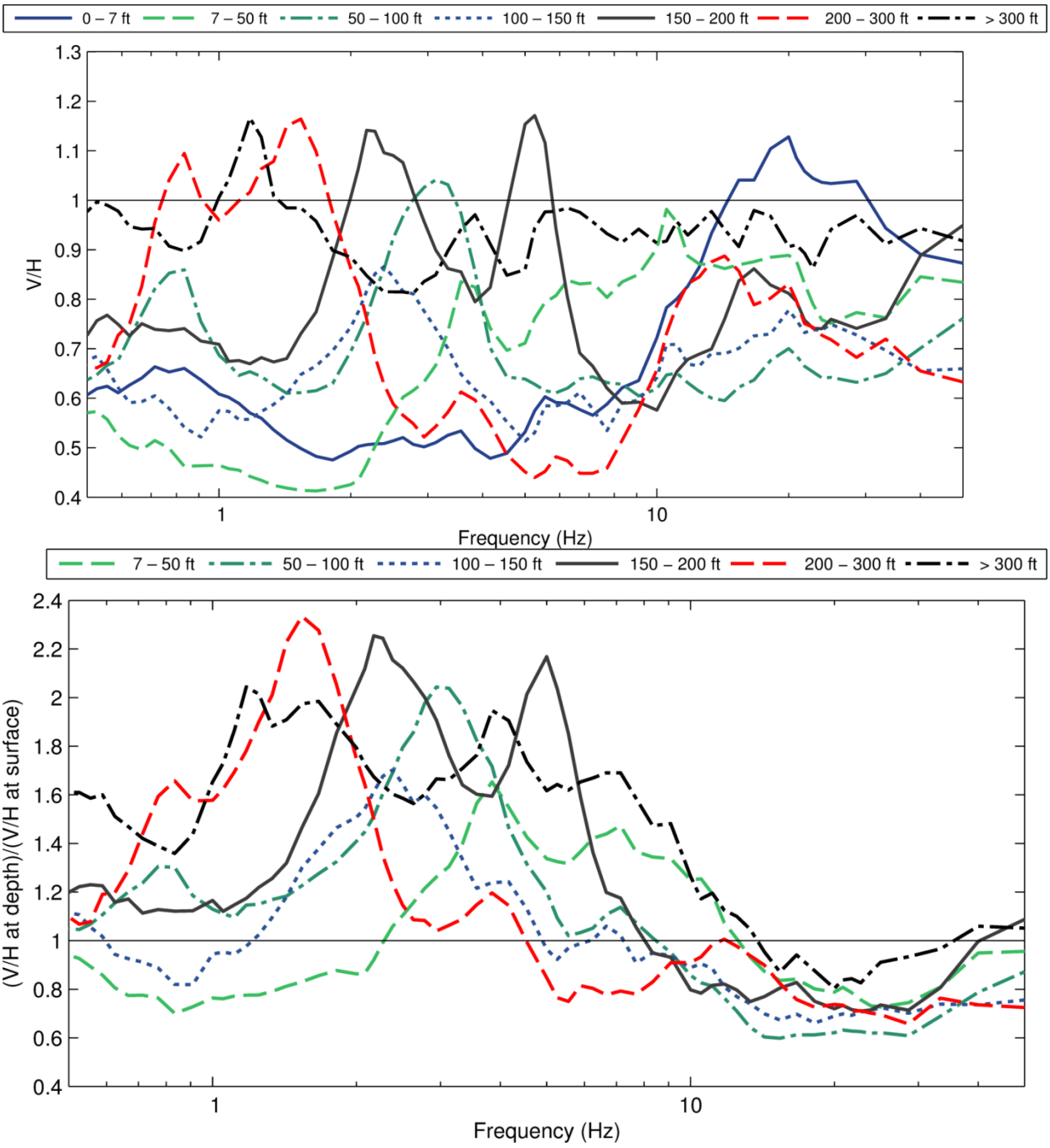

Figure 8 V/H ratios of all records obtained from arrays in class D1 sites. Average V/H ratios (top) and normalized average V/H ratios (bottom) for each of the seven depth bins:

0-7 ft (71 ratios), 7-50 ft (55 ratios), 50-100 ft (48 ratios), 100-150 ft (35 ratios), 150-200 ft (24 ratios), 200-300 ft (33 ratios), and >300 ft (31 ratios).

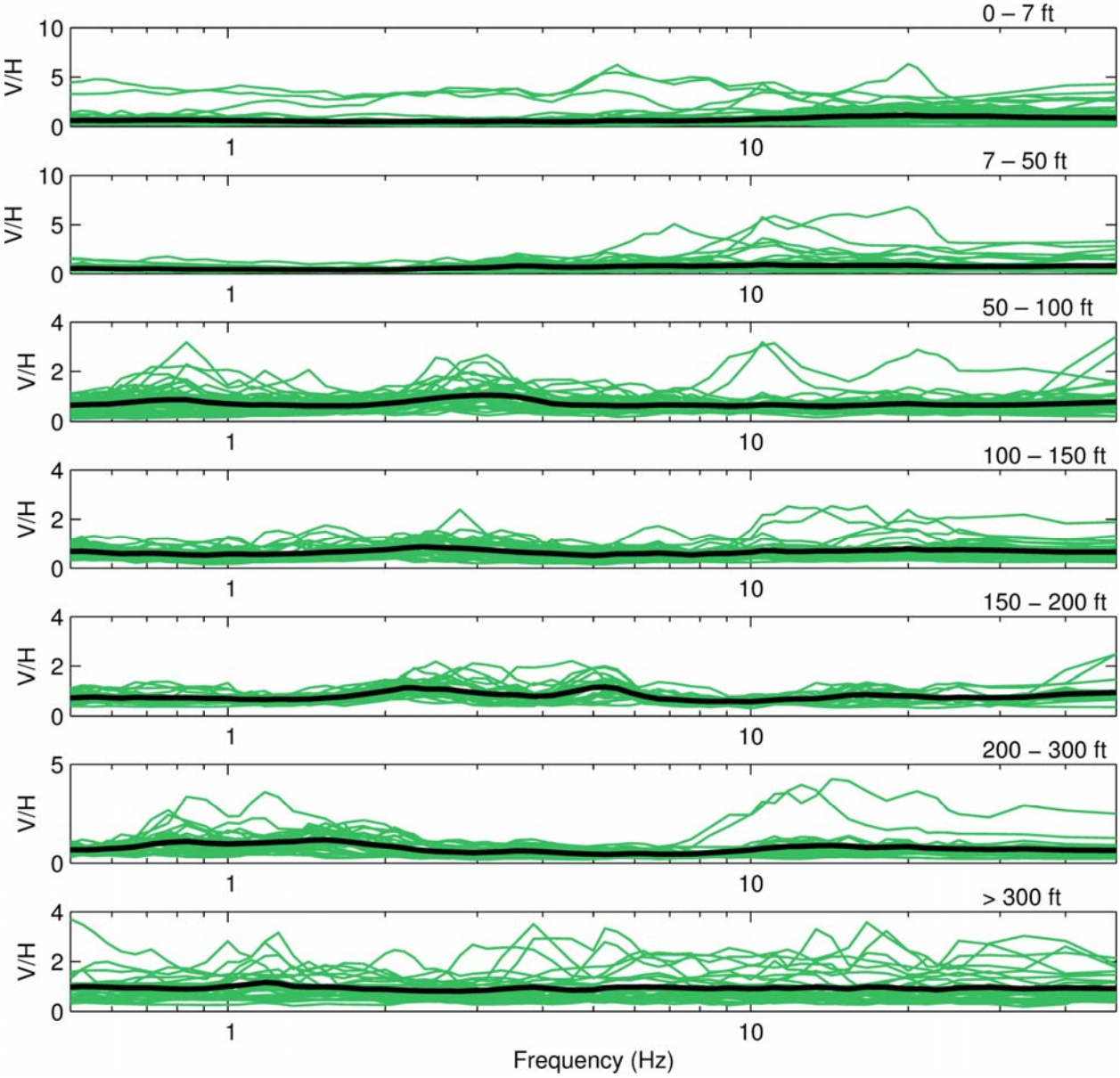

Figure 9 V/H ratios of all records obtained from arrays in class D1 sites. Total of 297 V/H ratios plotted in their corresponding depth bins:

0-7 ft (71 ratios), 7-50 ft (55 ratios), 50-100 ft (48 ratios), 100-150 ft (35 ratios), 150-200 ft (24 ratios), 200-300 ft (33 ratios), and >300 ft (31 ratios). The thick black lines correspond to the averages for each bin.

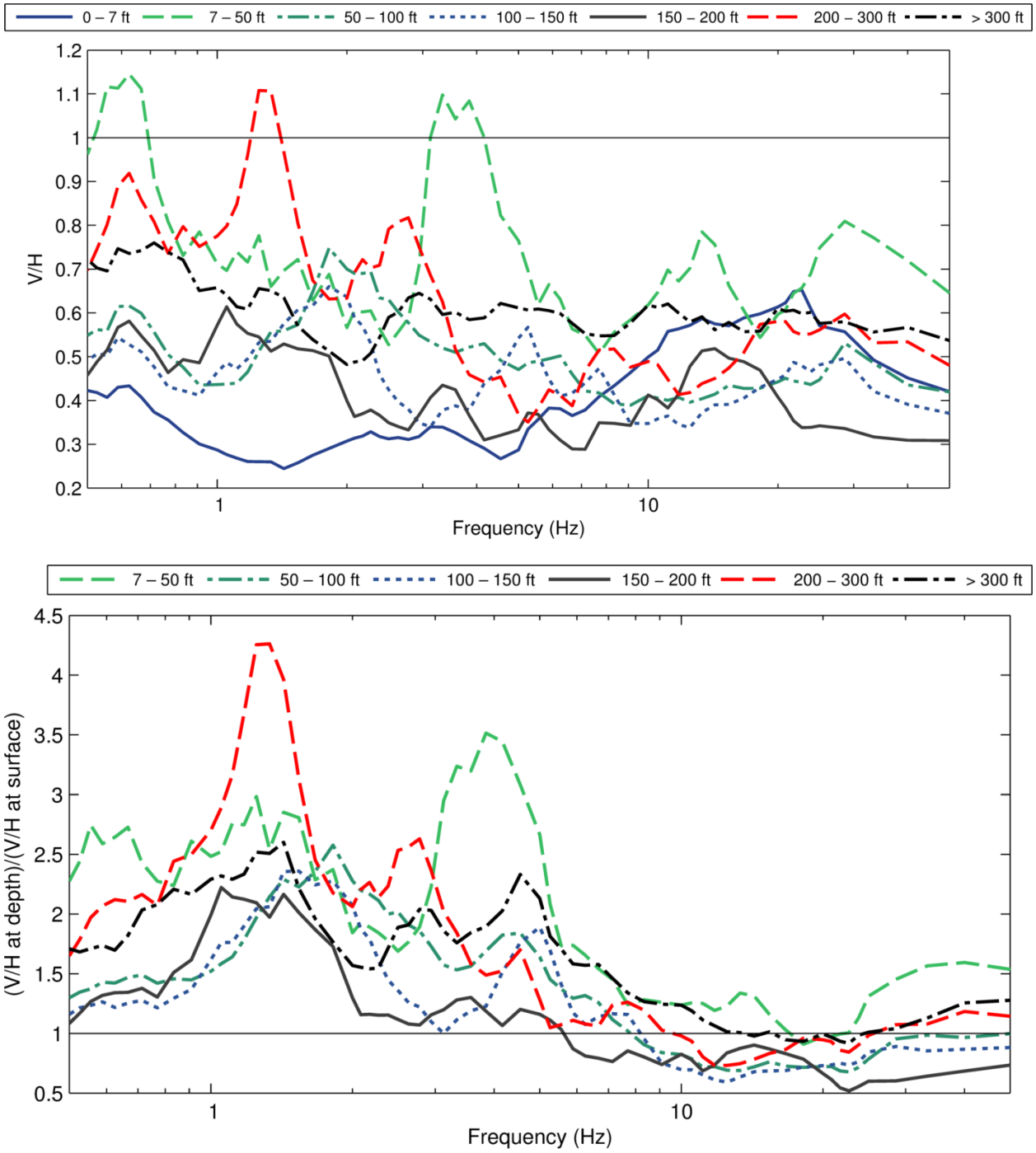

Figure 10 V/H ratios of all records obtained from arrays in class D2 sites. Average V/H ratios (top) and normalized average V/H ratios (bottom) for each of the seven depth bins:

0-7 ft (30 ratios), 7-50 ft (3 ratios), 50-100 ft (27 ratios), 100-150 ft (12 ratios), 150-200 ft (6 ratios), 200-300 ft (14 ratios), and >300 ft (18 ratios).

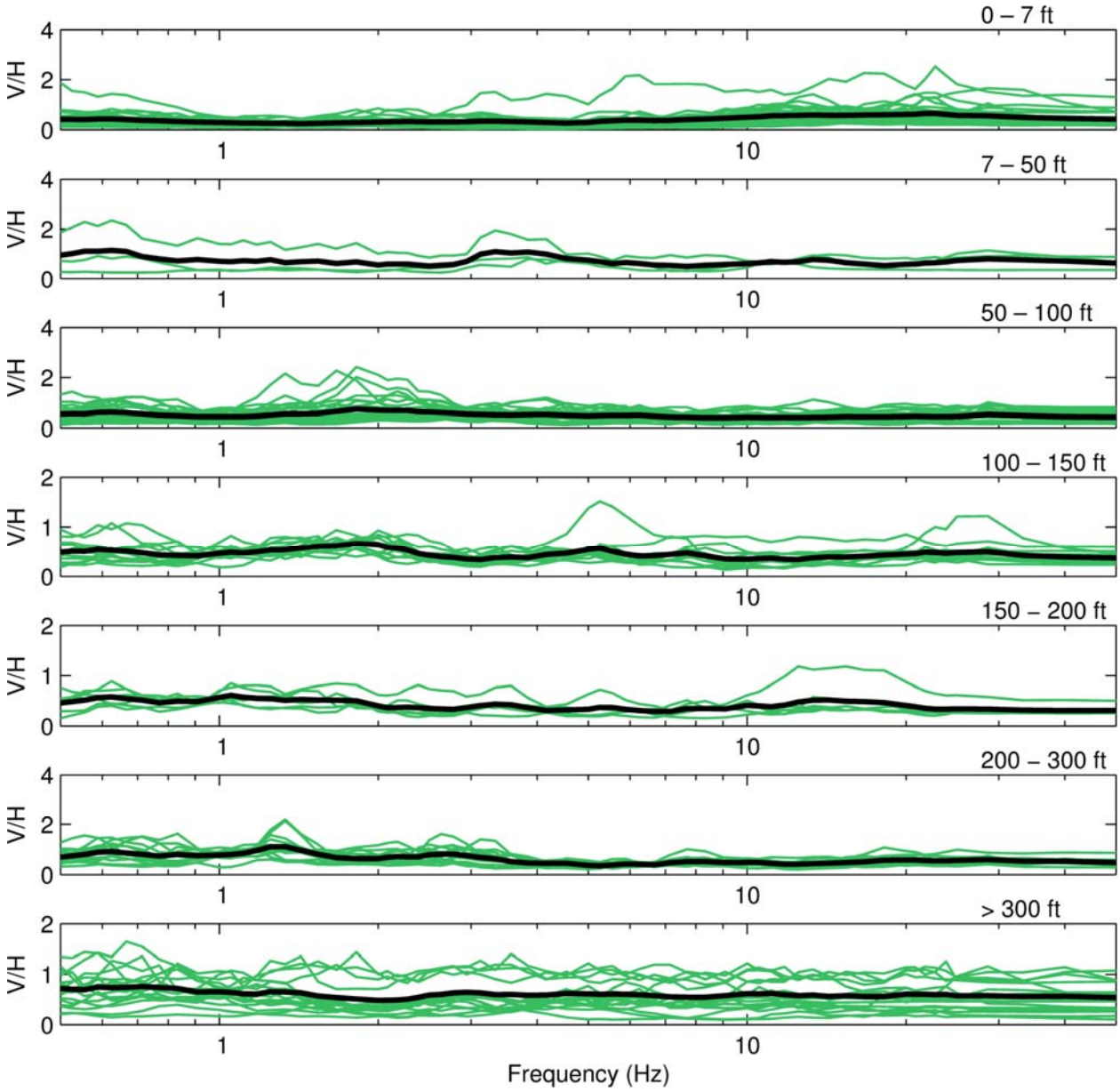

Figure 11 V/H ratios of all records obtained from arrays in class D2 sites. Total of 110 V/H ratios plotted in their corresponding depth bins:

0-7 ft (30 ratios), 7-50 ft (3 ratios), 50-100 ft (27 ratios), 100-150 ft (12 ratios), 150-200 ft (6 ratios), 200-300 ft (14 ratios), and >300 ft (18 ratios). The thick black lines correspond to the averages for each bin.

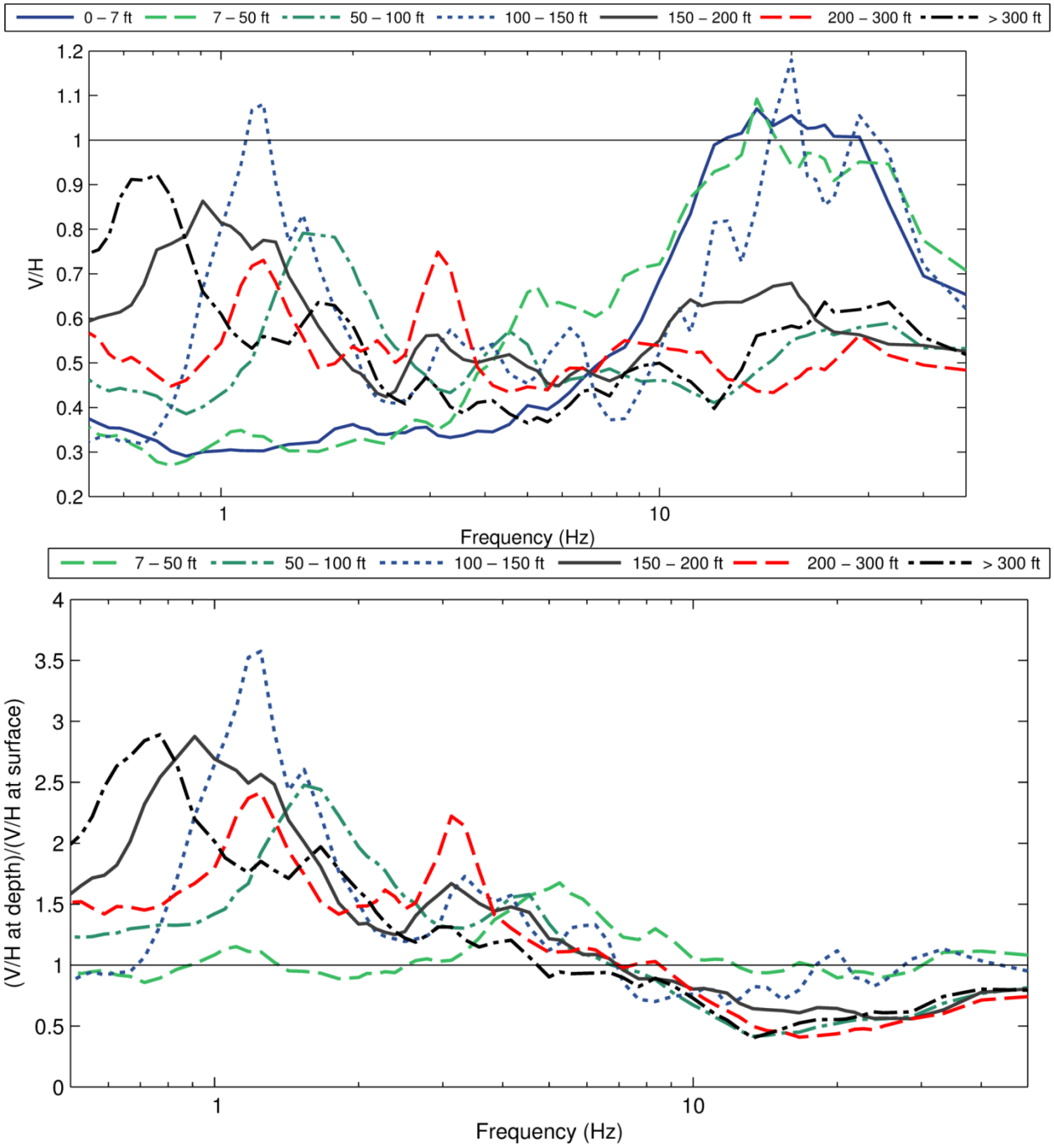

Figure 12 V/H ratios of all records obtained from arrays in class D3 sites. Average V/H ratios (top) and normalized average V/H ratios (bottom) for each of the seven depth bins:

0-7 ft (69 ratios), 7-50 ft (69 ratios), 50-100 ft (58 ratios), 100-150 ft (6 ratios), 150-200 ft (19 ratios), 200-300 ft (19 ratios), and >300 ft (29 ratios).

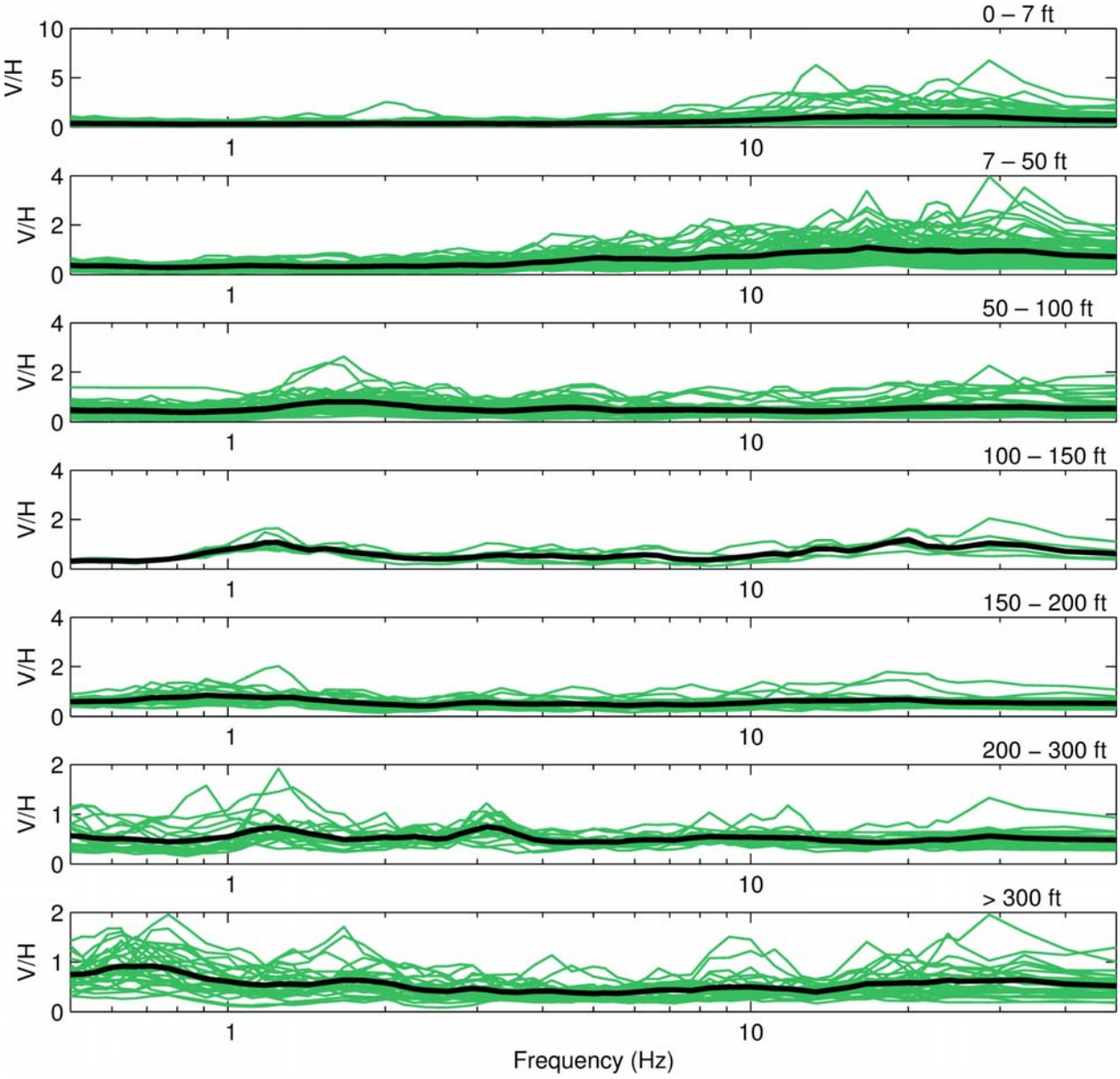

Figure 13 V/H ratios of all records obtained from arrays in class D3 sites. Total of 269 V/H ratios plotted in their corresponding depth bins:

0-7 ft (69 ratios), 7-50 ft (69 ratios), 50-100 ft (58 ratios), 100-150 ft (6 ratios), 150-200 ft (19 ratios), 200-300 ft (19 ratios), and >300 ft (29 ratios). The thick black lines correspond to the averages for each bin.

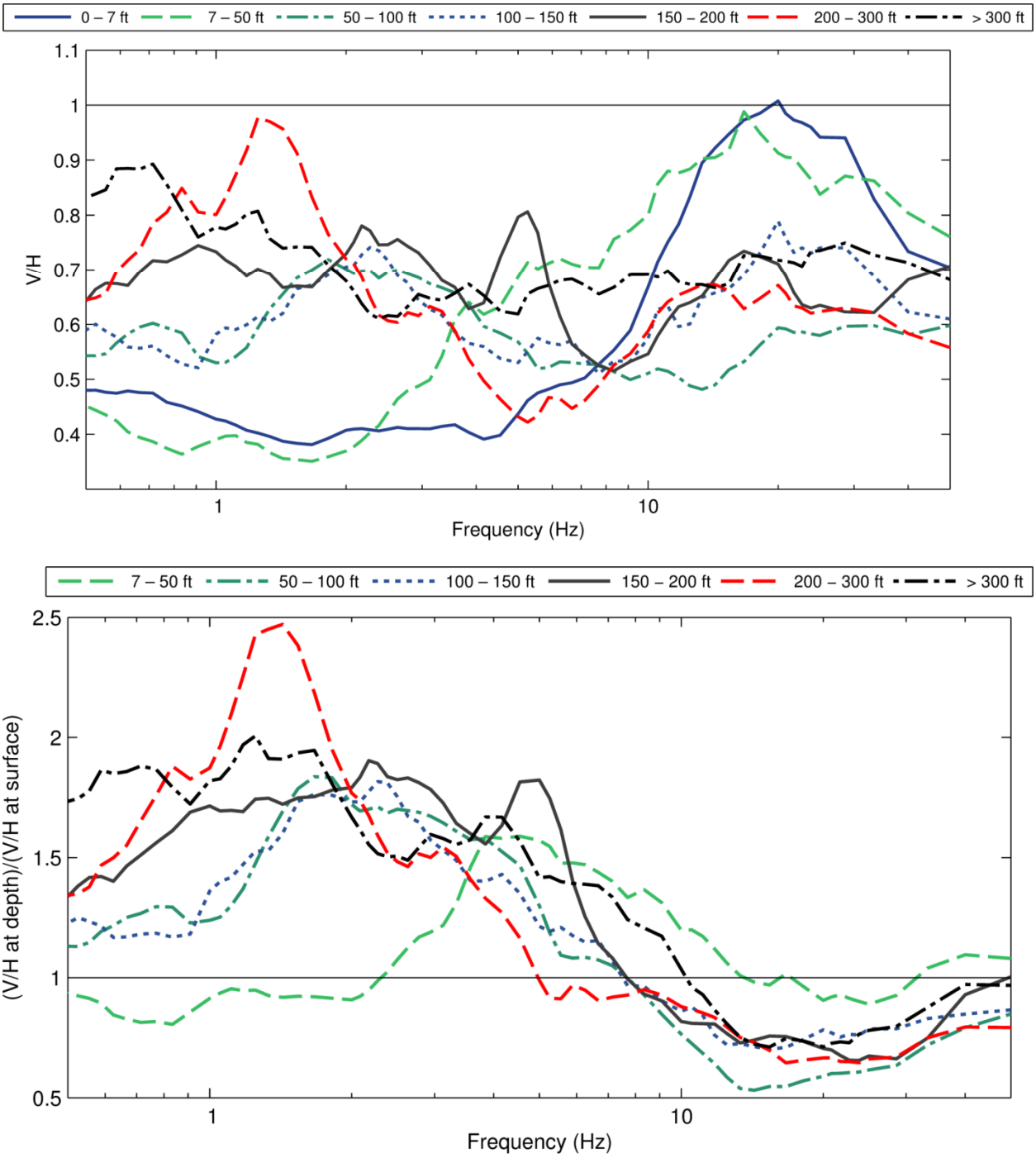

Figure 14 V/H ratios of all records obtained from arrays in class D (D1, D2, and D3) sites. Average V/H ratios (top) and normalized average V/H ratios (bottom) for each of the seven depth bins:

0-7 ft (170 ratios), 7-50 ft (127 ratios), 50-100 ft (133 ratios), 100-150 ft (53 ratios), 150-200 ft (49 ratios), 200-300 ft (66 ratios), and >300 ft (78 ratios).

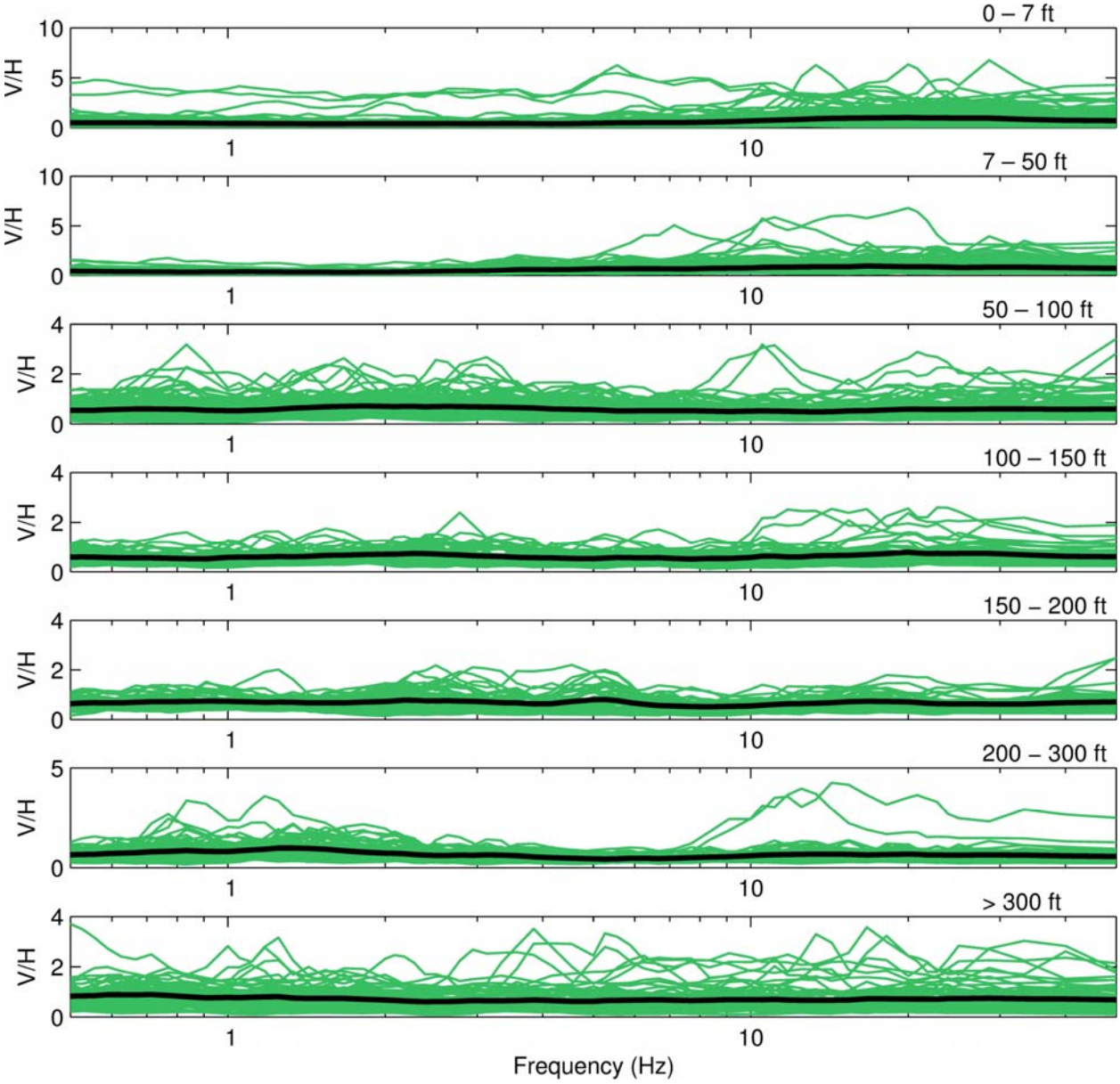

Figure 15 V/H ratios of all records obtained from arrays in class D (D1, D2, and D3) sites. Total of 676 V/H ratios plotted in their corresponding depth bins:

0-7 ft (170 ratios), 7-50 ft (127 ratios), 50-100 ft (133 ratios), 100-150 ft (53 ratios), 150-200 ft (49 ratios), 200-300 ft (66 ratios), and >300 ft (78 ratios). The thick black lines correspond to the averages for each bin.

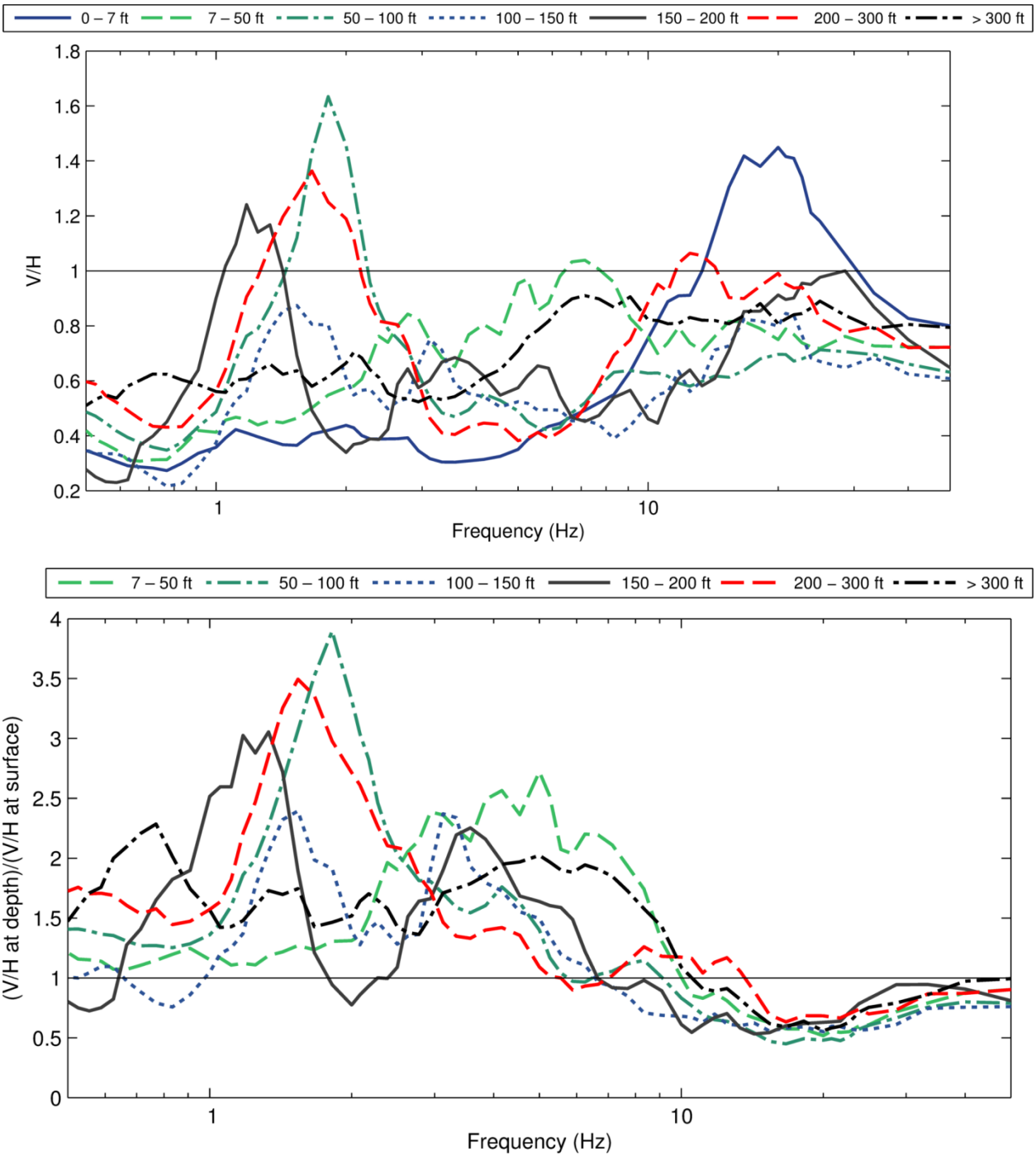

Figure 16 V/H ratios of all records obtained from arrays in class E sites. Average V/H ratios (top) and normalized average V/H ratios (bottom) for each of the seven depth bins:

0-7 ft (17 ratios), 7-50 ft (5 ratios), 50-100 ft (17 ratios), 100-150 ft (6 ratios), 150-200 ft (2 ratios), 200-300 ft (12 ratios), and >300 ft (6 ratios).

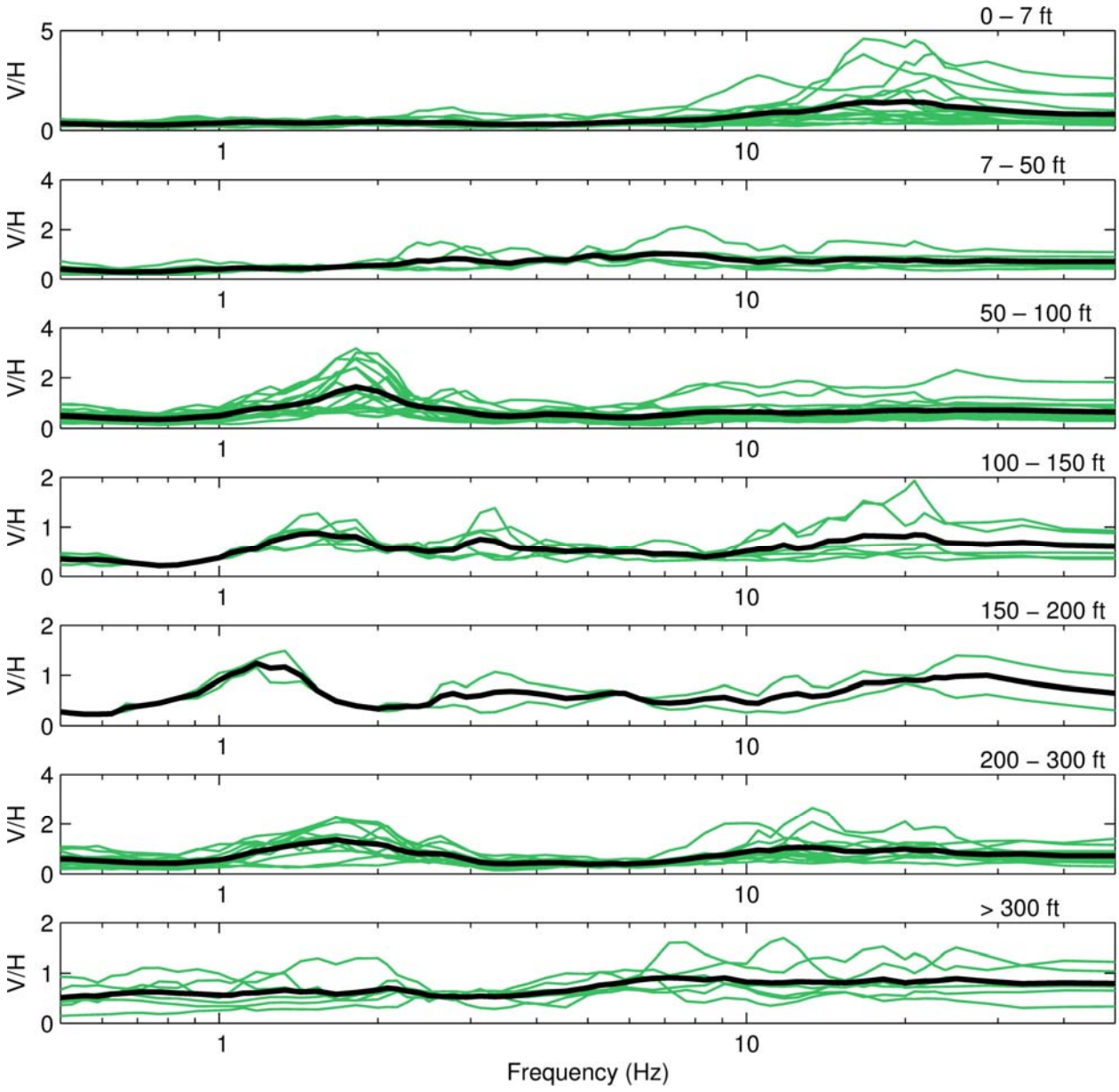

Figure 17 V/H ratios of all records obtained from arrays in class E sites. Total of 65 V/H ratios plotted in their corresponding depth bins:

0-7 ft (17 ratios), 7-50 ft (5 ratios), 50-100 ft (17 ratios), 100-150 ft (6 ratios), 150-200 ft (2 ratios), 200-300 ft (12 ratios), and >300 ft (6 ratios). The thick black lines correspond to the averages for each bin.

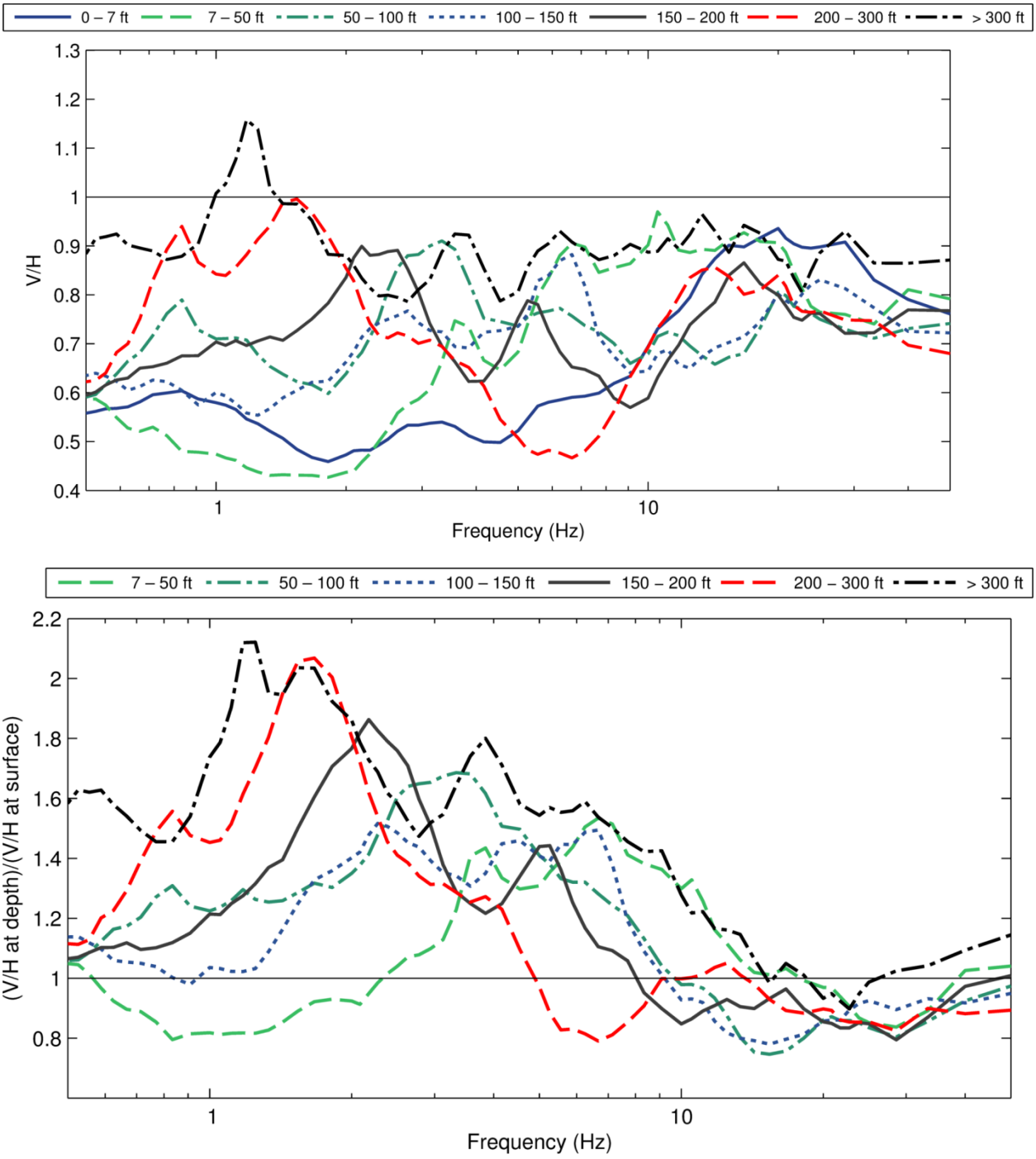

Figure 18 V/H ratios of all records obtained from events with PGA in the range 0.01-0.10 g (from arrays in class B, C, and D1 sites only). Average V/H ratios (top) and normalized average V/H ratios (bottom) for each of the seven depth bins:

0-7 ft (137 ratios), 7-50 ft (63 ratios), 50-100 ft (69 ratios), 100-150 ft (62 ratios), 150-200 ft (57 ratios), 200-300 ft (50 ratios), and >300 ft (28 ratios).

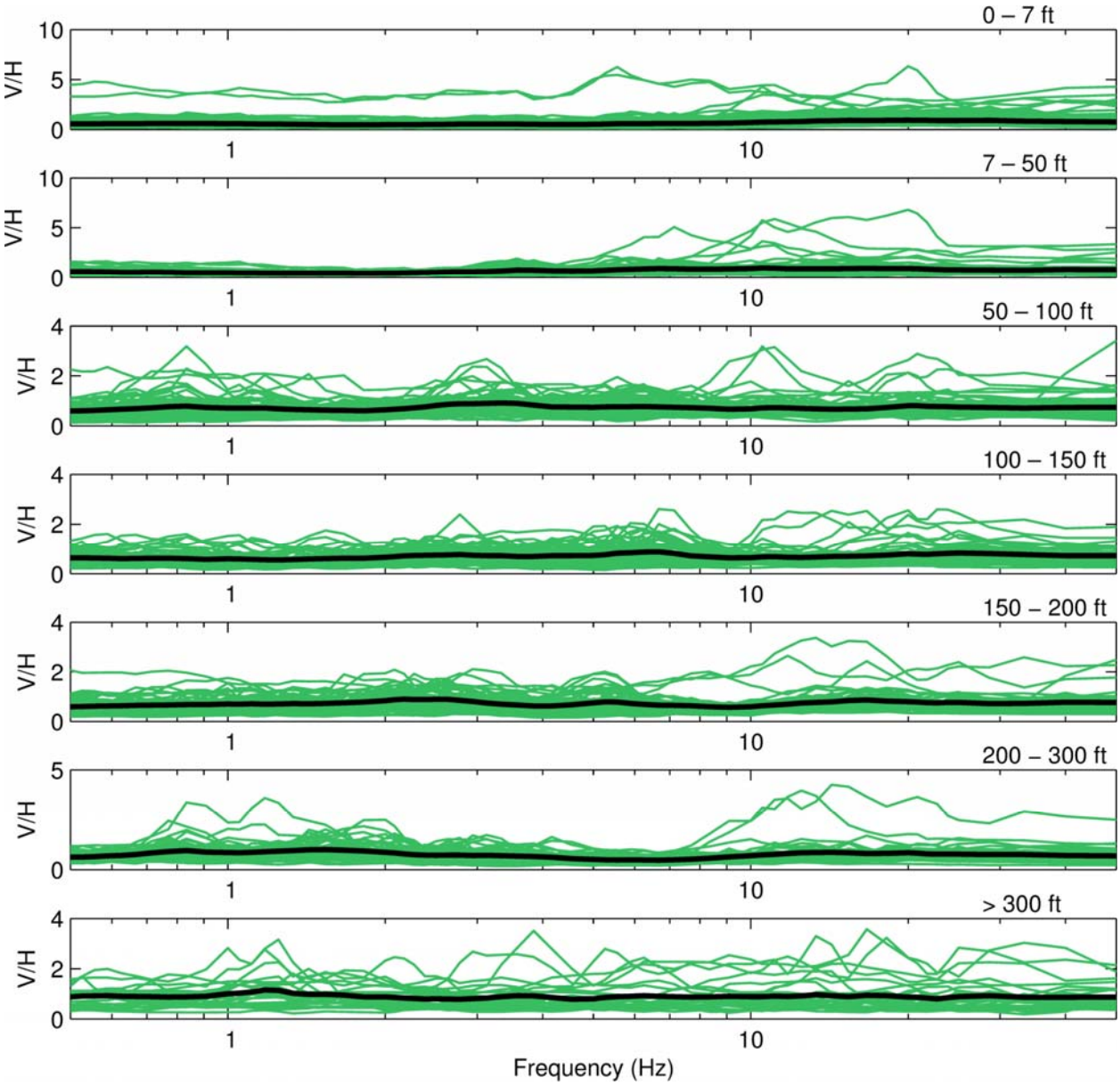

Figure 19 V/H ratios of all records obtained from events with PGA in the range 0.01-0.10 g (from arrays in class B, C, and D1 sites only). Total of 466 V/H ratios plotted in their corresponding depth bins:

0-7 ft (137 ratios), 7-50 ft (63 ratios), 50-100 ft (69 ratios), 100-150 ft (62 ratios), 150-200 ft (57 ratios), 200-300 ft (50 ratios), and >300 ft (28 ratios). The thick black lines correspond to the averages for each bin.

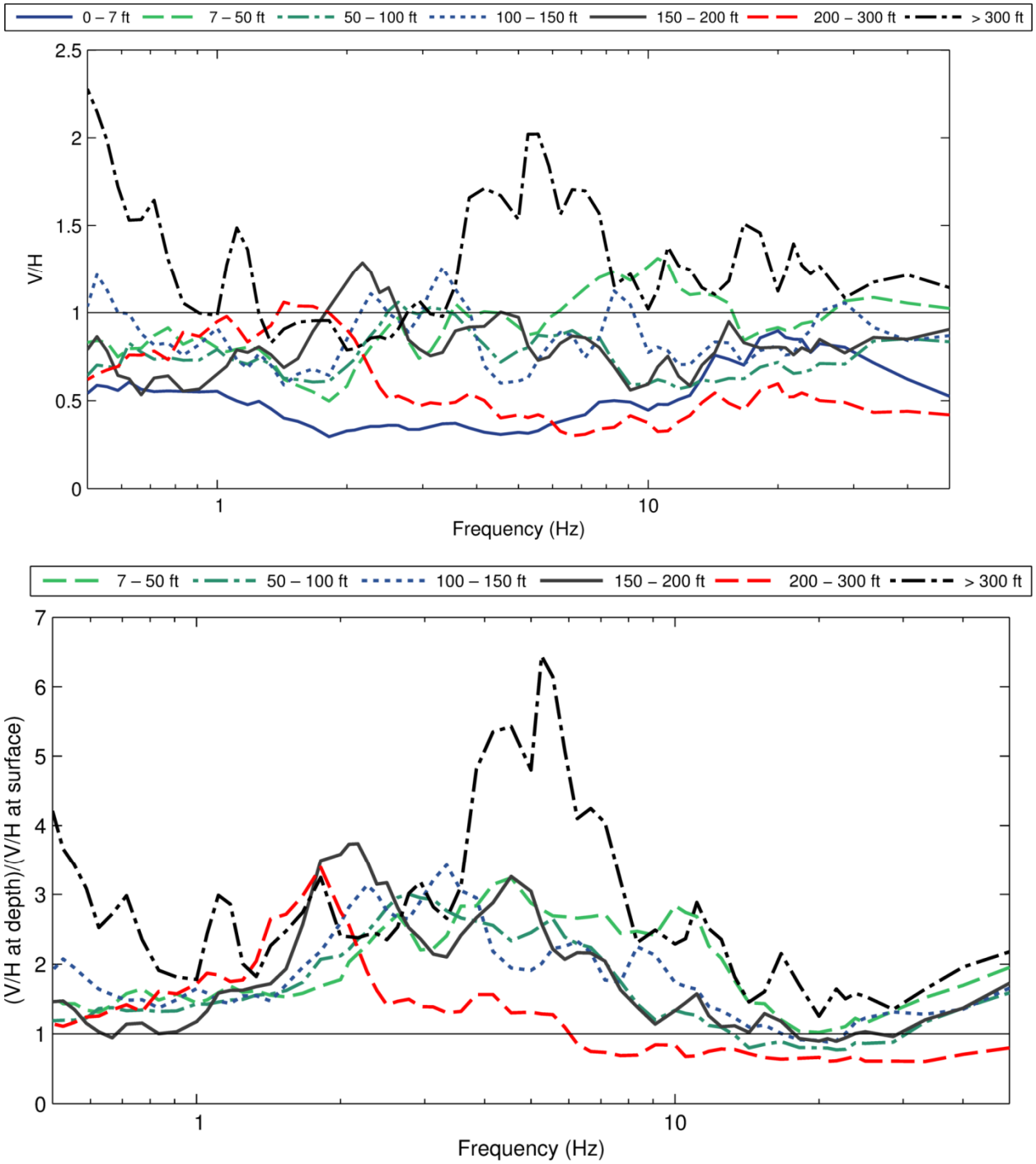

Figure 20 V/H ratios of all records obtained from events with PGA in the range 0.10-0.20 g (from arrays in class B, C, and D1 sites only). Average V/H ratios (top) and normalized average V/H ratios (bottom) for each of the seven depth bins:

0-7 ft (9 ratios), 7-50 ft (4 ratios), 50-100 ft (6 ratios), 100-150 ft (2 ratios), 150-200 ft (3 ratios), 200-300 ft (4 ratios), and >300 ft (2 ratios).

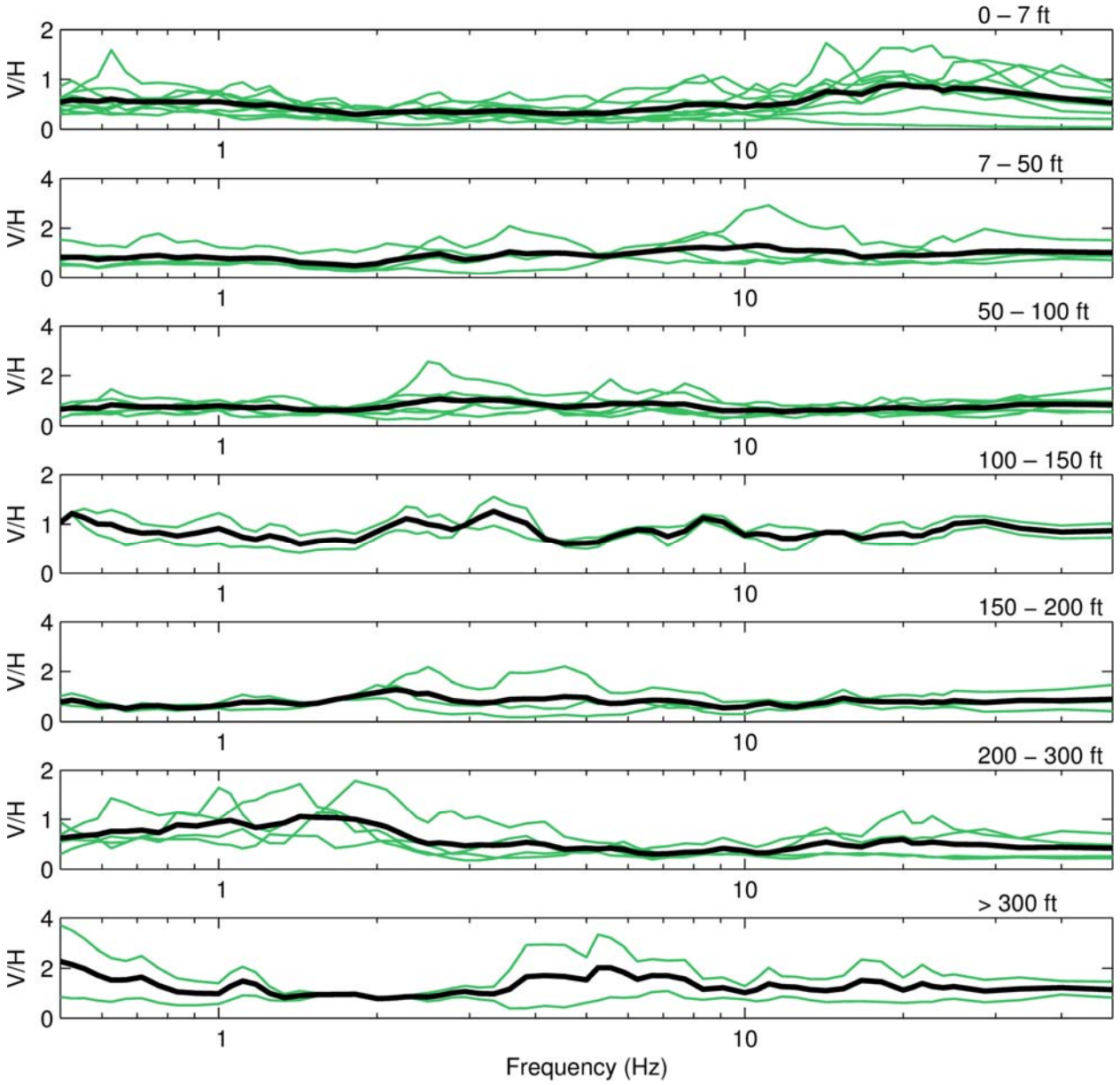

Figure 21 V/H ratios of all records obtained from events with PGA in the range 0.10-0.20 g (from arrays in class B, C, and D1 sites only). Total of 30 V/H ratios plotted in their corresponding depth bins:

0-7 ft (9 ratios), 7-50 ft (4 ratios), 50-100 ft (6 ratios), 100-150 ft (2 ratios), 150-200 ft (3 ratios), 200-300 ft (4 ratios), and >300 ft (2 ratios). The thick black lines correspond to the averages for each bin.

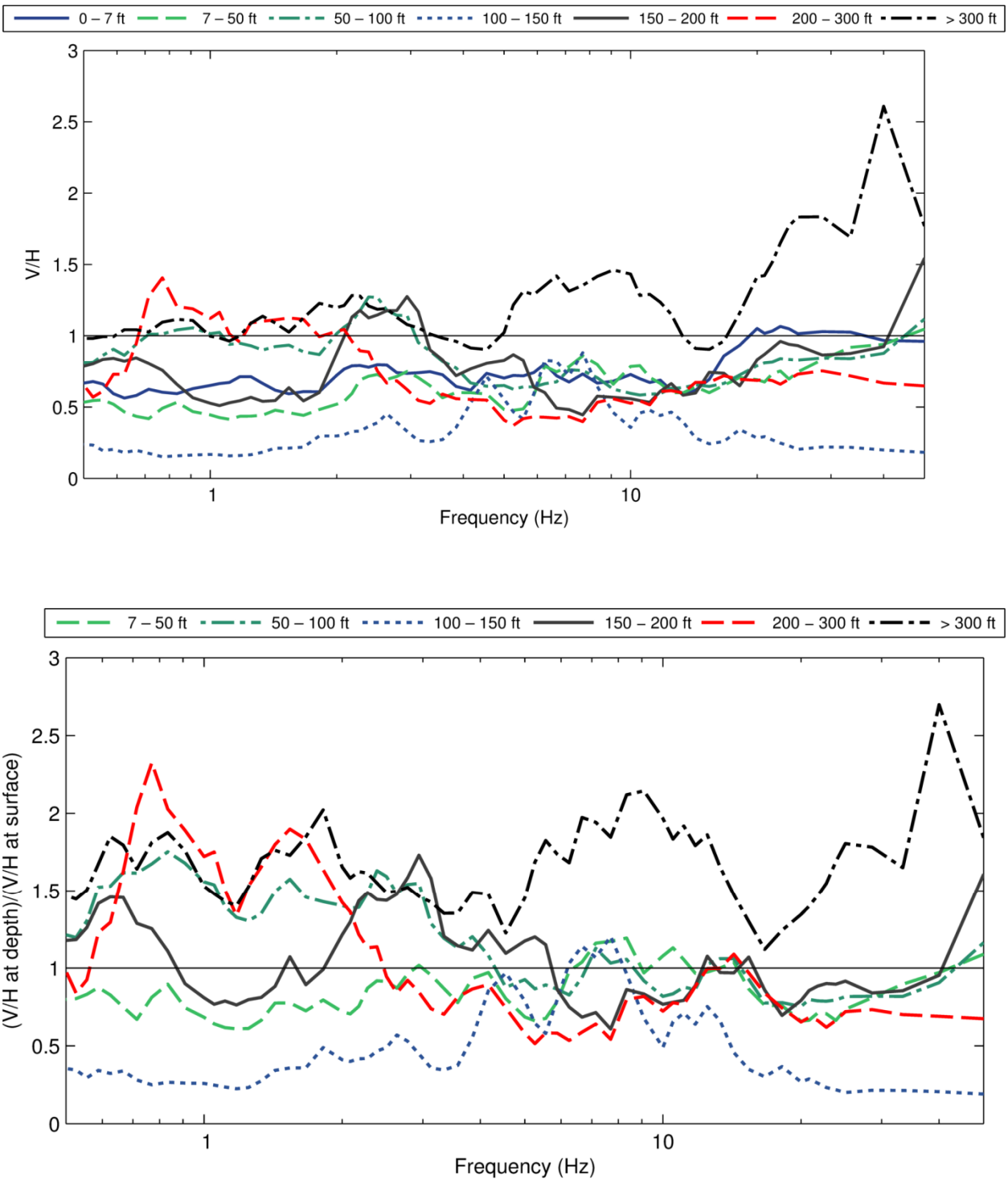

Figure 22 V/H ratios of all records obtained from events with PGA in the range 0.20-0.50 g (from arrays in class B, C, and D1 sites only). Average V/H ratios (top) and normalized average V/H ratios (bottom) for each of the seven depth bins:

0-7 ft (8 ratios), 7-50 ft (4 ratios), 50-100 ft (6 ratios), 100-150 ft (1 ratio), 150-200 ft (2 ratios), 200-300 ft (3 ratios), and >300 ft (1 ratio).

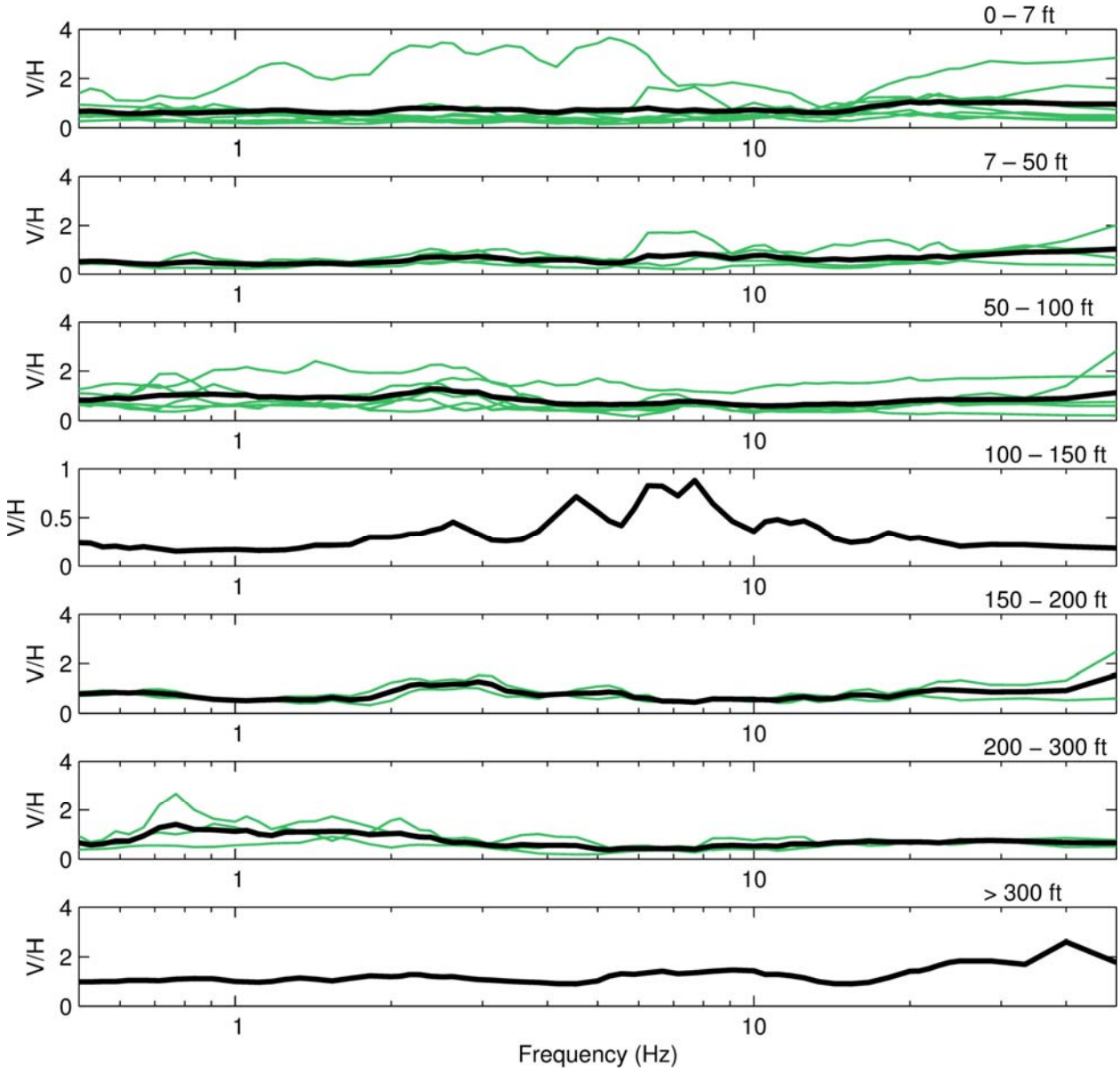

Figure 23 V/H ratios of all records obtained from events with PGA in the range 0.20-0.50 g (from arrays in class B, C, and D1 sites only). Total of 25 V/H ratios plotted in their corresponding depth bins:

0-7 ft (8 ratios), 7-50 ft (4 ratios), 50-100 ft (6 ratios), 100-150 ft (1 ratio), 150-200 ft (2 ratios), 200-300 ft (3 ratios), and >300 ft (1 ratio). The thick black lines correspond to the averages for each bin.

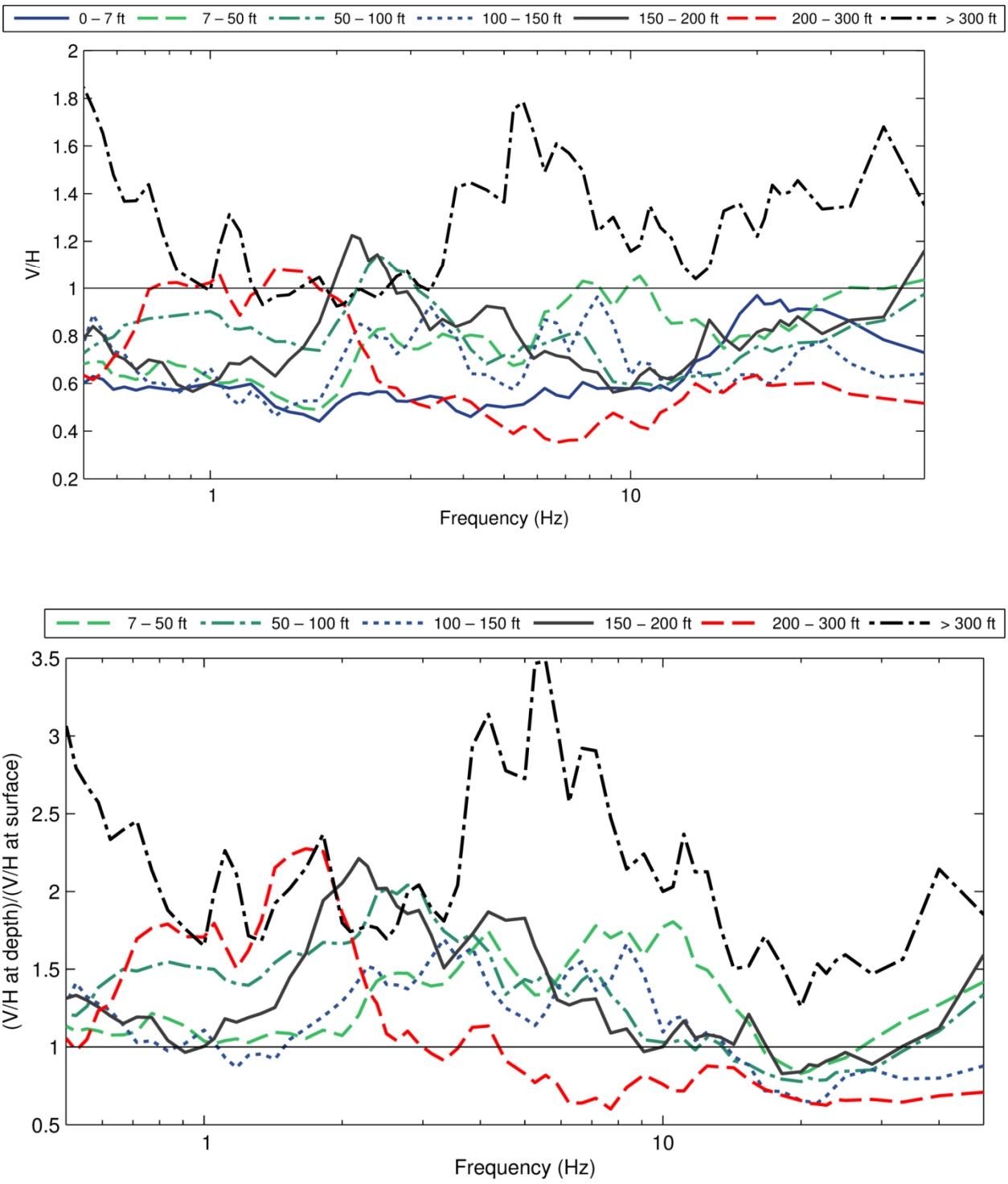

Figure 24 V/H ratios of all records obtained from events with PGA in the range 0.10-0.50 g (from arrays in class B, C, and D1 sites only). Average V/H ratios (top) and normalized average V/H ratios (bottom) for each of the seven depth bins:

0-7 ft (17 ratios), 7-50 ft (8 ratios), 50-100 ft (12 ratios), 100-150 ft (3 ratios), 150-200 ft (5 ratios), 200-300 ft (7 ratios), and >300 ft (3 ratios).

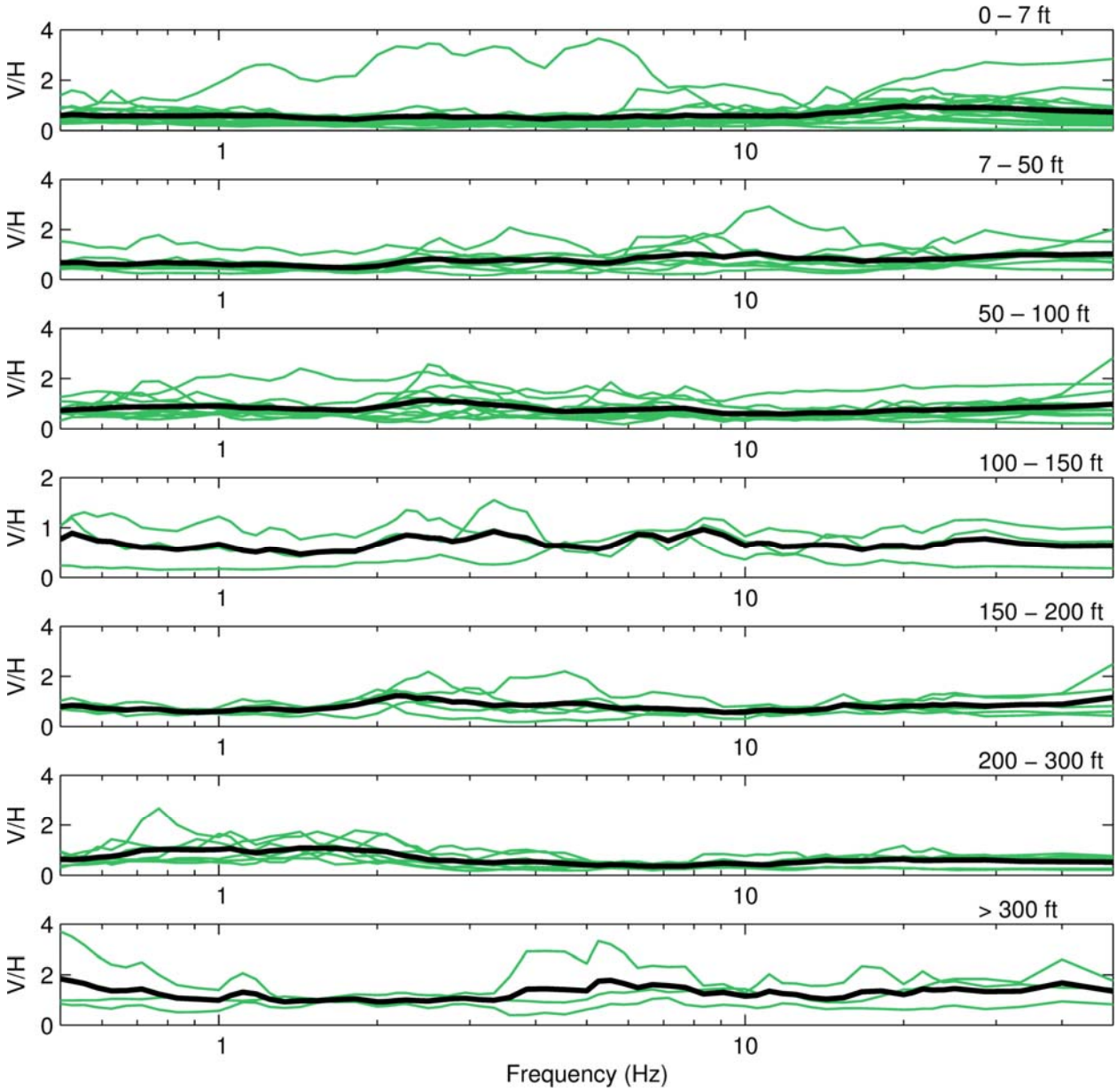

Figure 25 V/H ratios of all records obtained from events with PGA in the range 0.10-0.50 g (from arrays in class B, C, and D1 sites only). Total of 55 V/H ratios plotted in their corresponding depth bins:

0-7 ft (17 ratios), 7-50 ft (8 ratios), 50-100 ft (12 ratios), 100-150 ft (3 ratios), 150-200 ft (5 ratios), 200-300 ft (7 ratios), and >300 ft (3 ratios). The thick black lines correspond to the averages for each bin.

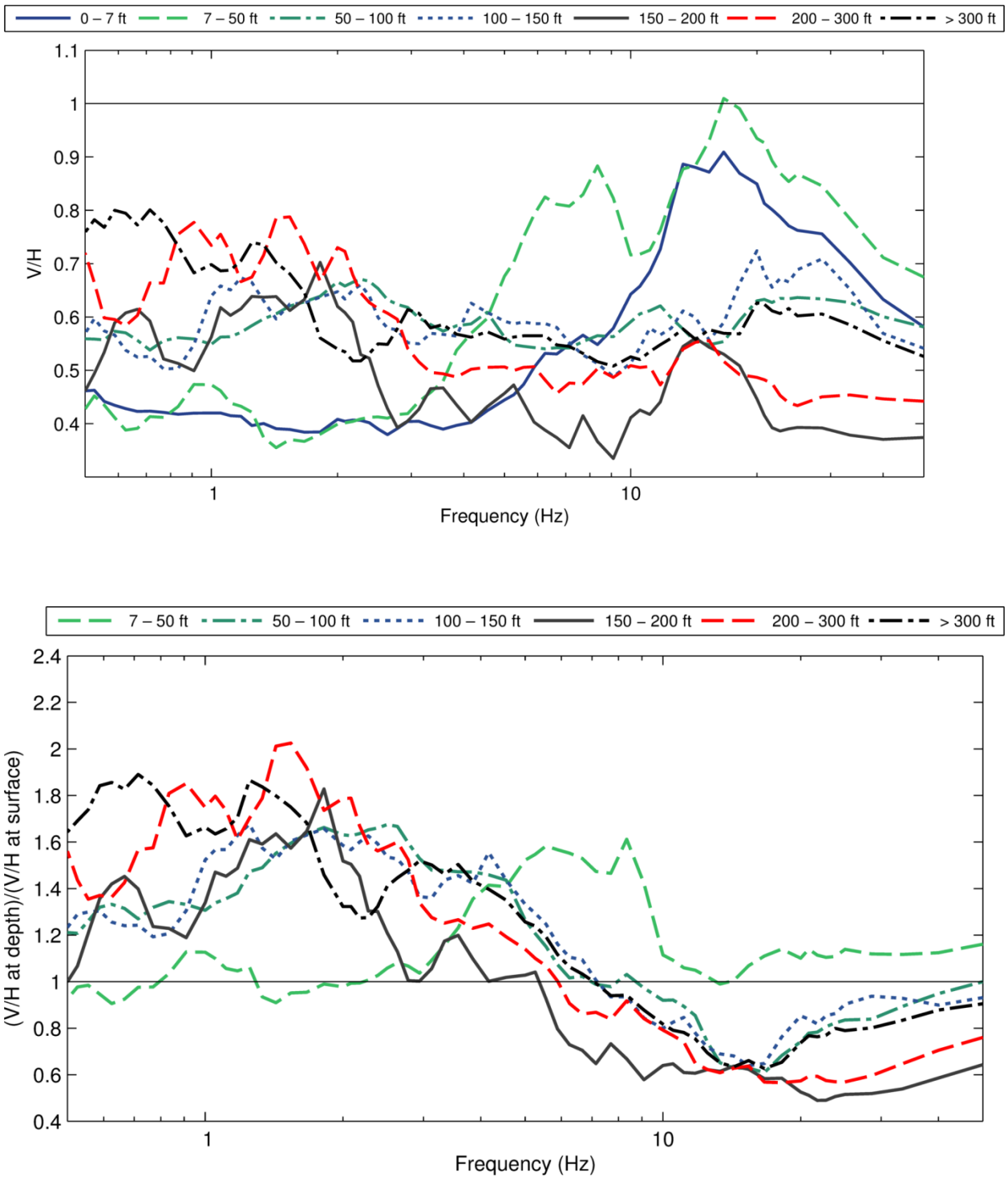

Figure 26 V/H ratios of all records obtained from CGS-CESMD and USGS-NSMP sites in California (arrays in class B, C, and D sites only). Average V/H ratios (top) and normalized average V/H ratios (bottom) for each of the seven depth bins:

0-7 ft (68 ratios), 7-50 ft (28 ratios), 50-100 ft (48 ratios), 100-150 ft (31 ratios), 150-200 ft (7 ratios), 200-300 ft (9 ratios), and >300 ft (34 ratios).

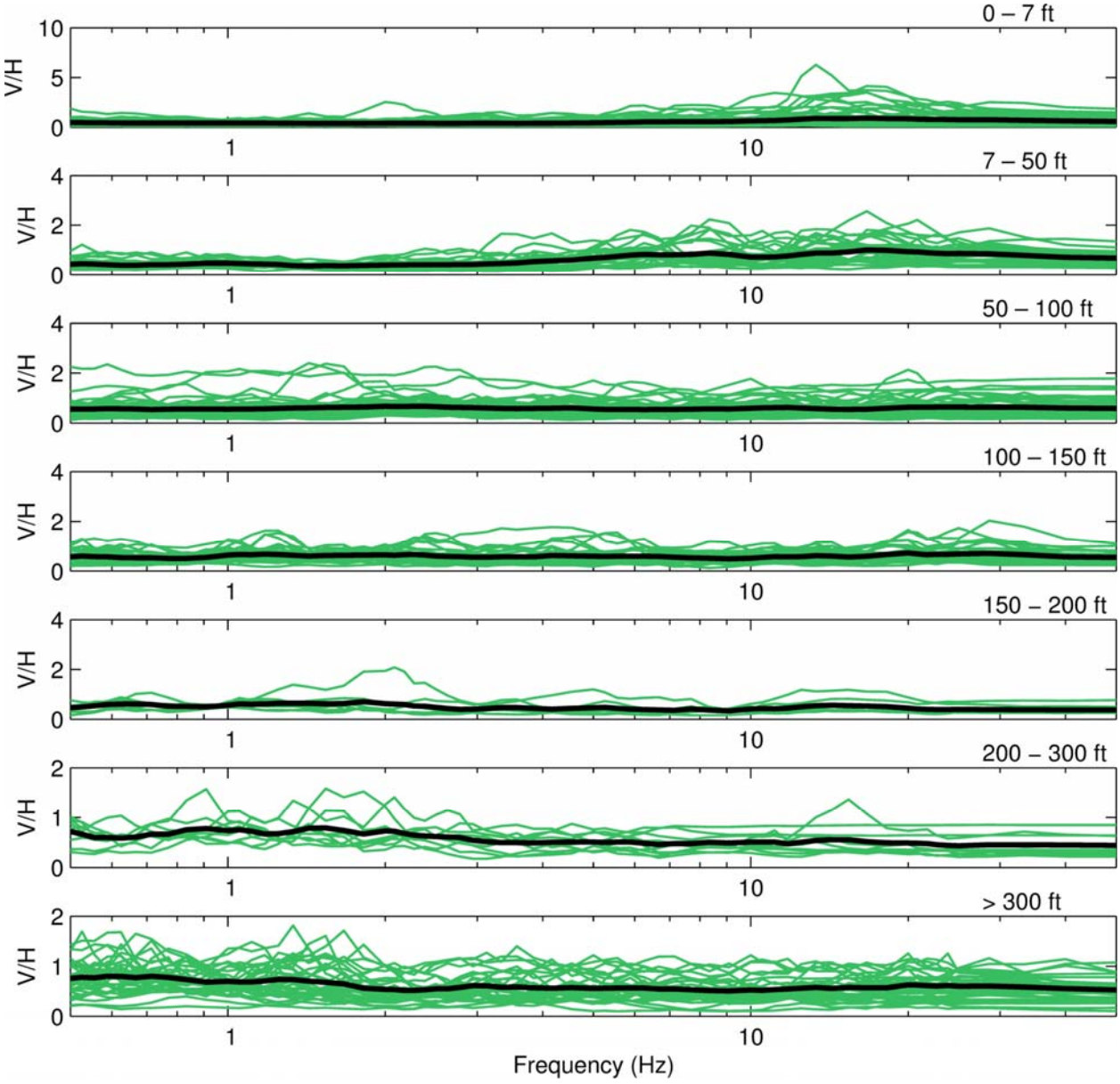

Figure 27 V/H ratios of all records obtained from CGS-CESMD and USGS-NSMP sites in California (arrays in class B, C, and D sites only). Total of 225 V/H ratios plotted in their corresponding depth bins:

0-7 ft (68 ratios), 7-50 ft (28 ratios), 50-100 ft (48 ratios), 100-150 ft (31 ratios), 150-200 ft (7 ratios), 200-300 ft (9 ratios), and >300 ft (34 ratios). The thick black lines correspond to the averages for each bin.

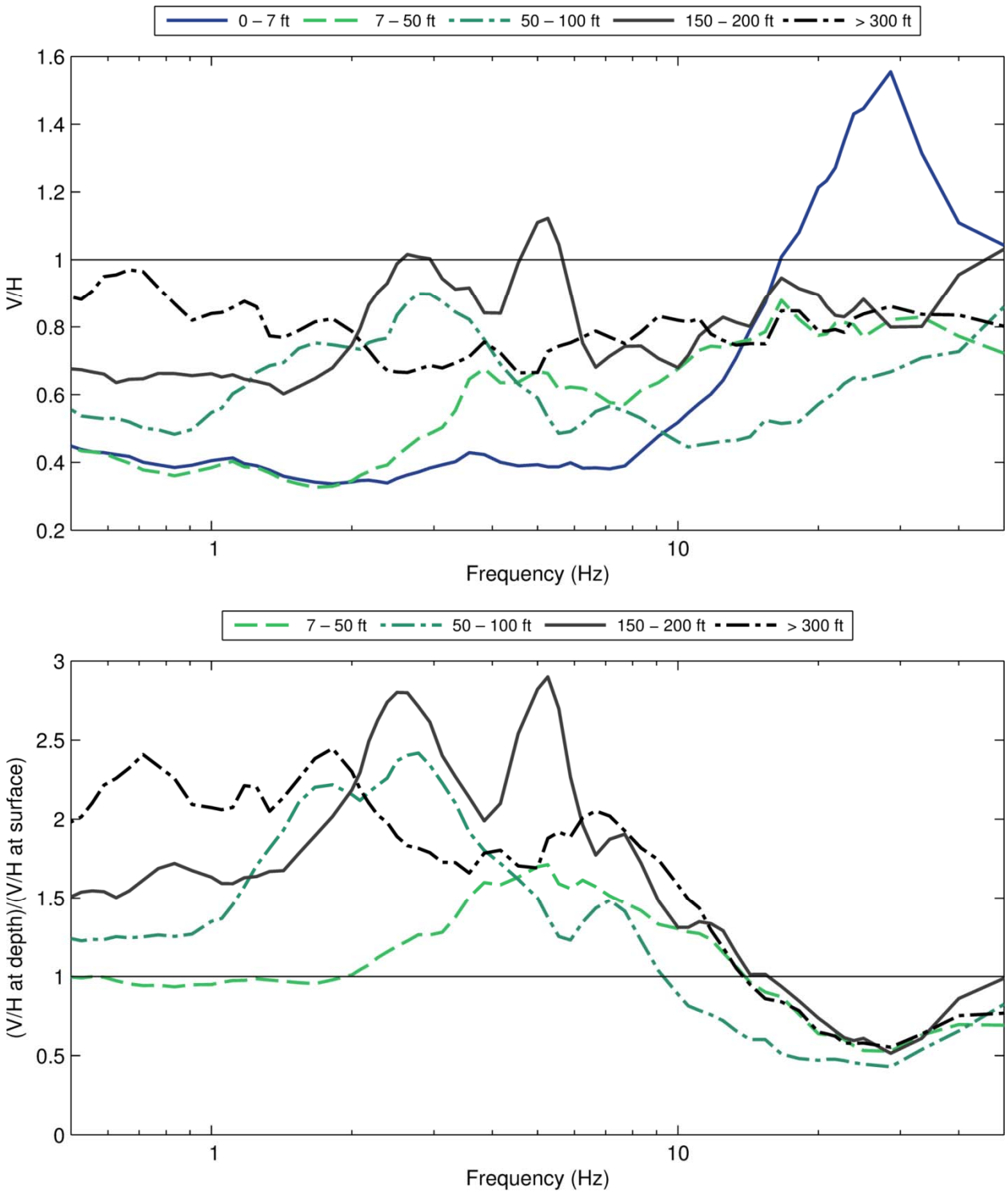

Figure 28 V/H ratios of all records obtained from NEES at UCSB sites in California (arrays in class C and D sites only). Average V/H ratios (top) and normalized average V/H ratios (bottom) for each of the seven depth bins:

0-7 ft (43 ratios), 7-50 ft (86 ratios), 50-100 ft (34 ratios), 150-200 ft (23 ratios), and >300 ft (44 ratios).

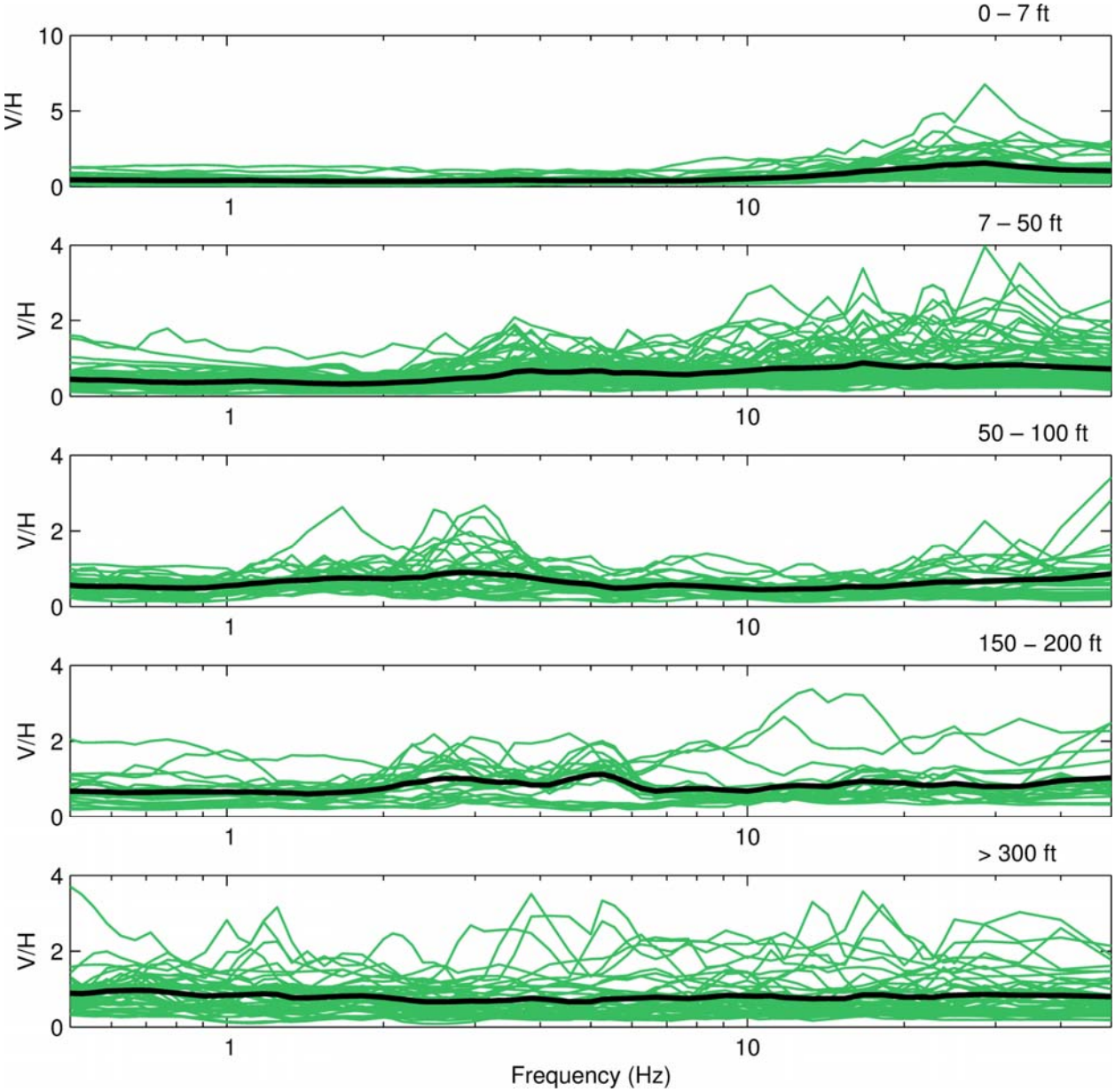

Figure 29 V/H ratios of all records obtained from NEES at UCSB sites in California (arrays in class C and D sites only). Total of 230 V/H ratios plotted in their corresponding depth bins:

0-7 ft (43 ratios), 7-50 ft (86 ratios), 50-100 ft (34 ratios), 150-200 ft (23 ratios), and >300 ft (44 ratios). The thick black lines correspond to the averages for each bin.

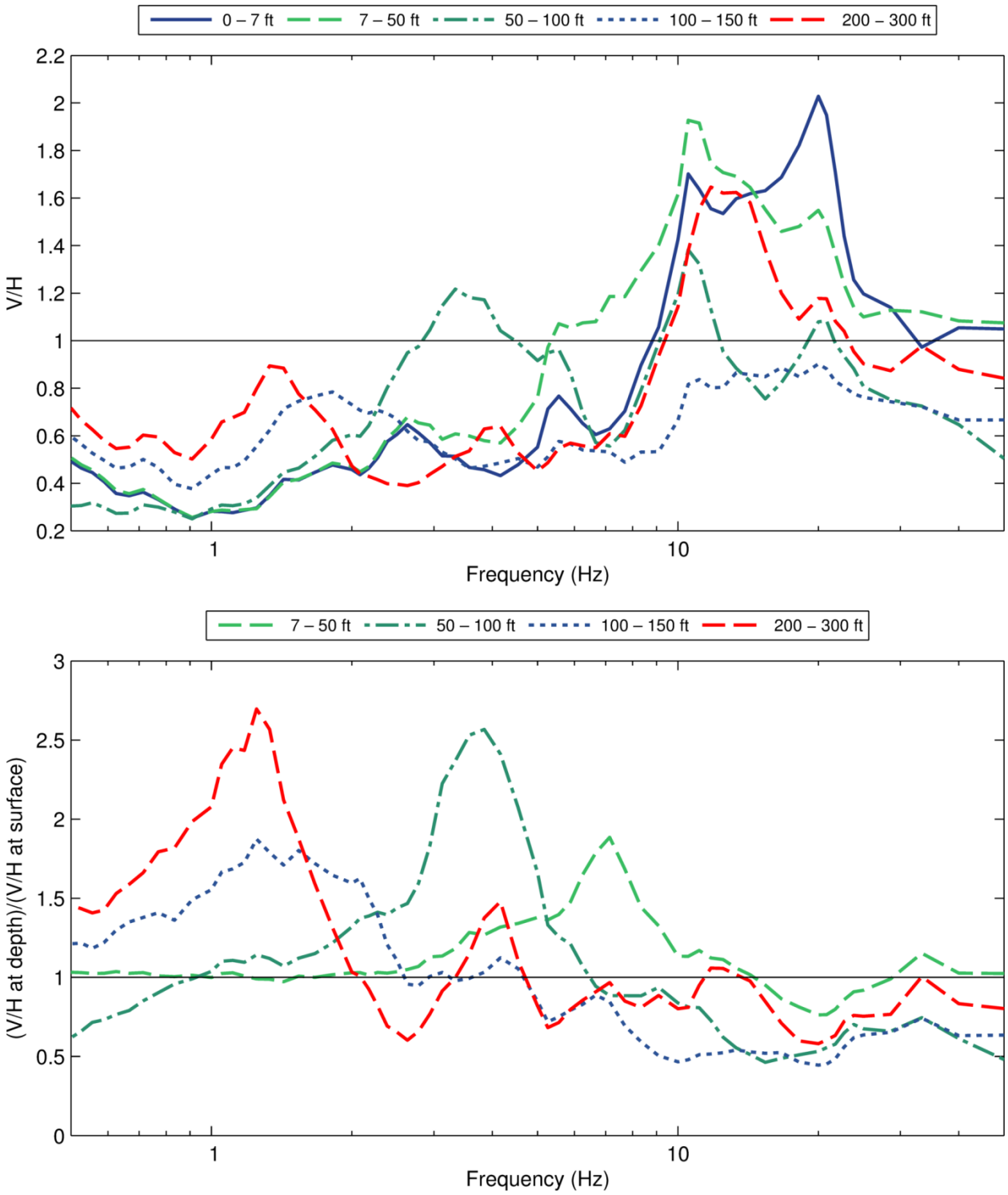

Figure 30 V/H ratios of all records obtained from the NEES at UCSB site in Anchorage, Alaska (array in class D site). Average V/H ratios (top) and normalized average V/H ratios (bottom) for each of the seven depth bins:

0-7 ft (8 ratios), 7-50 ft (16 ratios), 50-100 ft (8 ratios), 100-150 ft (15 ratios), and 200-300 ft (8 ratios).

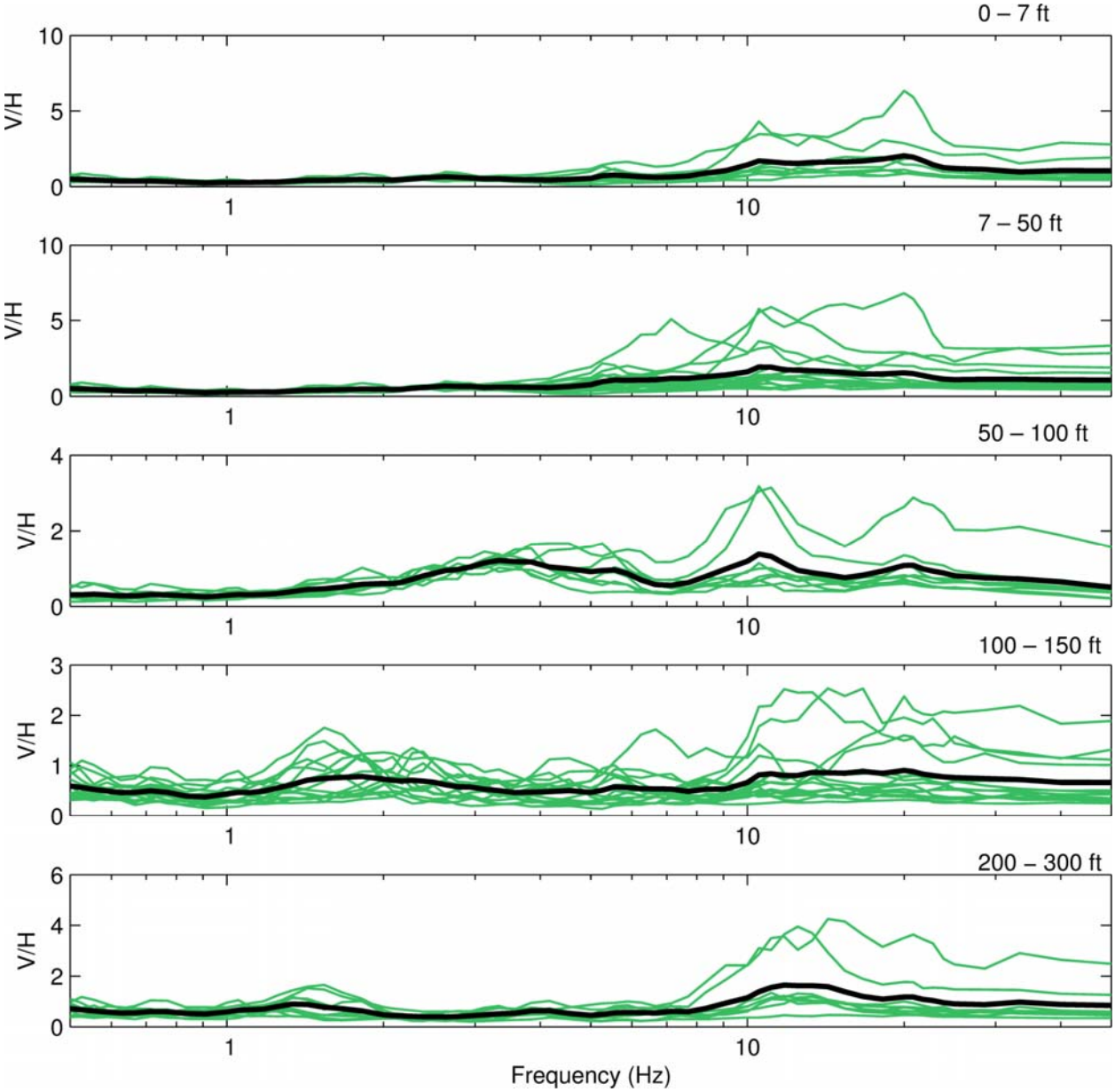

Figure 31 V/H ratios of all records obtained from the NEES at UCSB site in Anchorage, Alaska (array in class D site). Total of 55 V/H ratios plotted in their corresponding depth bins:

0-7 ft (8 ratios), 7-50 ft (16 ratios), 50-100 ft (8 ratios), 100-150 ft (15 ratios), and 200-300 ft (8 ratios). The thick black lines correspond to the averages for each bin.

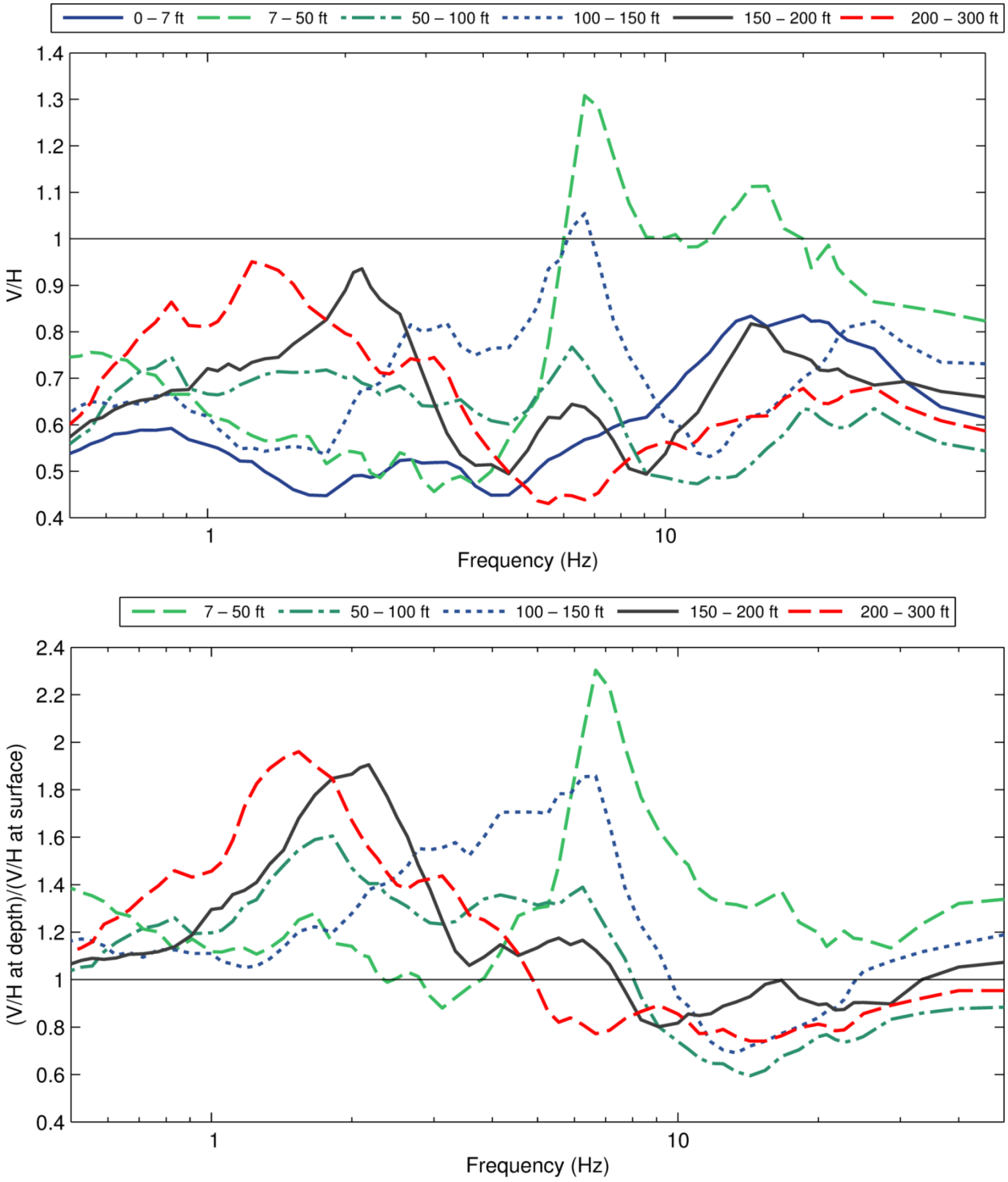

Figure 32 V/H ratios of all records obtained from the Sendai District, Japan (arrays in class B, C, and D sites only). Average V/H ratios (top) and normalized average V/H ratios (bottom) for each of the seven depth bins:

0-7 ft (114 ratios), 7-50 ft (13 ratios), 50-100 ft (61 ratios), 100-150 ft (37 ratios), 150-200 ft (38 ratios), and 200-300 ft (73 ratios).

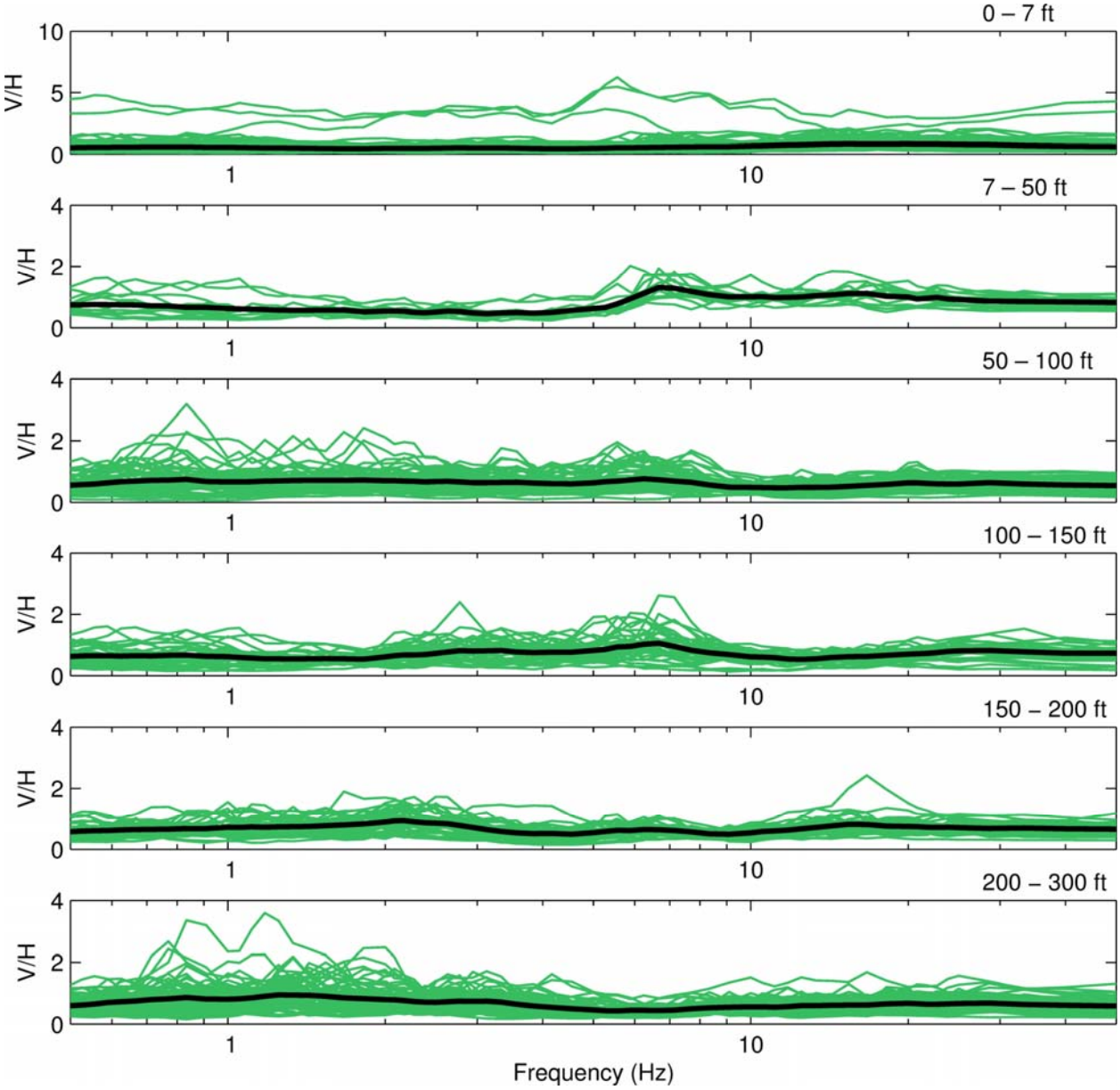

Figure 33 V/H ratios of all records obtained from the Sendai District, Japan (arrays in class B, C, and D sites only). Total of 336 V/H ratios plotted in their corresponding depth bins:

0-7 ft (114 ratios), 7-50 ft (13 ratios), 50-100 ft (61 ratios), 100-150 ft (37 ratios), 150-200 ft (38 ratios), and 200-300 ft (73 ratios). The thick black lines correspond to the averages for each bin.

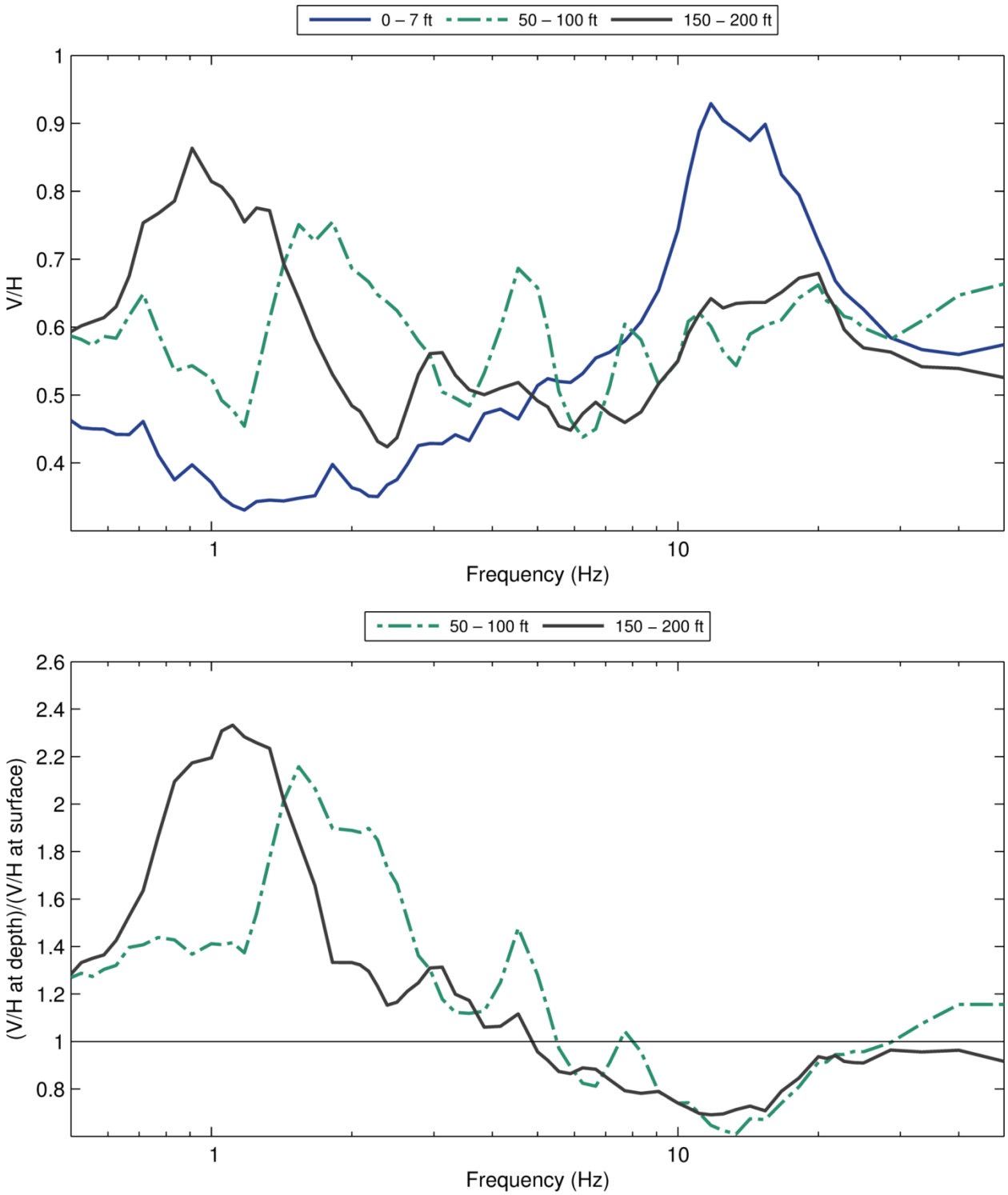

Figure 34 V/H ratios of all records obtained from the Taipei Basin, Taiwan (arrays in class D sites only). Average V/H ratios (top) and normalized average V/H ratios (bottom) for each of the seven depth bins:

0-7 ft (20 ratios), 50-100 ft (15 ratios), and 150-200 ft (19 ratios).

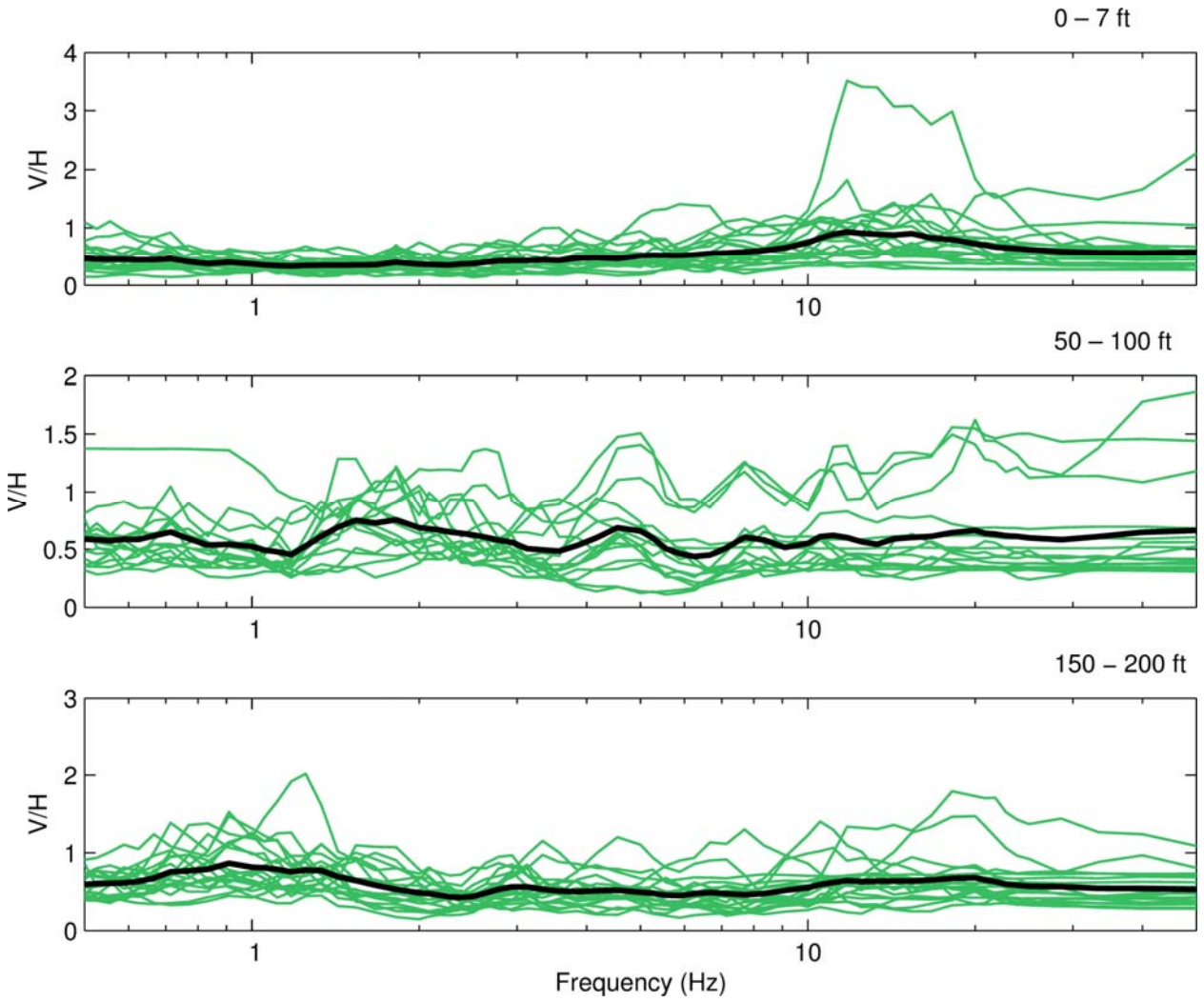

Figure 35 V/H ratios of all records obtained from the Taipei Basin, Taiwan (arrays in class D sites only). Total of 54 V/H ratios plotted in their corresponding depth bins:

0-7 ft (20 ratios), 50-100 ft (15 ratios), and 150-200 ft (19 ratios). The thick black lines correspond to the averages for each bin.

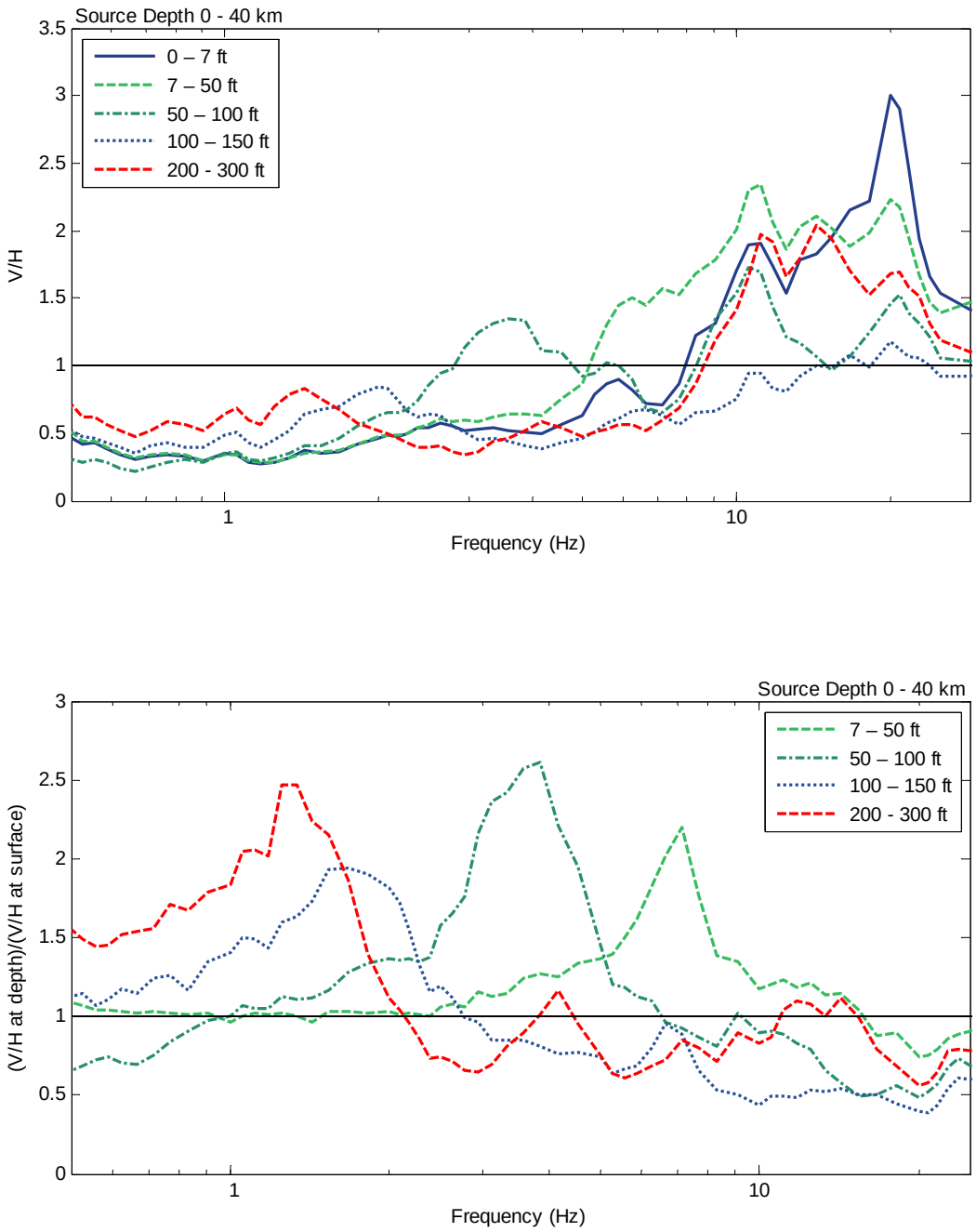

Figure 36 V/H ratios of all records obtained from events with source depths between 0 km and 40 km, from the NEES at UCSB site in Anchorage, Alaska (class D site)

Average V/H ratios (top) and normalized average V/H ratios (bottom) for each of the available depth bins.

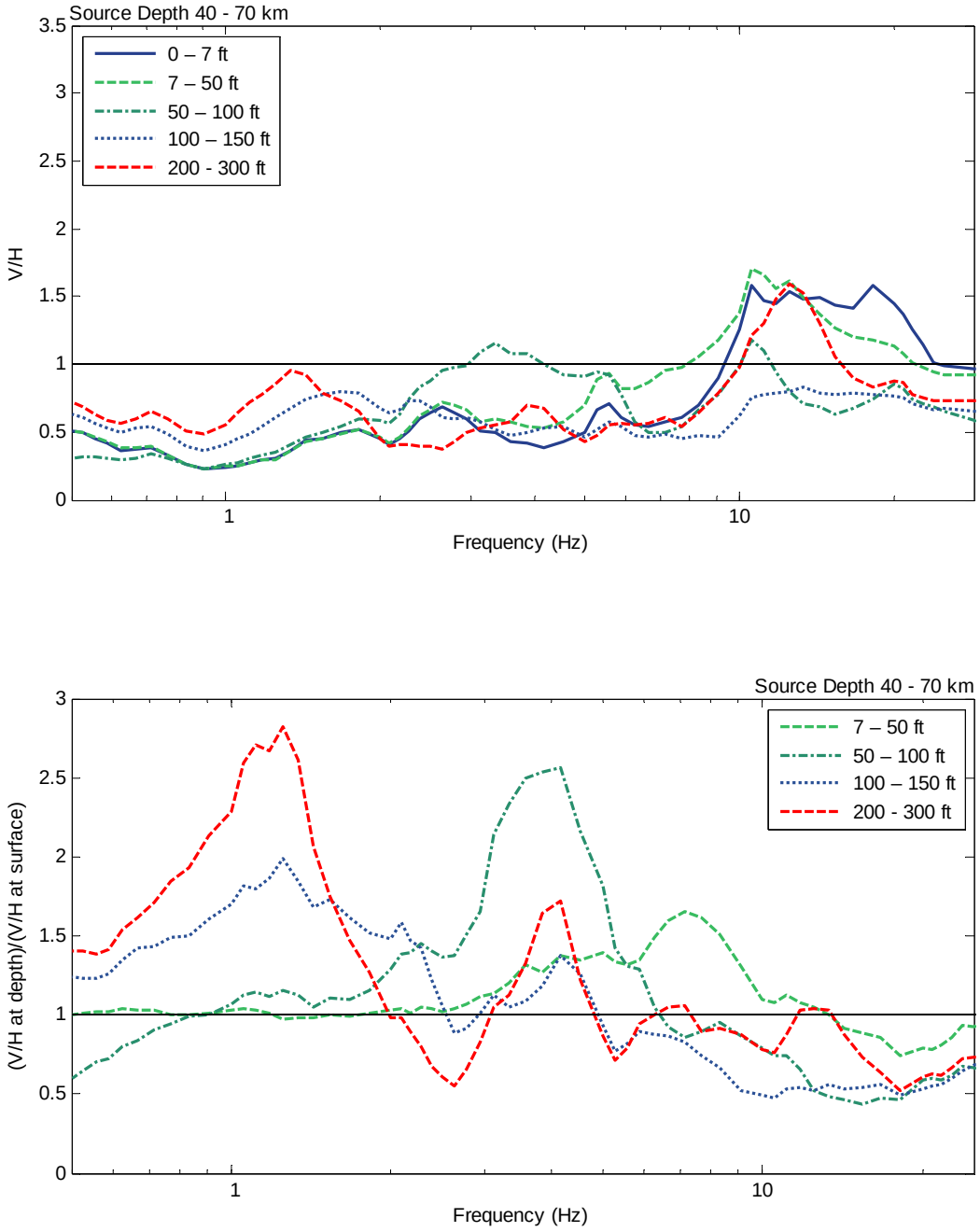

Figure 37 V/H ratios of all records obtained from events with source depths between 40 km and 70 km, from the NEES at UCSB site in Anchorage, Alaska (class D site)

Average V/H ratios (top) and normalized average V/H ratios (bottom) for each of the available depth bins.

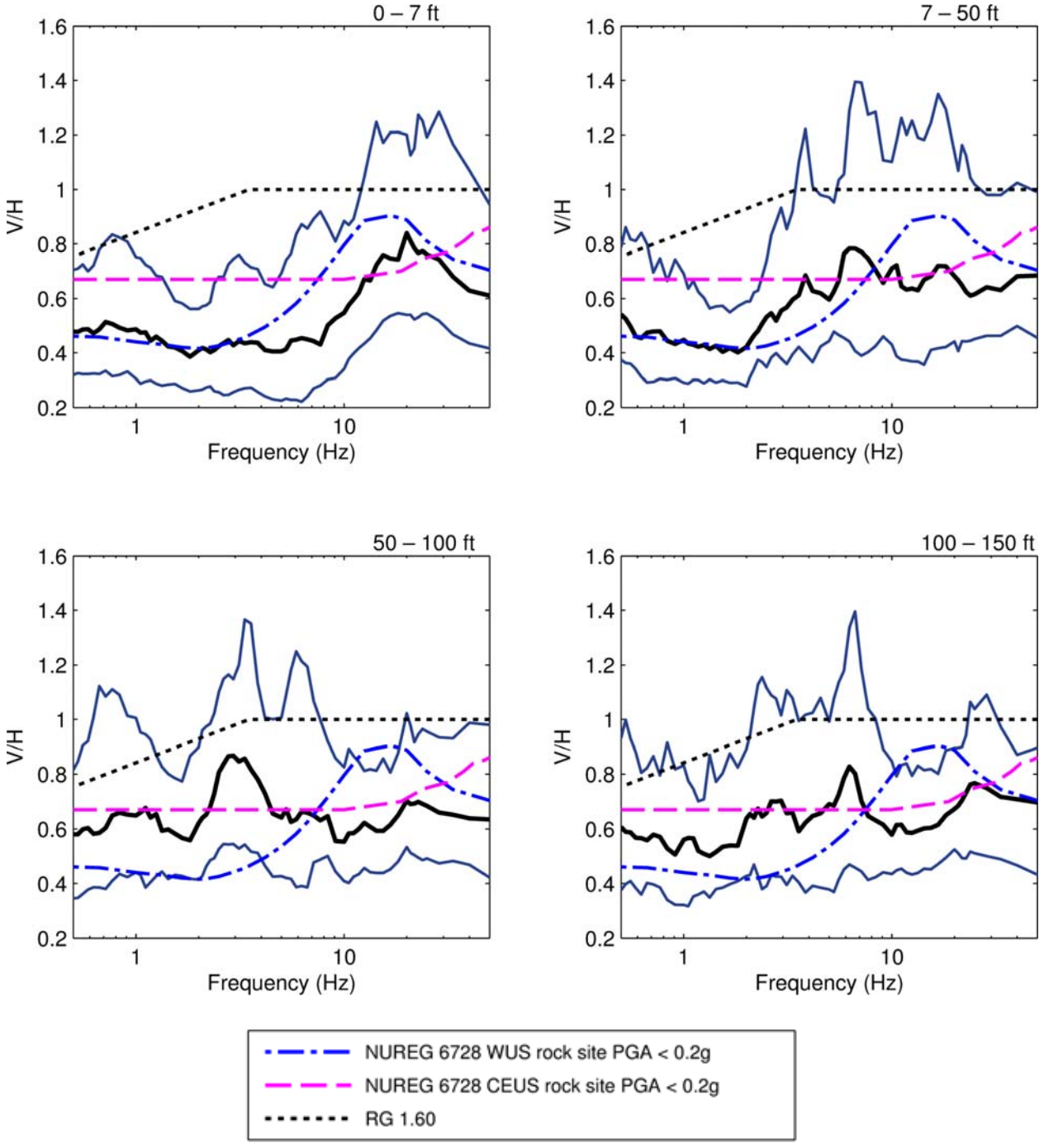

Figure 38 16th, 50th, and 84th percentiles of V/H ratios of all records obtained from arrays in class B, C, and D1 sites, and comparison to V/H ratios recommended in NUREG 6728 and RG 1.60

16th, 50th, and 84th percentiles are shown in solid lower blue, black, and upper blue lines, respectively. Figure shows depth bins 0-7 ft (top left), 7-50 ft (top right), 50-100 ft (bottom left), 100-150 ft (bottom right).

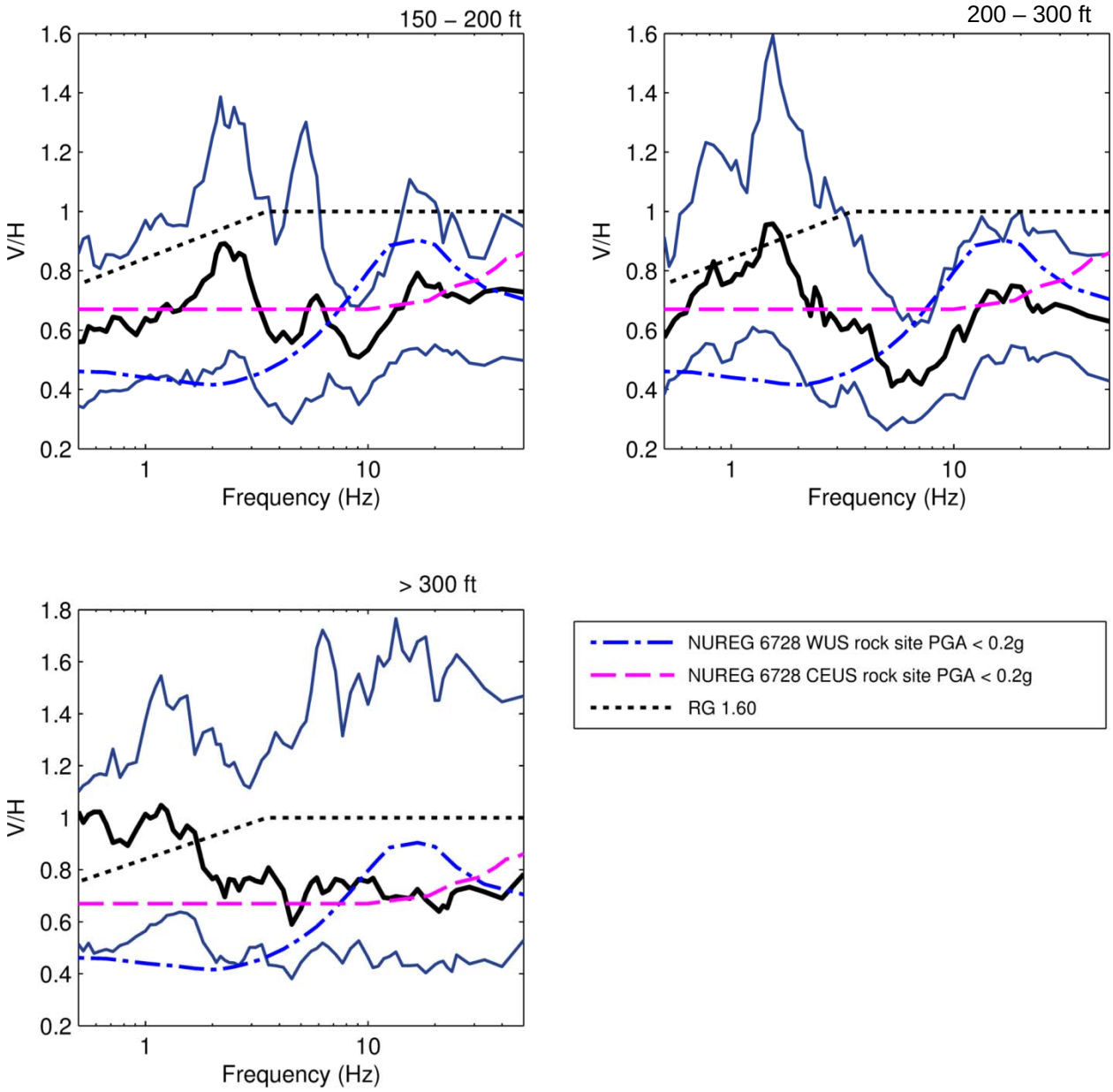

Figure 39 16th, 50th, and 84th percentiles of V/H ratios of all records obtained from arrays in class B, C, and D1 sites, and comparison to V/H ratios recommended in NUREG 6728 and RG 1.60

16th, 50th, and 84th percentiles are shown in solid lower blue, black, and upper blue lines, respectively. Figure shows depth bins 150-200 ft (top left), 200-300 ft (top right), and >300 ft (bottom left).